

## INFORMATION TO USERS

This manuscript has been reproduced from the microfilm master. UMI films the text directly from the original or copy submitted. Thus, some thesis and dissertation copies are in typewriter face, while others may be from any type of computer printer.

**The quality of this reproduction is dependent upon the quality of the copy submitted.** Broken or indistinct print, colored or poor quality illustrations and photographs, print bleedthrough, substandard margins, and improper alignment can adversely affect reproduction.

In the unlikely event that the author did not send UMI a complete manuscript and there are missing pages, these will be noted. Also, if unauthorized copyright material had to be removed, a note will indicate the deletion.

Oversize materials (e.g., maps, drawings, charts) are reproduced by sectioning the original, beginning at the upper left-hand corner and continuing from left to right in equal sections with small overlaps.

Photographs included in the original manuscript have been reproduced xerographically in this copy. Higher quality 6" x 9" black and white photographic prints are available for any photographs or illustrations appearing in this copy for an additional charge. Contact UMI directly to order.

ProQuest Information and Learning  
300 North Zeeb Road, Ann Arbor, MI 48106-1346 USA  
800-521-0600

UMI<sup>®</sup>



**University of Alberta**

**Determination of the Lipid-bound  
Conformation of the N-terminal Domain of  
Human Apolipoprotein E**

By

Carl Albert Fisher



A thesis to be submitted to the Faculty of Graduate Studies and  
Research in partial fulfillment of the requirements for the degree  
of Doctor of Philosophy

Department of Biochemistry

Edmonton, Alberta

Spring 2000



National Library  
of Canada

Acquisitions and  
Bibliographic Services

395 Wellington Street  
Ottawa ON K1A 0N4  
Canada

Bibliothèque nationale  
du Canada

Acquisitions et  
services bibliographiques

395, rue Wellington  
Ottawa ON K1A 0N4  
Canada

*Your file Votre référence*

*Our file Notre référence*

The author has granted a non-exclusive licence allowing the National Library of Canada to reproduce, loan, distribute or sell copies of this thesis in microform, paper or electronic formats.

The author retains ownership of the copyright in this thesis. Neither the thesis nor substantial extracts from it may be printed or otherwise reproduced without the author's permission.

L'auteur a accordé une licence non exclusive permettant à la Bibliothèque nationale du Canada de reproduire, prêter, distribuer ou vendre des copies de cette thèse sous la forme de microfiche/film, de reproduction sur papier ou sur format électronique.

L'auteur conserve la propriété du droit d'auteur qui protège cette thèse. Ni la thèse ni des extraits substantiels de celle-ci ne doivent être imprimés ou autrement reproduits sans son autorisation.

0-612-59958-2

**Canada**



# University of Alberta

## Library Release Form

**Name of Author:** Carl Albert Fisher

**Title of Thesis:** Determination of the Lipid-bound Conformation  
of the N-terminal Domain of Human  
Apolipoprotein E

**Degree:** Doctor of Philosophy

**Year this Degree Granted:** 2000

Permission is hereby granted to the University of Alberta Library to reproduce single copies of this thesis and to lend or sell such copies for private, scholarly, or scientific research purposes only.

The author reserves all other publications and other rights in association with the copyright in the thesis, and except as hereinbefore provided, neither the thesis nor any substantial portion thereof may be printed or otherwise reproduced in any material form whatever without the author's prior written permission.

  
\_\_\_\_\_

55 Struthers St.  
Etobicoke, Ontario  
M8V 1Y2

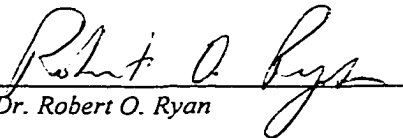
Dec. 15, 1999

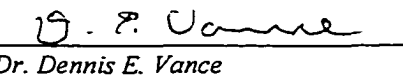
Date

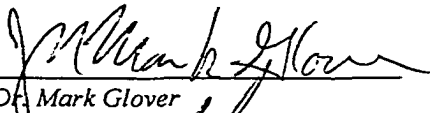
University of Alberta

Faculty of Graduate Studies and Research

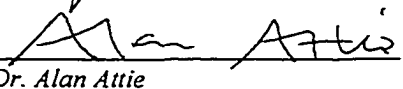
The undersigned certify that they have read, and recommend to the Faculty of Graduate Studies and Research for acceptance, a thesis entitled *Determination of the Lipid-Bound Conformation of the N-Terminal Domain of Human Apolipoprotein E* submitted by *Carl Albert Fisher* in partial fulfillment of the requirements for the degree of *Doctor of Philosophy*.

  
Dr. Robert O. Ryan

  
Dr. Dennis E. Vance

  
Dr. Mark Glover

  
Dr. Gary Lopaschuk

  
Dr. Alan Attie

1 November 1999  
Date Thesis Approved

## Abstract

Apolipoprotein E is an exchangeable apolipoprotein that is critical for lipid trafficking. ApoE contains two independently folding domains, a C-terminal lipid-binding domain and an N-terminal receptor binding domain, the latter of which only expresses this activity when lipid-associated. The lipid-free N-terminal domain of apoE is a globular bundle of four amphipathic  $\alpha$ -helices. Maintenance of secondary structure upon transition to the lipid-bound state suggests a conformational alteration of the helices. Several models have been proposed to predict the lipid-bound conformation of the N-terminal domain. I chose to test the Open Conformation Model which proposes that helices 1 and 2 move away from helices 3 and 4 about a "hinge" located between helices 2 and 3.

Recombinant apoE3(1-183), purified by affinity chromatography, was approximately 22 kDa in size, primarily  $\alpha$ -helical, and had stability properties comparable to the native protein. Functionality was confirmed by its ability to: i) form discoidal complexes with phospholipid, ii) prevent lipid loading-induced lipoprotein aggregation, and iii) bind the low density lipoprotein receptor (LDLr).

The lipid binding affinity of apoE3(1-183) was further characterized by analyzing its ability to compete for binding to a lipoprotein surface. ApoE3(1-183) displaced the resident exchangeable apolipoprotein but was itself displaced

by human apolipoprotein A-I. ApoE-enrichment generated particles that were able to effectively compete with LDL for LDLr binding.

Using Fourier transform infrared spectroscopy, it was then determined that the orientation of apoE3(1-183) helices with respect to the phospholipid acyl chains of discoidal complexes was perpendicular.

To determine the relative positioning of helices with respect to one another, fluorescence resonance energy transfer was employed. Proteins containing a single energy donor (tryptophan (Trp)) located on different helices were created and combined with an excess of a Trp-null mutant to create discs with minimal intermolecular energy transfer. Spectral analysis indicated that there was movement of helices 1, 2 and 4 away from 3 although helices 3 and 4 appeared to reestablish lipid-free like contacts but with an adjacent molecule. A new model was proposed in which helices 1 and 2 move away from 3 and 4, the latter two helices existing in an extended conformation.

## **Table of Contents**

---

<b>Chapter 1: Introduction</b>	<b>1</b>
<b>1.1 Lipoprotein Metabolism</b>	<b>2</b>
1.1.1 Dysfunction	3
i) Type III Hyperlipoproteinemia	3
ii) Familial Hypercholesterolemia	4
1.1.2 LDL Receptor Pathway	4
<b>1.2 Physical Characteristics of ApoE</b>	<b>5</b>
1.2.1 Polymorphism	7
i) Glycosylation	7
ii) Isoforms	7
a) E2	8
b) E4	10
1.2.2 Domains	10
1.2.3 ApoE Structure	12
<b>1.3 Functions of ApoE</b>	<b>14</b>
1.3.1 Lipoprotein Stabilization	14
1.3.2 Cholesterol Efflux	15
1.3.3 Hepatic Lipase Activation	16
1.3.4 Hormone Production	16
1.3.5 Platelet Aggregation	17
1.3.6 Neurology	17
i) Neuronal Plasticity	17
ii) Neurite Outgrowth	18
iii) Alzheimer's Disease	20
a) Amyloid $\beta$	20
b) Tau Protein	22
1.3.7 Receptor Binding	23
i) Interaction with Lipid	
a) Lipid Association	23

b) Lipoprotein Particle Size	26
c) Lipid Composition	29
ii) Heparan Sulfate Interaction	30
iii) Receptor Interaction	30
a) Binding Locus	32
b) LDLr	33
c) LRP	37
d) ApoER2	38
e) VLDLr	38
<b>1.4 Interactions of ApoE With Other Apolipoproteins</b>	<b>39</b>
1.4.1 ApoA	40
1.4.2 ApoB	41
1.4.3 ApoC	42
<b>1.5 Model Systems</b>	<b>44</b>
1.5.1 Peptide Analogs	44
1.5.2 ApoLp-III	47
1.5.3 Mice	48
i) Transgenic Mice	48
ii) Knockout Mice	50
<b>1.6 Specific Aims</b>	<b>51</b>
<b>1.7 Bibliography</b>	<b>53</b>
<b>Chapter 2: ApoE Expression, Characterization and Purification</b>	<b>71</b>
<hr/>	
<b>2.1 Introduction</b>	<b>72</b>
<b>2.2 Materials and Methods</b>	<b>72</b>

Materials	72
Expression Vector Construction	73
Bacterial Expression and Purification of Recombinant ApoE3(1-183)	74
Preparation and Isolation of DMPC Discs	74
Lipoprotein Binding Assay	75
LDL Receptor Binding Assay	75
Circular Dichroism Spectroscopy	75
Electron Microscopy	75
NMR Spectroscopy	76
Electrospray Ionization Mass Spectrometry	76
Analytical Procedures	76
<b>2.3 Results</b>	<b>77</b>
Expression and isolation of rApoE3(1-183)	77
Physical Characterization of rApoE3(1-183)	78
Functional Characterization of rApoE3(1-183)	80
NMR studies of recombinant apoE3(1-183)	83
<b>2.4 Discussion</b>	<b>87</b>
<b>2.5 Bibliography</b>	<b>91</b>
<b>Chapter 3: Relative Lipid Affinity of ApoE3(1-183)</b>	<b>94</b>
<hr/>	
<b>3.1 Introduction</b>	<b>95</b>
<b>3.2 Materials and Methods</b>	<b>95</b>
Isolation of lipoproteins and apolipoproteins	95
Apolipoprotein displacement studies	96
Receptor binding assay	96
<b>3.3 Results and Discussion</b>	<b>96</b>

Displacement of apoLp-III from LDLp by apoE3(1-183)	97
ApoA-I displacement of apoE3(1-183) from the surface of apoE3(1-183)-LDLp	98
Competition binding assays	100
ApoE3(1-183)-modified LDLp binding to the LDL receptor on cultured fibroblasts	101
<b>3.4 Bibliography</b>	<b>103</b>
<b>Chapter 4: The LDL Receptor Active Conformation of ApoE. Helix Organization in N-terminal Domain-phospholipid Disc Particles</b>	<b>105</b>
<hr/>	
<b>4.1 Introduction</b>	<b>106</b>
<b>4.2 Materials and Methods</b>	<b>106</b>
Materials	106
Purification of Apolipoprotein E3 N-terminal Domain	107
Preparation of DMPC:apoE3(1-183) disc complexes	107
Disc particle characterization	107
Analytical ultracentrifugation	107
IR spectroscopy	108
Sample preparation	108
Secondary structure determination	109
Orientation of the secondary structure	109
<b>4.3 Results and Discussion</b>	<b>111</b>
ApoE3(1-183):DMPC disc particles	111
Secondary Structure Characterization	111
Determination of the Orientation of the Helices	113
Model of Association	117
<b>4.4 Bibliography</b>	<b>121</b>



**Chapter 5: Lipid Binding Conformational changes in  
the N-terminal Domain of Human Apolipoprotein E** **124**

---

**5.1 Introduction** **125**

**5.2 Materials and Methods** **126**

Protein Expression and AEDANS Labeling 126

Fluorescence Measurements 127

Intramolecular Distance Calculations 127

Other Methods 128

**5.3 Results** **128**

AEDANS Labeling 128

Distance Measurements in the Lipid-free State 129

Guanidine HCl Titration of AEDANS•apoE3(1-183) 131

Trifluoroethanol Titration of AEDANS•apoE3(1-183) 132

Energy Transfer in AEDANS•apoE3(1-183)-DMPC

Discs and Detergent Micelles 134

**5.4 Discussion** **135**

**5.5 Bibliography** **141**

**Chapter 6: Elucidation of the Lipid-bound Structure  
of N-terminal ApoE by FRET** **143**

---

**6.1 Introduction** **144**

**6.2 Materials and Methods** **144**

Materials 144

Mutagenesis 145

Protein Expression, Purification, and Labeling	145
Phospholipid Disc Complex Formation	145
Fluorescence Measurement	145
Calculation of Donor-acceptor Separation	145
NMR Spectroscopy	146
Other Methods	146
<b>6.3 Results</b>	<b>147</b>
Protein Constructs	147
Maintenance of Structural Integrity	148
Efficient Energy Transfer in Lipid-free Protein	148
Monitoring Gross Conformational Changes with FRET	151
Altered Energy Transfer in Lipid-bound Protein	152
Minimization of Intermolecular Energy Transfer Indicates Movement of Helix 3 away from Helix 4	154
<b>6.4 Discussion</b>	<b>157</b>
<b>6.5 Bibliography</b>	<b>163</b>
<b>Chapter 7: General Discussion and Comment</b>	<b>166</b>
<hr/>	
<b>7.1 Development of an Expression and Purification System for ApoE3(1-183)</b>	<b>167</b>
<b>7.2 Displacement of ApoLp-III from LDLp to Create a Receptor-active Molecule</b>	<b>169</b>
<b>7.3 Determination of the Lipid-bound Orientation of ApoE3(1-183)</b>	<b>171</b>
<b>7.4 Determination of the Lipid-bound Conformation of ApoE3(1-183)</b>	<b>172</b>

<b>7.5 Comments</b>	<b>174</b>
<b>7.6 Bibliography</b>	<b>179</b>

## List of Tables

---

Table 1-1 Human lipoproteins and their characteristics	3
Table 4-1 Secondary structure components in apoE3(1-183)	113
Table 5-1 Parameters for resonance energy transfer in lipid-free and lipid-bound AEDANS labeled apoE3(1-183)	130
Table 5-2 Distance measurements derived from FRET analysis of AEDANS labeled apoE3(1-183) $\pm$ lipid	130
Table 6-1 Mutations introduced into apoE3(1-183) and the wavelength of Trp peak emission	147
Table 6-2 Efficiency of energy transfer for lipid-free and lipid-bound proteins	150
Table 6-3 Parameters of resonance energy transfer	151
Table 6-4 Distance measurements derived from FRET analysis of AEDANS-labeled proteins $\pm$ lipid	153

## List of Figures

---

Figure 1-1	LDLr model	6
Figure 1-2	ApoE3(1-191) amino acid sequence	13
Figure 1-3	ApoE(1-191) X-ray structure	14
Figure 1-4	Models of lipid-bound N-terminal domain of apoE	26
Figure 1-5	LDLr family	34
Figure 1-6	X-ray crystal structure of LDLr module 5	35
Figure 1-7	Sequence of LDLr module 5	36
Figure 2-1	SDS-PAGE of apoE3(1-183) bacterial expression	78
Figure 2-2	Immunoblot of rApoE3(1-183)	78
Figure 2-3	Reversed phase HPLC profile of purified rApoE3(1-183)	79
Figure 2-4	Circular dichroism spectra of rApoE3(1-183)	80
Figure 2-5	Electron micrograph of rApoE3(1-183)/DMPC complexes	81
Figure 2-6	The effect of rApoE3(1-183) on the turbidity of lipid-enriched LDL	82
Figure 2-7	Competition assay for binding to the LDLr	83
Figure 2-8	Effect of pH on ellipticity of rApoE3(1-183)	84
Figure 2-9	2-D HSQC spectrum of rApoE3(1-183)	86

Figure 3-1	Effect of exogenous apoE3(1-183) on the apolipoprotein composition of LDLp	97
Figure 3-2	Effect of exogenous apoA-I on the apolipoprotein composition of apoE3(1-183)-LDLp	99
Figure 3-3	Effect of exogenous apolipoproteins on the protein composition of LDLp	100
Figure 3-4	The ability of natural and hybrid LDLp to compete with <sup>125</sup> I-LDL for binding to cultured human skin fibroblasts	101
Figure 4-1	Basic FTIR setup	109
Figure 4-2	IR spectra of lipid-free and lipid-bound apoE3(1-183)	112
Figure 4-3	IR spectra of apoE3(1-183):DMPC complexes	114
Figure 4-4	Decomposition of the amide I region of spectra of apoE3(1-183):DMPC discs	116
Figure 4-5	Model representation of apoE3(1-183) helix orientation in DMPC disc complexes	118
Figure 5-1	Model depicting a lipid-association induced conformational change of apoE3 N-terminal domain	126
Figure 5-2	Fluorescence emission spectra of apoE3(1-183)	129
Figure 5-3	Effect of GdnHCl on the efficiency of energy transfer in AEDANS-apoE3(1-183)	131
Figure 5-4	Effect of trifluoroethanol on energy transfer in AEDANS-apoE3(1-183)	133

Figure 5-5	Effect of interaction with DMPC on the efficiency of energy transfer in AEDANS-apoE3(1-183)	134
Figure 5-6	Effect of detergent micelle interaction on the efficiency of energy transfer in AEDANS-apoE3(1-183)	136
Figure 6-1	Efficient energy transfer in AEDANS labeled {W39}	149
Figure 6-2	Protein unfolding monitored by FRET	152
Figure 6-3	Minor intermolecular energy transfer in {W39}	153
Figure 6-4	Intermolecular energy transfer reduction on discs containing Trp-null and {W162}	154
Figure 6-5	Emission spectra resulting from intermolecular energy transfer between AEDANS-labeled {Trp-null} and single Trp protein complexed with DMPC	157
Figure 6-6	Model depicting the lipid-bound conformation of the N-terminal domain of apoE	160

## List of Abbreviations

---

A $\beta$	beta amyloid
AD	Alzheimer's disease
Apo	apolipoprotein
ApoLp-III	apolipoprotein III
ATR	attenuated total reflection
CD	circular dichroism
CMC	critical micelle concentration
CNS	central nervous system
DMPC	dimyristoylphosphatidylcholine
DMEM	Dulbecco's modified eagle medium
ECM	extracellular matrix
EGF	epidermal growth factor
FAFA	fatty acid free albumin
FI	fluorescence intensity
FRET	fluorescence resonance energy transfer
FTIR	Fourier transform infrared spectroscopy
GdnHCl	guanidine hydrochloride
GST	glutathione S-transferase
HDL	high density lipoprotein
HDLc	HDL from hypercholesterolemic canines
HDLp	high density lipoprotein
HL	hepatic lipase
HMG CoA	3-hydroxy-3-methylglutaryl coenzyme A
HPLC	high-performance liquid chromatography
HSPG	heparan sulfate proteoglycan
HSQC	heteronuclear single quantum coherence
IAEDANS	N-iodoacetyl-N'-(5-sulfo-1-naphthyl)ethylenediamine
IDL	intermediate density lipoprotein
LBD	ligand binding domain
LDL	low density lipoprotein
LDLr	LDL receptor
LPL	Lipoprotein lipase



LRP	LDLr related protein
LTP	lipid transfer particle
MS	mass spectrometry
MW	molecular weight
NFI	normalized fluorescence intensity
PBS	phosphate buffered saline
PCR	polymerase chain reaction
PHF	paired helical filaments
PVDF	polyvinylidene difluoride
rApoE	recombinant apolipoprotein E
RAP	receptor associated protein
SDS-PAGE	sodium dodecyl sulfate polyacrylamide gel electrophoresis
TFE	trifluoroethanol
VLDL	very low density lipoprotein
WT	wild-type

### **Amino Acid Residues**

#### *Nonpolar*

Alanine	Ala	A
Isoleucine	Ile	I
Leucine	Leu	L
Methionine	Met	M
Phenylalanine	Phe	F
Proline	Pro	P
Tryptophan	Trp	W
Valine	Val	V

#### *Uncharged polar*

Asparagine	Asn	N
Cysteine	Cys	C
Glutamine	Gln	Q

Glycine	Gly	G
Serine	Ser	S
Threonine	Thr	T
Tyrosine	Tyr	Y

*Polar*

Arginine	Arg	R
Aspartate	Asp	D
Glutamate	Glu	E
Histidine	His	H
Lysine	Lys	K

# Chapter 1

## Introduction

---

Apolipoprotein E (apoE), a multi-domain exchangeable apolipoprotein, is one of the most intensely studied proteins due to its anti-atherogenic properties stemming from its critical role in the transport and clearance of lipoprotein remnant particles. Research on this protein has intensified in the last decade following the discovery of its association with amyloid plaques and neurofibrillary tangles, clinical features of Alzheimer's disease, a debilitating neurodegenerative disease which is the most common cause of dementia in humans<sup>1</sup>. While apoE has been implicated in several processes required for normal mammalian development and whole body homeostasis, this thesis will focus on the participation of this protein in lipoprotein metabolism and, more specifically, the conformational alterations that allow it to adopt a lipid-bound, receptor competent state. Based upon my research, I will present a model that depicts the lipid-bound form of apoE and discuss the implications that this may have on the ability of this protein to bind to its primary receptor, the low density lipoprotein receptor.

## **1.1 Lipoprotein metabolism**

In the body, there is a requirement for a readily available supply of lipid that must be tempered by the detrimental effect of having excessive amounts in circulation, namely, the development of atherosclerosis. The hydrophobic character of lipid necessitates a vessel in which it can be transported in the aqueous environment of the plasma. This complex, the lipoprotein, is a mixture of lipids (phospholipid, cholesterol and triacylglycerols), and apolipoproteins. Apolipoproteins that can exist free of lipid in the plasma are referred to as exchangeable, and include the apoA's, apoC's, and apoE. The only nonexchangeable apolipoproteins are apoB-48 and apoB-100. The two primary sources of lipoprotein particles in human plasma are the liver (very low density lipoprotein; VLDL ) and the intestines (chylomicrons; see **Table 1-1**). In the periphery, these particles are lipolysed in the capillaries to form remnants (intermediate density lipoprotein (IDL), low density lipoprotein (LDL) and chylomicron remnants. Remnant lipoprotein particles are then taken up by the

liver, primarily via LDL receptor (LDLr)-mediated endocytosis (discussed below).

**Table 1-1** Human lipoproteins and their characteristics. Adapted from Davis and Vance<sup>2</sup>.

	Chylomicrons	VLDL	IDL	LDL	HDL
Density, g/ml	<0.95	0.95-1.006	1.006-1.019	1.019-1.063	1.063-1.210
Diameter, nm	75-1200	30-80	25-35	18-25	5-12
Composition, % dry weight					
Protein	1-2	10	18	25	33
Triacylglycerol	83	50	31	9	8
Cholesterol + cholesterol ester	8	22	29	45	30
Phospholipid	7	18	22	21	29
Apolipoproteins	A-I, -II B-48 C-I, -II, -III E	B-100 C-I, -II, -III E	B-100 C-I, -II, -III E	B-100	A-I, -II C-I, -II, -III E

### 1.1.1 Dysfunction

Dysfunction in lipoprotein clearance can lead to a number of dyslipidemias including two which are of particular relevance to my thesis: i) type III hyperlipoproteinemia (dysbetalipoproteinemia) and ii) familial hypercholesterolemia.

#### i) Type III Hyperlipoproteinemia

This disease is characterized by an accumulation of remnant particles in circulation, collectively referred to as  $\beta$ VLDL<sup>3</sup>. Some of the clinical features include xanthomas (formed by cholesterol deposits) and premature atherosclerosis. Havel and Kane were the first to suggest that this disease may involve an apolipoprotein, based on elevated levels of an arginine-rich protein in the plasma of affected individuals<sup>4</sup>. It has since been determined that this accumulation is primarily due to the presence of a rare isoform of apoE (apoE2)

that has a diminished receptor binding capacity<sup>5</sup> (discussed in section 1.2.1). Several other naturally occurring variants have been identified that display only moderately defective LDLr binding but do not bind properly to cell surface-associated heparan sulfate proteoglycans (HSPG) and yet possess dominant type III hyperlipoproteinemia<sup>3</sup>. While apoE has been identified as a culprit in the development of this disease, its overt manifestation is dependent on additional genetic and environmental factors<sup>3</sup>.

## **ii) Familial Hypercholesterolemia (FH)**

FH is a disease of autosomal dominant inheritance characterized by an elevated level of LDL cholesterol in plasma, xanthomas, and premature atherosclerosis resulting from the accumulation of coronary atherosclerotic plaques<sup>6</sup>. Determination of the molecular defect that resulted in this disorder led to the discovery of a cell surface receptor, the LDLr, and subsequent research led to the elucidation of the LDL receptor pathway as outlined below. FH results from mutations in the LDLr. The resultant protein alterations may have a direct effect on ligand interaction or the disease may manifest itself due to problems in protein synthesis, transport through the Golgi, clustering in coated pits or recycling in endosomes<sup>7</sup>. Homozygotes can have mutations in both alleles of the same gene or they may have mutations in genes coding for different components of the LDLr pathway. Analysis of these mutations have provided considerable insight into the requirements, at a molecular level, for the normal functioning of this protein.

### **1.1.2 LDL Receptor Pathway**

The biochemical characterization of fibroblast cells isolated from FH homozygotes led Brown and Goldstein to identify a dysfunction in a cell surface protein intimately associated with lipoprotein uptake, the low density lipoprotein receptor (LDLr)<sup>8-10</sup>. The ability to saturate binding, the relative temperature independence, the diminishment of high affinity interaction following protease treatment, and the ability to compete LDL binding with

VLDL, indicated that this process must be receptor mediated<sup>10</sup>. A non-saturable, low affinity binding component was also identified, probably resulting from interaction with components of the extracellular matrix (ECM). Both the high and low affinity binding interactions led to the same degradation of LDL via an endocytic process resulting in lysosomal processing. Additionally, binding was found to be  $\text{Ca}^{2+}$  dependent and resulted in a decrease in the activity of the rate-limiting enzyme in cholesterol biosynthesis, 3-hydroxy-3-methylglutaryl coenzyme A (HMG CoA) reductase. Cells isolated from homozygous hypercholesterolemic individuals lacked this high affinity binding component and, consequently, there was diminished clearance of LDL and no reduction in the activity of HMG CoA reductase<sup>9</sup>. It was concluded that this high affinity binding was the rate-limiting step in the degradation pathway of LDL.

The cell culture system that was developed to analyze defects in receptor binding has become a valuable tool to further our understanding of the consequences that alterations in the molecular components of lipoproteins and recombinant particles have on cell surface receptor interactions.

Fig. 1-1 outlines the LDL receptor pathway as it is known today. Following binding to receptors, clustered in clathrin coated pits, endocytosis commences by a "pinching off" of proximal membrane to create an endosome. As the pH in this compartment decreases, the LDLr dissociates and is recycled to the cell surface for further rounds of lipoprotein internalization. The endosome then fuses with lysosomes where the lipoprotein components are hydrolyzed to their constituents which are transported to areas of storage or utilization.

## **1.2 Physical Characteristics of ApoE**

The importance of apoE in lipid metabolism was first suggested by its relative abundance in VLDL that had been isolated from Type III hyperlipoproteinemic

patients when compared to normal individuals<sup>4</sup>. Since that time, apoE has been extensively studied both physically and functionally.

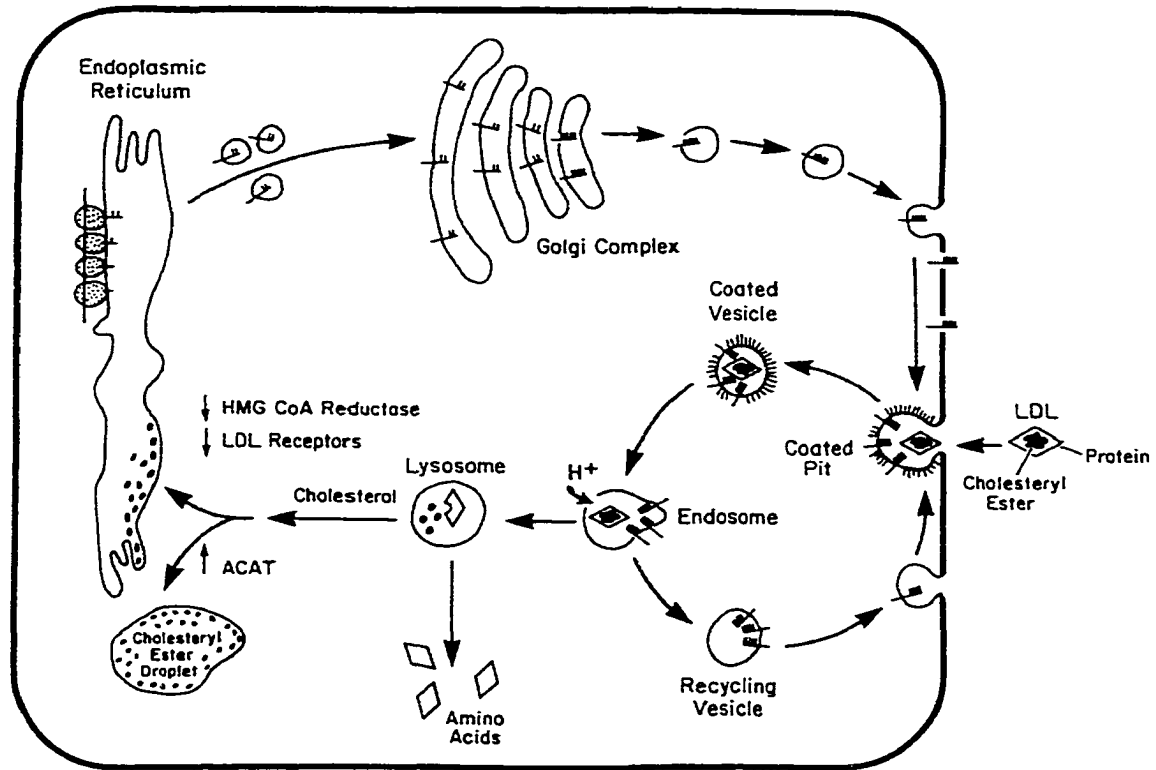


Fig. 1-1 The LDL receptor pathway<sup>6</sup>.

ApoE is synthesized with an 18 amino acid N-terminal signal peptide that undergoes intracellular processing to produce a 37 kDa glycoprotein composed of 299 amino acids<sup>11-13</sup>. The allele for this protein is encoded by a 3.6 kbp, four exon gene at a single locus on the long arm of chromosome 19 (ref.<sup>14,15</sup>). It is expressed in most organs of the body with significant quantities present in liver, brain, spleen, lung, adrenal gland, ovary, kidney and muscle<sup>16</sup>. The liver accounts for up to 3/4 of total production while the brain is second producing approximately one-third that level<sup>16</sup>. The widespread expression of this protein suggests that it may participate in a myriad of activities possibly unrelated to lipid metabolism, in ways that have yet to be fully defined.



## 1.2.1 Polymorphism

### i) Glycosylation

Early on, it was determined that more than one form of apoE existed. Using isoelectric focussing<sup>17,18</sup>, it was discovered that apoE separates into more than one band, suggesting post-translational modification and/or amino acid sequence alteration. To further investigate this phenomenon, apoE isolated from normal and lipidemic subjects was incubated with neuraminidase, a glycosidase which cleaves terminal sialic acid residues, resulting in the disappearance of bands in a 2-D electrophoresis gel<sup>19</sup>. This finding indicated that apoE was modified by the attachment of sugar moieties, later identified as galactose, N-acetylglucosamine, glucosamine, N-acetylgalactosamine, galactosamine, and sialic acid<sup>20</sup>. Amino acid analysis of a single tryptic peptide identified Thr 194 as the sole residue modified by glycosylation and it was determined that this modification was not essential for its expression<sup>21</sup>. Although the role of these sugars has yet to be determined, it was postulated that this moiety may provide some protection to the proteolytically sensitive loop region in which it is contained (see section 1.2.2). Alternatively, glycosylation may affect receptor binding or the preference of apoE for different lipoprotein particles *in vivo*<sup>16,22</sup>.

### ii) Isoforms

Shore and Shore were the first to suggest that there may be some heterogeneity in apoE<sup>23</sup>. During their pioneering isolation and characterization of VLDL proteins, it was determined that there were multiple ion-exchange chromatography peaks corresponding to protein which had similar amino acid composition and electrophoretic mobility. Additionally, serum collected from hyperlipidemic individuals contained VLDL which lacked some proteins while the concentration of a protein rich in arginine (now known as apoE) was elevated. Using 2-D gel electrophoresis, Zannis and Breslow presented evidence that several isoforms of apoE may exist. They speculated that one of these isoforms, having a pattern shifted to a more acidic isoelectric point, may be

the underlying factor in the development of type III hyperlipoproteinemia (i.e. apoE2)<sup>24</sup>. Subsequently, three major isoforms of apoE differing by a single unit of net charge were identified<sup>25</sup> resulting from amino acid differences at positions 112 and/or 158<sup>26</sup>. ApoE3, the most common isoform, has a cysteine at position 112 and an arginine at 158. ApoE2 has Cys at both 112 and 158, while apoE4 has Arg at both of these positions. The allele frequencies in the North American population are  $\epsilon 3 = 0.77\%$ ,  $\epsilon 4 = 0.15\%$ , and  $\epsilon 2 = 0.08\%$ <sup>17</sup>.

a) **ApoE2.** Although apoE2 possesses only 1% of full receptor binding activity, less than 5% of individuals who are homozygous for this allele express type III hyperlipoproteinemia<sup>27</sup>. In order for overt expression of this disease, other genetic or environmental factors such as obesity or a high fat diet, must be present<sup>3</sup>.

It was determined that modification of Cys by cysteamine to a positively charged lysine analog could increase receptor binding of apoE2 approximately 8-fold, suggesting that charge may be a critical factor for receptor interaction<sup>28</sup>. Alterations in binding were believed to be due to modification of residue 158, since modification of Cys 112 in apoE3 did not alter binding. While binding was increased, levels were still considerably below that achieved by apoE3 suggesting that merely introducing a charge at this location was not sufficient to restore full receptor binding. Other features specific to the presence of an Arg may be required.

The binding ability of apoE2 can be increased to the level of full-length apoE3 by digesting apoE2 with thrombin, producing a 10 kDa C-terminal and a 22 kDa N-terminal fragment, and treating the 22 kDa portion with cysteamine<sup>29</sup>. When this protein was complexed with lipid, receptor binding was increased 100-fold, to the level of apoE3, and this binding capacity was maintained even following incubation of complexes with a reducing agent. These results suggest that once the protein has bound lipid and adopted the necessary conformation for receptor binding, the resultant orientation of residues may be more important than the presence of any individual charged group. It may also

indicate that the charge at residue 158 is involved in intramolecular interactions which aid in the adoption of the proper conformation for receptor interaction. Additionally, removal of the C-terminus appears to eliminate some structural constraint that this region imposes on the N-terminus in the full length protein. This inter-domain interaction remains poorly characterized.

The mechanism of faulty receptor binding by apoE2 was clarified by solving the X-ray crystal structure of this isoform and comparing it to that of apoE3<sup>30</sup>. This structure revealed that, in apoE2, a Cys at position 158 eliminates the salt bridge between Arg 158 and Asp 154 that is present in apoE3, resulting in the formation of a new salt bridge between Asp 154 and the previously unbridged Arg 150. As a consequence, the side chain of Arg 150 is no longer available for receptor interaction. Replacement of this residue by Ala reduced binding to 24% of that of apoE3<sup>31</sup>, still considerably greater than the 1% of apoE2, suggesting that an alteration in salt bridges may result in modification of the side chain orientation of basic residues that contribute to the pattern of charge presented for receptor interaction. In regards to the requirement of secondary factors for the development of type III hyperlipoproteinemia, the authors speculated that dietary intake of lipid may alter the size of apoE2-containing lipoproteins, affecting salt bridge formation and, thereby, modulating its receptor binding ability.

A reason for the low levels of LDL cholesterol and high plasma triglyceride levels in type III individuals was suggested by studies of transgenic mice expressing the E2 isoform<sup>32</sup>. When apoE2 was overexpressed in LDLr null (knockout) mice, plasma cholesterol levels were decreased in a concentration dependent manner indicating that this reduction is independent of the LDLr. There was also a positive correlation of apoE2 levels with plasma triglyceride, suggesting an impairment of lipoprotein lipolysis which appeared to be due to diminished concentrations of apoC-II (a co-factor for lipoprotein lipase) on VLDL particles. Thus, while increased plasma cholesterol levels are due to decreased clearance, increased triglyceride levels appear to result from an inhibition of lipolysis by apoE2 preventing the conversion of lipoprotein particles to remnants.

**b) ApoE4.** While apoE3 is considered the “wild-type” form of this protein, apoE4 may actually be the ancestral form since almost all animals have Arg 112/Arg 158 at the homologous positions in their sequence<sup>3</sup>. This isoform is associated with decreased plasma apoE concentrations and elevated levels of plasma cholesterol and LDL. It is, thus, a risk factor for the development of cardiovascular disease<sup>27,33</sup>. A decrease in apoE levels presumably results from the almost two-fold more rapid clearance of apoE4 than apoE3 from circulation which triggers a reduction in LDLr expression leading to reduced LDL clearance<sup>34</sup>. A contributing factor to the excess of plasma components may be its preference for larger lipoprotein particles, such as VLDL and chylomicron remnants, versus the HDL-sized particle preference of apoE3<sup>34,35</sup>. The molecular mechanism of this preference was delineated by Dong et al. who indicated that this preference stemmed from interaction of Arg 61 in the N-terminal domain with Glu 255 in the C-terminus<sup>36</sup>. Comparison of the X-ray structure of apoE3 and apoE4 revealed that, in the latter protein, a salt bridge was present between Glu 109 and Arg 112, causing reorientation of Arg 61, thus making it more accessible for possible interaction with acidic residues in the C-terminus. In 1996, this same group was able to complete this work by naming the critical C-terminal residue. Substitution of acidic amino acids in the C-terminus (244, 245, 255, 256, 370, and 271) by Ala, identified Glu 255 as critical for the VLDL preference of apoE4 and implicated the interaction of this residue with Arg 61<sup>37</sup>. How this interaction is able to dictate lipoprotein particle preference is still unclear.

### **1.2.2 Domains**

ApoE is unique in comparison to other apolipoproteins that have been characterized to date in that it has two independently folding domains with quite distinct properties. The first thorough analysis of the domain structure of apoE was by Wetterau et al. in 1988<sup>38</sup>. By monitoring secondary structure indices during guanidine HCl denaturation, a biphasic curve with transition midpoints at 0.7 and 2.5 M GdnHCl was generated, suggesting that there were

two structurally independent domains having significantly different stabilities. Additionally, proteolysis with a battery of enzymes identified two protease-resistant fragments of approximately 10 and 22 kDa in size and their identity was determined by immunoreactivity and amino acid sequencing to be the C-terminus and N-terminus, respectively. The authors suggested that the relatively low stability and structural flexibility of the C-terminus of apoE may facilitate lipid binding in a similar manner to that of the apo A's and apoC-II.

As is the case with many exchangeable apolipoproteins, apoE forms a multimeric complex in aqueous solution. Using sedimentation velocity analytical ultracentrifugation, Yokoyama et al. were able to determine that the propensity of full-length apoE to self-associate as tetramers is due primarily to the C-terminal domain<sup>39</sup>. In contrast, the isolated N-terminal fragment is monomeric up to 15 mg/ml<sup>40</sup>. Additionally, there was no association of the two major fragments when aliquots of thrombin-digested apoE3 were analyzed by high-performance liquid chromatography (HPLC) suggesting that there are no strong interactions between these two regions of the protein. It was also noted that the C-terminus appears to be more elongated while the N-terminus is globular based upon analysis of the Stokes radius and hydrodynamic parameters.

While the two domains of apoE appear to be structurally independent, there is evidence of an influence of one domain on the other as was suggested by Gianturco and colleagues<sup>41</sup>. Incubation of VLDL with thrombin abolished the ability of these particles to compete with LDL for binding to the surface of fibroblast cells. Immunoreactivity indicated that there was an alteration in the protein structure of apoE on the cell surface. Western blot analysis revealed that thrombin had cleaved some of the protein into 22 and 10 kDa fragments which presumably corresponded to the N- and C-terminal domains of this protein, respectively. Addition of the isolated 10 kDa fragment to thrombin-inactivated VLDL had little effect while addition of the 22 kDa fragment could only restore approximately 50% of the activity. It was concluded that the intact protein, possessing the appropriate conformation, was required for optimal binding and uptake by fibroblast cells. It is somewhat surprising that

the isolated 22 kDa fragment could not restore full receptor binding activity. There may be numerous reasons for this including the possible detrimental effects of the purification process (i.e. delipidation) or a diminished ability to form a complex with these particles. It has since been demonstrated that complexes of the 22 kDa fragment of apoE with phospholipid can effectively compete with LDL for binding to the LDLr<sup>42</sup>.

Further support for inter-domain interaction stems from the finding of a 10-fold enhancement in apoE2 receptor binding following removal of the C-terminal domain<sup>29</sup>, and the lipoprotein preference of apoE3 for HDL-sized particles and apoE4 for VLDL/IDL<sup>35,36</sup>.

### 1.2.3 ApoE Structure

Exchangeable apolipoproteins are composed of amphipathic  $\alpha$ -helices and this characteristic is critical for their functioning. The presence of both hydrophobic and hydrophilic attributes permits the existence of both lipid-free and lipid-bound states, thereby allowing apolipoproteins to act as protein detergents<sup>43</sup>. Secondary structure prediction (e.g. Chou and Fasman<sup>44,45</sup>) and spectroscopic techniques including circular dichroism (CD)<sup>40</sup> and Fourier transform infrared spectroscopy (FTIR)<sup>46</sup>, have indicated that apoE is composed primarily of  $\alpha$ -helices (62%<sup>11</sup>) with some  $\beta$ -strand being present in the predicted C-terminal domain.

Our understanding of the interaction of structure with the functioning of the N-terminus of apoE was greatly aided by the determination of the X-ray crystal structure of the first 191 amino acids of this protein by Wilson and co-workers<sup>47</sup>. The amino acid sequence of the segment crystallized is shown in **Fig. 1-2** as are the helical boundaries: helix 1 residues 24 to 42; helix 1' residues 44 to 53; helix 2 residues 54 to 81; helix 3 residues 87 to 122; and helix 4 residues 130 to 164.



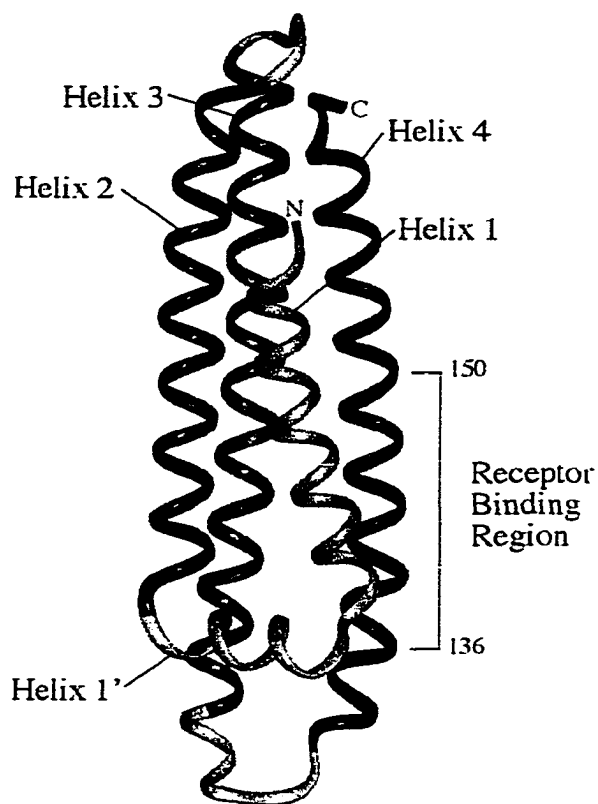


**Fig. 1-3** Ribbon diagram of the X-ray crystal structure of apoE amino acid residues 23-164 (ref.<sup>47</sup>).

It was suggested that the putative class A amphipathic helix between residues 181-192, disordered in the X-ray structure, may adopt a more ordered structure when it is lipid-associated<sup>43</sup>. This latter suggestion is supported by the relative resistance of this region to proteolysis when the N-terminal domain is lipid-bound<sup>48</sup>.

### **1.3 Functions of ApoE**

---

#### **1.3.1 Lipoprotein Stabilization**

Apolipoproteins stabilize lipoprotein particles by shielding hydrophobic patches, thereby assisting in the solubilization of lipids for transport in the plasma. Insight into this aspect of apoE was provided by the analysis of



lipoprotein particles that were produced by insects (*Manduca sexta*) infected with a baculovirus harboring an expression vector for human apoE.<sup>349</sup> Expression of apoE in these insects caused a dramatic alteration of the host's lipoprotein profile. ApoE allowed the resident particles to accommodate more lipid, facilitating the formation of larger particles. Since the resident exchangeable apoprotein was unable to alter the lipoprotein profile in the same manner, the high degree of structural similarity between apolipoprotein III (apoLp-III; see section 1.5.3) and the N-terminus of apoE suggests that the bulk of this lipoprotein remodeling may be mediated by the C-terminus of apoE.

### 1.3.2 Cholesterol Efflux

Apolipoprotein A-I (apoA-I) has been the primary focus of research on the efflux of cholesterol from cells. Another participant in this pathway may be apoE.

Koo et al. identified a subclass of HDL that was produced by cultured mouse peritoneal macrophages that contained apoE as the major apolipoprotein in addition to lesser amounts of apoA-I<sup>50</sup>. More recently, Huang et al. identified a  $\gamma$  migrating (agarose gel) lipoprotein in normal human and murine plasma that contained only apoE as its protein component<sup>51</sup>. This spherical particle was a potent acceptor of fibroblast-derived cholesterol which it subsequently transferred to  $\alpha$ -HDL, similar to the activity of pre- $\beta$ -HDL which contains only apoA-I. This finding suggested that apoE may have potent anti-atherosclerotic activity, not only by clearing lipoprotein particles but also by aiding in cholesterol efflux from cells. Further support for this function came from the demonstration that apoE can mediate the efflux of cholesterol from human monocyte-derived macrophages, decreasing their cholesterol content in the absence of other apolipoproteins or HDL<sup>52</sup>. In normal human plasma, apoE-rich HDL is believed to be present in very small quantities and, thus, the importance of such associations *in vivo* is unclear.

### 1.3.3 Hepatic Lipase Activation

The unique ability of apoE to enhance hepatic lipase (HL)-catalyzed hydrolysis of a phosphatidylethanolamine monolayer led Thuren et al. to propose that phospholipid in an apoE-rich HDL is the preferred substrate of HL, an enzyme

that is implicated in the lipolysis of HDL, IDL and chylomicron remnants<sup>53</sup>. This enhancement was believed to be due to a protein-protein interaction rather than simply a disruption in the lipid surface since enhancement was absent with other exchangeable apolipoproteins. Thuren et al. confirmed this hypothesis and demonstrated that the C-terminus of apoE was primarily responsible for this activity<sup>54</sup>. However, maximal activity could only be achieved with the intact protein suggesting that some domain-domain interaction may be necessary for optimal enhancement. This conclusion was also supported by the isoform-specific effect on HL activity in which apoE4 activated the enzyme to a lesser extent than did apoE3 or apoE2. The mechanism of apoE activation of HL is still under investigation.

#### **1.3.4 Hormone Production**

Through its ability to recruit cholesterol-rich lipoprotein particles to cells, apoE may affect steroidogenesis in endocrine tissues such as testes, ovaries and the adrenals. The importance of apoE was suggested by the comparable level of protein and mRNA in both hepatic and adrenal tissues (0.15-1.2 % of total tissue protein)<sup>55</sup>. Additionally, there is a positive correlation between adrenal gland cholesterol content and apoE mRNA concentration<sup>56</sup>. Williams and colleagues have implicated apoE in the efficient functioning of adrenal cells by their demonstration that this protein forms a “blanket” on the surface of rat adrenal cells<sup>57</sup>. ApoE may be anchored to the surface by heparan sulfate proteoglycans and the authors speculated that this localization may facilitate binding of HDL particles to these cells in preparation for cholesterol transfer or it may facilitate uptake of these particles by activating HL, which can promote the selective uptake of free and esterified cholesterol<sup>58</sup>.

Recently, Swarnakar and co-workers determined that the selective uptake of cholesterol ester (CE) from LDL by murine adrenocortical cells overexpressing apoE was increased 2.5 fold<sup>59</sup>. The authors suggested that cell surface apoE may interact with apoE-enriched lipoprotein particles to enhance

the uptake pathways in a fashion similar to that which appears to be occurring in hepatoma cells (i.e. via enhanced cell surface binding).

### **1.3.5 Platelet Aggregation**

Another potential anti-atherogenic role for apoE was recently suggested by Riddell and colleagues who demonstrated an inhibition of platelet aggregation when platelets were incubated with full-length apoE/DMPC complexes<sup>60</sup>. Lipid-free apolipoprotein did not have any effects on aggregation suggesting that this function is acting through a process that is dependent upon the lipid-associated state, such as receptor interaction. This hypothesis was supported by the inability of cyclohexanedione (which modifies Arg, disrupting receptor binding)-modified apoE-DMPC to prevent aggregation. Platelet aggregation as a key component in the development of atherosclerotic plaques was further implied by the correlation of coronary heart disease with platelet count and aggregability in apparently healthy middle-aged men<sup>61</sup>. A similar correlation was shown between ischemic heart disease and platelet aggregation<sup>62</sup>. The binding of apoE to its receptor may prime the cells to respond to some agonist or other agent resulting in the observed effects.

### **1.3.6 Neurology**

#### **i) Neuronal Plasticity**

After neuronal cell loss or terminal deafferentation in the central nervous system (CNS), a large amount of lipid (including cholesterol) is lost from degenerating membranes and myelin<sup>63</sup>. In response to this, apoE is upregulated in astrocytes (CNS<sup>64</sup>) and macrophages (peripheral nervous system (PNS)<sup>65</sup>), presumably to scavenge lipid and cholesterol for transport to sites of storage for eventual utilization for nerve regeneration<sup>66</sup> and CNS reinnervation<sup>67</sup>. Additionally, the LDLr is present at high concentrations at regenerating peripheral nerve

processes<sup>68</sup> suggesting the importance of the uptake of lipoprotein particles for this process.

Since apoA-I and apoB are not expressed in the CNS of mammals, apoE's role in the nervous system may be significant. Masliah and colleagues demonstrated that apoE knockout mice have a significant loss of synapses and a reduction in the dendritic cytoskeleton in neurons as the mice aged<sup>69</sup>. These mice also had impaired plastic synaptic changes, suggesting a role for this protein in neuronal repair<sup>70</sup>.

Additional support for a role in neuronal plasticity was offered by Corder and co-workers<sup>71</sup> who compared the presence of the apoE4 genotype with development of dementia in HIV-infected subjects. The authors found that, compared to apoE2 or apoE3 subjects, homozygous apoE4 individuals had twice as high an incidence of dementia or peripheral neuropathy, suggesting that the E4 isoform was somehow incompetent to participate in the repair process that may be induced by viral-derived nerve damage.

## ii) Neurite outgrowth

In the peripheral nervous system, apoE is thought to play a role in nerve regeneration<sup>72</sup> although considerable controversy exists.

Nathan et al. found that, in the presence of  $\beta$ -VLDL, apoE3 promoted neurite growth (specifically extension) of rabbit dorsal root ganglia cells while apoE4 inhibited growth<sup>73</sup>. Their data suggested that interaction of apoE-enriched  $\beta$ -VLDL with neurons was receptor-mediated since these effects were not observed when a monoclonal antibody to apoE was added to the media or the protein was reductively methylated. Additionally, lipid-free protein had no effect on neurite branching or extension. The binding and/or internalization of apoE4 or apoE3 may differentially affect the activity of intracellular components or signaling pathways that regulate neuronal growth. This same group presented evidence suggesting that the E4 isoform may promote the depolymerization of microtubules, affecting the cytoskeleton of neuronal cells<sup>74</sup>. Microtubules and their associated proteins play a crucial role in the

development of neurons, therefore, disruption of these structures would be detrimental to neurite growth. The stability of these structures has been linked to neurodegenerative disorders including Alzheimer's disease (AD)<sup>75</sup> and, thus, apoE4 may promote the development of this disease by destabilizing microtubules.

Fagan and colleagues decided to analyze whether the isoform-specific effects seen with  $\beta$ VLDL also applied to apoE-enriched HDL-like particles, these apparently being the size which is normally found within cerebral spinal fluid<sup>76</sup>. Neuronal cells were incubated with recombinant apoE or protein purified from plasma along with plasma- and CNS-derived HDL and the extent of outgrowth was determined. As with larger sized particles, the E3 isoform promoted growth to a greater extent than the E4 isoform. Co-incubation with receptor associated protein (RAP) or anti-LRP IgG indicated that stimulation was via the LDLr related protein (LRP). These results provide further support for the contention that Alzheimer's disease patients having the E4 allele may be more susceptible to neurological abnormalities due to a potential deficiency in the ability of their nervous system to remodel as a consequence of synaptic or dendritic injury requiring replacement or repair.

While the studies of Fagan et al. and others indicated that there were isoform-specific differences in the ability of apoE to stimulate neurite outgrowth, DeMattos and co-workers pointed out that in all of these studies, native CNS HDL, which already contains apoE, required the addition of exogenous apoE to see any effects, making it difficult to delineate the physiologically relevant form of this protein<sup>77</sup>. While the presence of lipid appears to be a requisite, the minimal lipid content requirement was unknown. DeMattos et al. tackled this question by expressing apoE isoforms in a neuronal cell line. Cell derived, minimally lipidated apoE3 stimulated neurite outgrowth while apoE4 did not. The addition of  $\beta$ VLDL actually had an inhibitory effect on growth perhaps through sequestration of secreted apoE, altering its conformation and preventing it from interacting with cells. The authors speculated that apoE may act to direct neurite extension or as a paracrine factor to stimulate neurite outgrowth (perhaps via an unknown receptor).

Isoform-specific effects of apoE are further supported by the work of Raber et al. who induced neuron-specific apoE3 or apoE4 expression in apoE null mice<sup>78</sup>. An isoform-dependent, sex-specific difference in cognition was readily apparent with apoE4-expressing females performing significantly poorer in learning and exploratory behavior than did males or apoE3 expressing females.

ApoE appears to be playing some critical role in the nervous system, although it is not indispensable since apoE knockout mice do not seem to have an obvious problem with nerve repair or development<sup>79</sup> although there was some indication of neurodegeneration as the mice aged<sup>70</sup>.

### iii) Alzheimer's Disease

As noted above, apoE is implicated in nerve maintenance. There is circumstantial evidence that it also participates directly in the pathogenesis of AD. The apoE4 isoform has been shown to be a risk factor for the development of AD (late onset familial, early onset<sup>1,80</sup>, and sporadic<sup>81,82</sup>). In individuals having late onset AD, the apoE4 allele is present at a 2- to 3-fold higher rate than in the general population<sup>81,83</sup>. Up to 80% of all clinically identified cases of AD carry at least one  $\epsilon 4$  allele<sup>84</sup>. Additionally, French centenarians showing no signs of mental illness had an  $\epsilon 4$  allele frequency of less than 5%<sup>85</sup>. Conversely, Corder et al. discovered that the allele frequency of  $\epsilon 2$  was reduced in AD patients (4.5% versus 12.6% for controls) suggesting that this allele may provide some protection from the development of late-onset AD while the  $\epsilon 4$  allele confers considerable risk in a dose-dependent manner<sup>86,87</sup>.

### a) $\beta$ Amyloid

One of the neuropathological hallmarks of Alzheimer's patients is the presence of extracellular senile plaques composed primarily of aggregated  $\beta$  amyloid ( $A\beta$ ) peptide (residues 1-40), a proteolytic digestion fragment of amyloid precursor protein. Interaction of  $A\beta$  and apoE has been implicated by their colocalization in senile plaques although apoE has been found intimately associated with a

wide variety of other cerebral and systemic amyloids<sup>88</sup>. ApoE may be a 'pathological chaperone' whereby it mediates the formation of amyloid, but is not necessarily itself a component of the final fibrils.

While the precise means by which AD and apoE polymorphism are linked is not clear, a number of hypotheses have been proposed. A $\beta$  and delipidated apoE4 may form structures of fibrils that are denser and which form more rapidly than in the presence of other isoforms<sup>89-91</sup>. Additionally, the *in vitro* rate of fibril formation from A $\beta$  is enhanced by apoE with apoE4 being more effective than apoE3<sup>92</sup>.

In contrast to the delipidated protein, lipidated apoE has a different isoform-specific effect<sup>93</sup>. When the A $\beta$  binding affinity of unpurified apoE was compared to that of protein purified by delipidation of lipoprotein complexes, apoE3 bound preferentially (approximately 20-fold greater) to A $\beta$  compared to apoE4. Following purification, there was little apparent isoform-specific difference in binding. Thus, the subtle alterations in protein structure induced by the purification process, may have a pronounced effect on the protein's functioning. A similar lipidation effect on apoE function has been shown for the promotion of neurite extension of primary dorsal root ganglia <sup>73</sup> consistent with a hypothesis that proposes that the enhanced binding of the E3 isoform with A $\beta$  may facilitate clearance of this compound inhibiting the formation of potentially pathological aggregates.

Recently, Winkler et al.<sup>94</sup> demonstrated that A $\beta$ (1-43) was able to inhibit the exogenous apoE-mediated enhancement of  $\beta$ VLDL binding to the surface of fibroblast cells via a non-LDLr mediated process. Cross reactivity of apoE with a polyclonal antibody to A $\beta$  (to A $\beta$ (1-28)) suggested that there might be a common sequence or structural motif. Epitope mapping identified sequences on both apoE (144-148) and A $\beta$  (9-19) that are known to be heparin-binding domains indicating that competition for cell uptake may occur via the HSPG/LDL receptor related protein (LRP) pathway. Some of the isoform-specific effects seen with AD and apoE may be due to the heightened affinity of apoE4 (125%) vs. apoE3 (100%) vs. apoE2 (33%) for heparin and thus, it was

speculated that apoE4 may be better able to compete for binding of  $A\beta$  to cells thereby inhibiting its degradation, resulting in greater probability that it will aggregate. Enhancement of LDLr interaction may mask the inhibitory effects on LRP binding. Thus, binding may be influenced by the receptors that predominate in a given cell type.

While, the relevance of these findings awaits further clarification, there is clearly an isoform-specific effect on the interaction of apoE and  $A\beta$ . It is interesting to note that even though the amino acid residue differences that distinguish apoE isoforms are located in the amino terminal domain, the region identified as responsible for  $A\beta$  interaction is in the C-terminal domain, residues 244-272<sup>95</sup>.

### **b) Tau Protein**

Tau normally binds to and stabilizes microtubules in the brain. Phosphorylated tau has a propensity to form paired helical filaments (PHF) which then lack their microtubule stabilizing capacity. PHF are the primary component of neurofibrillary tangles, abnormal intracellular structures that are a histological hallmark of AD. Whether PHF contribute to AD-associated dementia or are merely a byproduct of this development is unclear. Destabilized microtubules may have a diminished capacity to assist neurons in their functioning/development, thereby limiting their effectiveness in cognitive function.

ApoE3 binds readily to unphosphorylated tau *in vitro* and, thus, may modulate its function and metabolism<sup>96</sup>. This binding may prevent tangle formation by blocking the access of kinases to possible phosphorylation sites or it may inhibit disulfide formation, a prerequisite for helical filament development<sup>96</sup>. It has been hypothesized that, since apoE4 associates only weakly with tau, more rapid phosphorylation is permitted, conferring protease resistance and promoting the formation of helical filaments<sup>96,97</sup>. Conversely, apoE2 may have a protective effect in comparison to apoE3 due to the presence in tau of one or two cysteines (isoform dependent)<sup>98</sup> which are



located in the microtubule binding and putative self-assembly region<sup>99</sup>. If apoE can sequester these residues, the likelihood that PHF will form is diminished. Disulfide bonds might more readily form with apoE2 due to the presence of two Cys rather than just one. The protective effect of apoE2 has been supported by several studies of sporadic and familial late-onset AD<sup>81,100</sup>. Thus, it may not be the case that apoE4 causes AD, but that apoE3 and apoE2 protect against its formation<sup>96</sup>, a hypothesis that was supported by Ohm et al. who, using postmortem analysis of neurohistological developmental stage, determined that neurofibrillary changes increased in parallel with  $\epsilon 4$  gene dose<sup>101</sup>.

It is still unclear precisely how apoE is able to interact with tau protein since apoE is normally degraded in the lysosome following receptor-mediated endocytosis. Some of its effects may occur through a signaling pathway or via another route in which physical interaction is not required<sup>5</sup>.

### **1.3.7 Receptor Binding**

There are several factors that can modulate ligand-receptor interaction between apoE and the LDLr.

#### **i) Interaction with Lipid**

##### **a) Lipid Association**

While the bulk of apoE's lipid binding affinity resides in the C-terminal domain (specifically residues 244-272<sup>36</sup>), the N-terminal domain does bind to lipid and it was determined quite early that at least some lipidation is required in order for receptor binding to occur. Innerarity and Mahley<sup>102</sup> found that apoE-rich lipoproteins (HDLc; cholesterol-rich particles produced by cholesterol feeding of dogs or swine) had a 10-100 fold greater receptor binding activity than did human LDL. This activity was maintained when lipoprotein particles were partially delipidated to form discs while total delipidation abolished all binding activity. This finding suggested that lipid-association induces a conformational change in apoE, thereby permitting receptor interaction.

Innerarity et al. were able to mimic the high affinity binding capability of HDLc using reconstituted complexes composed of DMPC and protein isolated from human plasma by delipidation<sup>103</sup>. These complexes were internalized and degraded comparably to native lipoproteins. It was concluded that phospholipid was able to confer upon apoE the ability to bind the LDLr by altering the conformation of this apolipoprotein in such a manner that it assumed the requisite structure.

There does appear to be a difference in the structure of apoE on discoidal particles versus spherical lipoproteins. Lund-Katz et al. found that apoE on HDLc had approximately 10% less  $\alpha$ -helical content than did protein associated with DMPC discoidal complexes<sup>104</sup>. There may be different, more restrictive structural requirements around the periphery of a disc compared to the surface of a spherical particle, resulting in differing degrees of helix-helix versus helix-lipid interactions. Following introduction of <sup>13</sup>C by reductive methylation of the Lys residues, 1-D NMR indicated a heterogeneity in the Lys microenvironments for DMPC complexes versus HDLc, suggesting significant structural differences.

A structural propensity to adopt an alternate conformation is a characteristic that would be a desirable attribute for any exchangeable apolipoprotein. This conformational flexibility has been studied by several groups. Molecular dynamics simulations recently performed by Prévost and Kocher on the receptor binding domain of apoE suggested that this domain has relatively weak tertiary compactness in comparison to proteins of similar size, as evidenced by a higher incidence of atomic-size cavities<sup>105</sup>. The authors went on to suggest that, in comparison to other globular proteins, N-terminal apoE has molten globule-like properties primarily due to its loose tertiary contacts. A number of other exchangeable apolipoproteins have a similar conformational looseness. Thermal denaturation studies on human apoA-I using scanning calorimetry and circular dichroism indicated that this protein displays several properties that are characteristic of the molten globule state<sup>106</sup>. These include low-cooperativity, non-two-state thermal unfolding, high polypeptide chain mobility, and an  $\alpha$ -helical structure that is only weakly stabilized by tertiary

interactions. Further evidence for conformational plasticity was suggested by spectroscopic analysis of apoLp-III<sup>107</sup>. As the sample pH decreased below 6.5, an enhancement in Tyr fluorescence intensity was noted, indicative of a conformational alteration, without any apparent change in secondary structure. This finding suggested that there was a conformational state intermediate between the native and denatured structure. Additionally, the low accessibility to Tyr of fluorescence quenchers between pH values 5.2 and 7.4 indicated that this intermediate had a compact shape. Under pH conditions in which the intermediate is believed to predominate, DMPC-liposome clearance was significantly more rapid, suggesting that this conformation facilitates protein insertion, and it was concluded that it may represent the most active and metabolically relevant conformation of apoLp-III. The discovery of such an intermediate suggests that such forms may be present in other exchangeable apolipoproteins and may represent a distinct population of molecules that is primed for lipid interaction.

Complexes of apoE with phospholipid are a model of the bioactive state of this protein whose constituents are well defined, allowing the controlled manipulation of some of the factors that affect receptor binding, primarily the protein itself. Additionally, understanding the conformation that the protein adopts on these molecules can further enhance our understanding of its ability to perform its biological activity.

The complexes produced by combining protein with phospholipid are discoidal in shape and it is presumed that, in such a structure, protein is oriented around the periphery (in a relative orientation that is still controversial<sup>46,108</sup>) shielding the acyl chains of the lipid from the aqueous milieu.

Several models have been proposed to reconcile the necessity of the N-terminal domain of apoE to alter its conformation to permit the interaction of its hydrophobic interior with a lipid surface. These models are explained in more detail in a later chapter but will be mentioned here (Fig. 1-4). One of the models that has gained considerable support is the "Open Conformation Model" proposed by Karl Weisgraber to explain the area occupied by the N-terminal domain at an air-water interface<sup>109</sup>. Another model, the "Picket Fence", was

suggested by de Pauw and colleagues following analysis of spectroscopic data and based on geometric considerations<sup>46</sup>. A final model can be envisioned that is analogous to that adopted by an N-terminal deletion mutant of apoA-I presented by Borhani et al.<sup>110</sup>

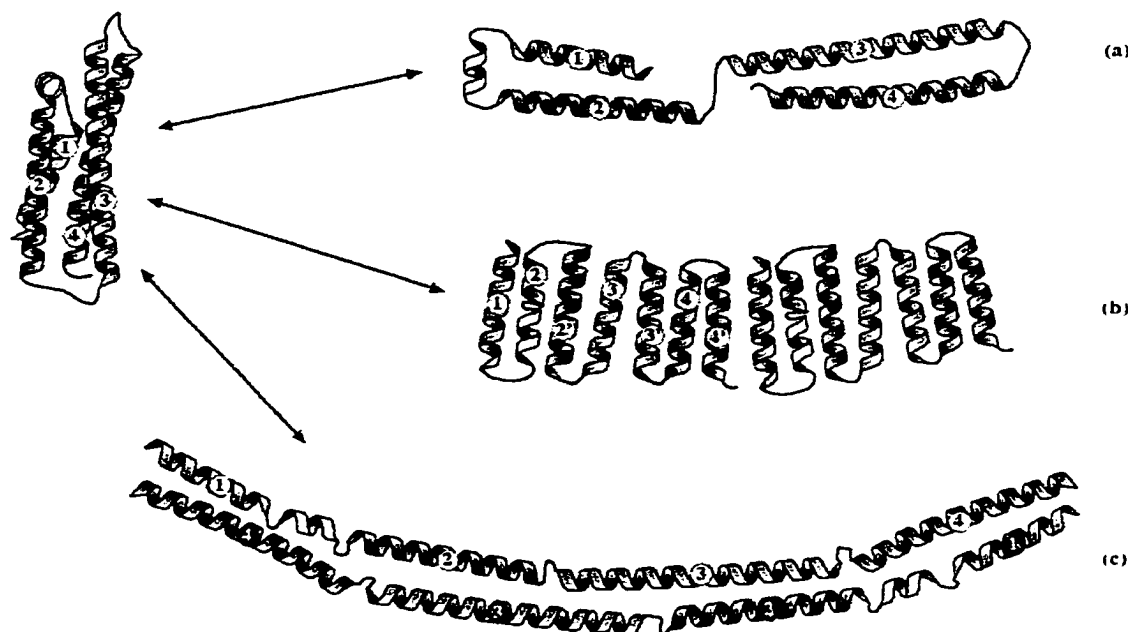


**Fig. 1-4** Models detailing the conformation of lipid-bound N-terminal domain apoE. a) Open Conformation<sup>109</sup>; b) Picket Fence<sup>46</sup>; c) Extended Belt (analogous to ref.<sup>110</sup>).

### b) Lipoprotein Particle Size

This is one of the few instances in which size does seem to matter. Chylomicrons are only cleared in the remnant form and this ability appears to be due to the loss of surface phospholipid<sup>111-113</sup> concomitant with lipoprotein (or hepatic) lipase-mediated lipolysis in the peripheral blood vessels. Lack of a significant change in the apoprotein profile as a result of phospholipid removal suggests that this surface perturbation allows apoE to adopt a receptor-competent conformation.

Binding of apoE to lipid is necessary but is not sufficient to confer receptor binding ability. Linga et al. found that, on LDL, only a small proportion of the apoE present was reactive with the N-terminal domain-

specific antibody 1D7 and, thus, was presumably not in a receptor competent form<sup>114</sup>, suggesting that receptor binding of these particles must occur primarily via apoB-100.

Jonas and colleagues<sup>115</sup> generated recombinant lipoprotein molecules of differing sizes using the cholate dialysis method and altered the sizes of the resultant with the aid of LDL and lecithin:cholesterol acyltransferase (LCAT). It was determined that apolipoproteins E and A-IV had similar abilities to apoA-I to form particles of such small size that a reduction in the number of helices in contact with lipid would be necessary, demonstrating the adaptability of these proteins to conform to surfaces of differing curvature.

The size/curvature of lipoprotein particles also appears to play a role in the ability of apolipoproteins to bind receptors. It was determined that apoB on large VLDL particles was not capable of specific binding to the LDLr on human skin fibroblasts and it was only when apoE was added that these particles exhibited saturable binding<sup>116</sup>. However, on LDL-sized particles, apoB was sufficient for binding to the LDLr suggesting that there is some conformational change induced during lipolysis which may expose particular residues essential for receptor interaction that are masked or not in the right orientation in larger particles. This suggestion was further supported by Bradley et al.<sup>117</sup> who demonstrated that, even though IDL contained 1 mole of apoE per 4 moles of IDL, thrombin did not diminish the binding capacity of this particle. This digestion abolished apoE mediated binding in larger particles, implicating apoB as the primary mediator of receptor binding for these particles. They also determined that there appears to be a switch in the apolipoprotein responsible for binding at VLDL<sub>3</sub> sized particles as VLDL is being catabolized to LDL with an associated surface area reduction. As a consequence, conformational alterations in the associated lipoproteins occur as they attempt to adapt their structure to the changing surface environment, altering their receptor binding ability. While there is a gradual loss of apoE from the lipoprotein surface during this process, the reduction in its receptor binding capability precedes this loss. Such a diminishment could be due to subtle changes in conformation on these particles and/or more pronounced alterations which may involve the gradual

displacement of helices, as is suggested by Ana Jonas and her hypothesized alterations in lipid association as a requisite to forming complexes with smaller discoidal particles<sup>115</sup>. This may be particularly relevant for the N-terminal domain of apoE which has a much lower lipid binding capacity in comparison to the C-terminus.

Sehayek and colleagues lipolysed VLDL particles and measured the rates at which particles were taken up by the LDLr<sup>118</sup>. Lipoprotein lipase-mediated lipolysis of VLDL enhanced its uptake by fibroblasts cells suggesting that the reduction in particle size somehow exposed regions of apoE that were then competent to bind to the receptor. An intriguing finding was that the addition of exogenous apoE to lipolysed particles did not increase lipoprotein uptake to as great an extent as anticipated, suggesting that there was some conformational difference between the exogenous and endogenous protein. Perhaps there is some difference in the manner in which the helices associate with one another when they first interact with lipoprotein particles that is altered as the particle size is diminished.

Granot et al. found that smaller triglyceride-rich lipid emulsion particles (triolein and PC), in the absence of any apoE, were taken up more rapidly by J-744 (murine macrophage-like) cells than larger ones (20-100 fold)<sup>119</sup>. This may have been due to the increased surface area exposed to the cells. The authors suggested that adsorptive endocytosis was the mechanism of uptake of emulsions lacking apoE. When this apolipoprotein was added to these emulsions, VLDL-sized particle uptake was enhanced 4-5-fold while IDL-sized particles were enhanced up to 2-fold. It was estimated that the larger particles bound about ten times more apoE molecules than the smaller (40 vs. 4, respectively). Thus, the enhanced binding of the larger apoE-containing particles may have been due to the presence of a larger number of apoE molecules which may have enabled multivalent receptor binding. Alternatively, the curvature of the lipoprotein particles may have induced a more receptor-competent structure. The increased uptake of larger particles appeared to be due to an increased receptor affinity. It was suggested that receptor-mediated uptake alone could not account for the high rate of lipoprotein uptake at

physiological concentrations and that adsorptive endocytosis may play a significant role.

Earlier work by Mims et al. demonstrated a different relationship, one in which smaller apoE-rich particles were better ligands for the LDLr<sup>120</sup>. Granot et al. noted that differences in the efficiency of particle uptake based on size, when compared to the results of Mims et al., may have been due to their use of triglyceride-PC versus Mims's cholesterol-DMPC complexes and comparisons based on mass rather than particle size as they have done in the Granot study.

Thus, particle size may modulate the mode of uptake of apolipoproteins with receptor interaction dominating for larger particles and non-receptor uptake for smaller particles. Non-receptor pathways may be an important clearance mechanism in the absence of fully functioning apoE such as in hyperlipidemia or in the case of apoE knockout mice.

### **c) Lipid Composition**

The type of lipid present in lipoprotein particles can have a dramatic effect on apolipoprotein activity. The binding affinity of apoE for the particle surface may be influenced by the sphingomyelin and the n-3 fatty acid content of surface phospholipids which can be altered by diet (fish oils versus lard)<sup>121</sup>. Braschi et al. reconstituted lipoprotein particles with apoA-I and various concentrations of triacylglycerol, diacylglycerol, and cholesterol ester with palmitoyl-oleoylphosphatidylcholine (POPC)<sup>122</sup>. The electrophoretic mobility and immunoreactivity of the particles indicated that the lipid constituents affected the protein charge and conformation. These changes were able to modulate the catabolism of lipoproteins with the more positively charged particles being cleared more rapidly from rabbit plasma. It was suggested that the charge and conformation of apoA-I may be intimately related such that conformational alterations vary the complement of charged amino acid side chains that are exposed and available for interaction with other molecules. ApoE, and consequently receptor binding, may be affected by lipid constituents in a similar manner, especially considering the importance of charged residues for receptor binding.

## ii) Heparan Sulfate Interaction

Receptor interaction is believed to be a two step process in which there is an initial binding to cell surface-associated HSPG followed by interaction with proximal receptors.

Mahley and colleagues<sup>123</sup> were able to distinguish between the requirements for heparin and for receptor binding by chemically modifying the positively charged amino acid residues, Lys and Arg. It was determined that reductive methylation of Lys, which maintained its positive charge, did not alter the binding of apoE to heparin but did prevent LDLr binding. Only alterations in positive charge interfered with heparin binding. The heparin-binding regions of apoE have been localized to residues 142-147 and 243-272 by defining the epitopes at which monoclonal antibodies, that were able to inhibit this interaction, bound<sup>124</sup>. The second site is only recognized when it is lipid-free, suggesting that this region participates in lipid interaction, but is not involved directly in receptor binding.

A greater than 4-fold increase in apoE secretion was detected following treatment of apoE overexpressing macrophages with heparinase suggesting that a significant amount of protein may actually be sequestered in the ECM<sup>125</sup>. The authors also showed that cells incubated with phosphatidylcholine vesicles enhanced the release of apoE at 4°C but this enhancement was abolished for proteoglycan-depleted cells. The ECM may also retard protein release via proteolysis which can occur during apoE's residence there. Burgess et al. presented data that suggests that lipid-poor apoE, associated with the ECM, can dissociate from the cell surface upon presentation of and complexation with a lipoprotein particle, enhancing this particle's ability to bind to the LDLr or LRP<sup>126</sup>. Thus, the ECM may harbor a pool of apoE that is available for association with lipoprotein particles.

## iii) Receptor Interaction

One of the primary roles of apoE is as a ligand for binding to cell surface receptors preceding endocytosis. Several receptors have been identified to



which this protein binds with high affinity including LDLr, LRP, apoE receptor 2 and VLDLr.

Pitas, Innerarity and Mahley delineated the means by which HDLc was able to bind to the LDLr with an 80-100 fold greater binding activity than LDL<sup>127</sup>. These authors created discoidal particles containing DMPC and varying amounts of active, full-length or inactivated (diketene-treated to acetoacetylate Lys residues) apoE. They determined that the apoE content was approximately 4 apoE's per disc based on the size and phospholipid/protein ratio of the complexes. The ratio of active to inactive protein was varied based on this number. The authors confirmed that modified and unmodified proteins partitioned into lipid in the ratios in which they were added by [<sup>125</sup>I] labeling apoE and determining the rates of incorporation into discs. When the ability of the complexes to compete for binding to the LDLr was compared, it was determined that the binding affinity was dependent upon the number of active apoE molecules present on discs and as the number of active apoE approached 1, the binding affinity approximated that of LDL. Additionally, at receptor saturation, approximately 4 times the number of LDL particles were bound than HDLc suggesting that HDLc is able to bind 4 receptors per particle. Thus, the higher affinity interaction of apoE-containing particles appears to be due to multiple receptor binding. Analysis of the ability of apoE-enriched spherical lipid microemulsion particles to compete with LDL for binding to the LDLr was confirmed by Funahashi and colleagues to require at least four apoE per particle for optimal binding<sup>128</sup>.

Thus, a critical requirement for high affinity receptor interaction may be the formation of multiple contacts by the same particle. That is, the close spatial association of apoE molecules may allow the binding of up to four LDL receptors per lipoprotein particle, increasing the affinity for the cell surface several fold over that of a single copy or of apoB-100<sup>127</sup>. As important as the structural changes induced by lipid binding may be, providing a platform that allows several copies to be in close enough proximity to permit extensive protein-protein interactions between an individual particle and cell surface receptors may be just as critical.

### **a) Binding Locus**

Mahley and co-workers<sup>129</sup> indicated the importance of charged residues to receptor binding by demonstrating that treatment of apoE with cyclohexanedione abolished all receptor binding activity.

The receptor binding residues of apoE have been isolated to a specific region in the N-terminal domain of apoE. Innerarity et al. demonstrated that a cyanogen bromide digestion fragment encompassing residues 126-218, following conversion of DMPC bilayer micelles to discs, had a binding ability similar to that of LDL<sup>42</sup>. This region was further defined to the area of residues 139-169 by the identification of an antibody (1D7) that bound to this epitope and interfered with receptor binding<sup>130</sup>. Natural mutations in which basic amino acids at positions 142, 145, 146, or 158 were substituted with a neutral residue, possessed greatly reduced receptor binding ability, narrowing this region down even further<sup>16</sup>. It is now commonly accepted that the receptor binding region lies between residues 136 and 150<sup>5</sup> (see Fig. 1-3).

Lalazar and co-workers investigated the contribution of various amino acid residues in the receptor binding region to high affinity receptor interaction<sup>31</sup>. Substitution of basic amino acids in this region by alanine reduced the ability to compete with LDL for binding sites, although no single substitution totally abolished binding, suggesting that the charged residues may act cooperatively in this process. A double mutation replacing a Ser 139 with Arg and Leu 149 with Ala, increased the receptor binding activity by 150% indicating that not all mutations are disruptive to binding. The authors did not speculate on the precise mechanism of this enhancement although one would anticipate that introduction of another positive charge could enhance charge-mediated interactions, while removal of a leucine (which is in close proximity to another (Leu 150)) may alter the orientation of the hydrophilic face of this portion of the helix, affecting the precise charge profile that would be presented. There was no indication of the effect that single mutations of these residues would have. While it is implied that direct ionic interaction with the receptor is disrupted, the authors recognized that there may be intramolecular

salt bridge disruption resulting in a conformational change that diminishes binding.

The region of apoE that is most critical for receptor interactions was further explored by combining C-terminal deletion mutants with DMPC and analyzing receptor binding<sup>131</sup>. Fragment apoE(1-170) had only 1% binding, apoE(1-183) had 85%, while apoE(1-174) was intermediate at 19%. Thus, residues 171-183 appear to be critical for maintaining the primary binding region in a receptor competent orientation.

## **b) LDLr**

Early evidence as to the identity of the ligands for the LDLr was provided by Hofmann and colleagues who demonstrated that overexpression of the LDLr in transgenic mice resulted in a greater than 90% reduction in the plasma levels of both apoE and apoB-100, while apoA-I levels were unaltered<sup>132</sup>.

The LDLr is the progenitor of a large class of integral membrane cell surface receptors which concentrate in clathrin coated pits and mediate the endocytosis of macromolecules. This 839 amino acid protein (Fig. 1-5) is composed of five domains: i) an amino terminal ligand binding domain (LBD) containing 7 Cys-rich repeats (modules) of 40 amino acids in length; ii) an epidermal growth factor (EGF) precursor domain containing 3 cysteine-rich repeats which mediates ligand release in the endosome via a pH-dependent conformational change prior to recycling<sup>133</sup>; iii) an O-linked sugar domain; iv) a transmembrane spanning region; and v) a cytoplasmic tail which contains the sequence NPxY, believed to cause the clustering of these proteins into coated pits.

Determination of the 3-D structure of the whole LDLr has proven difficult due to its large size and its membrane integration. However, there has been success in obtaining structural data on a few of the ligand binding repeats.

Daly et al. presented the NMR solution structures of the first two repeats in the LBD<sup>134,135</sup>. Both structures were quite similar although this was not surprising considering the degree of sequence similarity (40-50%)<sup>136</sup>. The structures were composed of an amino terminal  $\beta$  hairpin followed by a

succession of  $\beta$  turns. The authors noted that many of the acidic side chain residues were clustered on one face of the module. While the importance of  $\text{Ca}^{2+}$  for structural stability was alluded to, this ion was not a component of the structures presented.

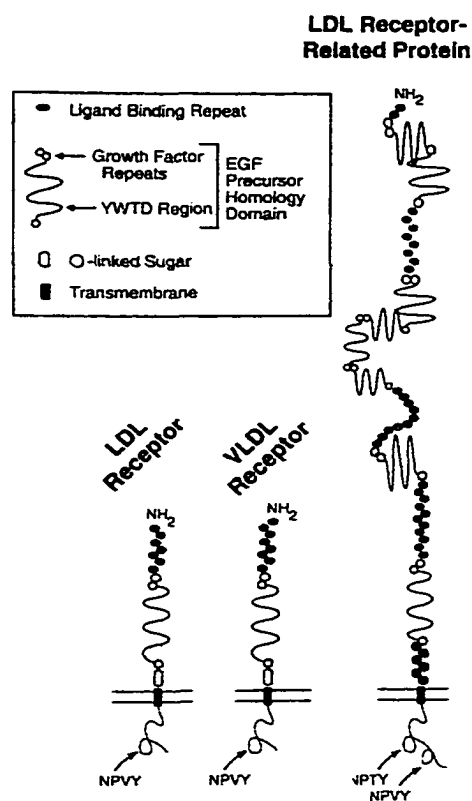


**Fig. 1-5** Members of the LDLr family to which apoE is known to bind *in vivo*. Adapted from Goldstein et al.<sup>6</sup>

All of the cysteine-rich repeats in the LBD can contribute to apoE binding, however, module 5 has been shown to be of seminal importance for the binding of apoE<sup>137</sup>. The major difference between this module and all the others in this domain is the presence of an additional glutamic acid residue at position 207 resulting in a stretch of three negatively charged residues (Asp-Glu-Glu). It was postulated that this concentration of charge may play a pivotal role in apoE interaction.

It had long been assumed that the basic residues in the receptor binding region of apoE participated in a charge-charge interaction with an acidic motif in the ligand binding modules of the LDLr. Publication of the crystal structure of module 5 of the LDLr suggested that this charge-charge interaction may not be quite as paramount as had previously been thought<sup>138</sup>. This structure (Fig. 1-6) revealed that four of the highly conserved acidic residues (3 Asp and a Glu) were buried and, therefore, not available for ligand binding since they were participating in the coordination of a calcium ion, the latter being critical for the adoption the module's proper fold.

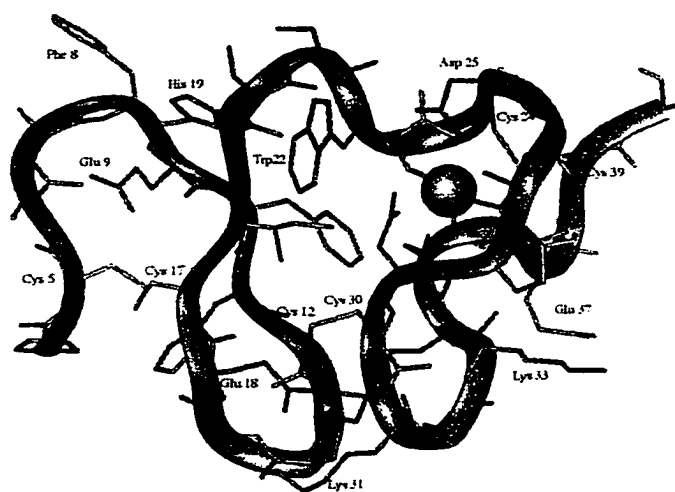


**Fig 1-6** X-ray structure of LDLr module 5. The position of the amino acid side chains on the ribbon backbone are indicated. The Ca<sup>2+</sup> is denoted by a blue sphere.

As a result, the stretch of negative charge that distinguished this module from the others presents only one acidic residue (Glu37) for ligand interaction (see Fig. 1-7). The only other negatively charged residue available in this region is Asp 32. The authors suggested that a hydrophobic concave face may provide a surface for lipoprotein binding. The ligand that interacts with this surface presumably requires a complimentary architecture. Lipid-associated apoE may present such a surface although, if this is the case, it is not certain how the charge density in the region of the fourth helix participates in this process. The



endocytosed and degraded but some appears to escape this fate. Protein release may occur via an increased concentration density at the surface beyond a certain threshold. There may also be a modification in the associated lipid (a requisite for receptor binding) such that there is a conformational alteration that causes its release. It was postulated that apoE secretion could be modulated by maintaining this protein's expression levels while altering that of the LDLr. Thus, in terminally differentiated macrophages (foam cells), reduced receptor expression would presumably maximize apoE secretion, increasing its availability for participation in lipid transport.

### c) LRP

LRP is postulated to be a remnant receptor. Its presence was alluded to by the ability of individuals with homozygous FH or Watanabe-heritable hyperlipidemic rabbits (WHHL) (having no functional LDLr) to clear chylomicron remnant particles<sup>141</sup>. It was determined that LRP (or what may be its homolog in humans) can bind the apoE component of remnants and does not bind apoB-48<sup>142,143</sup>. Expressed most abundantly in liver, brain and lung, this receptor was cloned and sequenced in 1988 by Herz et al.<sup>144</sup>. It is a member of the LDLr family of proteins, is calcium dependent, and contains 4 imperfect copies of the 767 amino acid external domain of the LDLr giving it a total of 31 ligand binding repeats and 22 growth factor homology repeats versus 7 and 3 respectively for LDLr. Presumably the large number of ligand binding modules enables this receptor to bind multiple ligands. In contrast to the LDLr, its expression is not repressed by cholesterol loading. It is believed to be endocytosed in a manner similar to the LDLr since radiolabelled protein was taken up by cells (intact WHHL rabbit livers) along with lipid<sup>141</sup>.

The involvement of this receptor with remnant clearance was further suggested by chemical crosslinking studies which revealed that apoE liposomes were able to bind a protein expressed on the surface of HepG2 cells and human liver membranes that was immunologically identified as LRP<sup>145</sup>. Kowal et al. demonstrated that interaction of apoE-enriched lipoproteins with LRP and the subsequent enhancement of cellular cholesterol ester formation (an indicator of

cholesterol uptake) could be inhibited by a polyclonal antibody directed against the external domain of LRP expressed on the surface of fibroblast cells, demonstrating that this protein may function as an endocytosis-mediating receptor in the clearance of such particles<sup>146</sup>. It is noteworthy that  $\beta$ -VLDL required apoE enrichment before it would bind to LRP even though it already contained significant amounts of apoE. It was suggested that excess apoE may be required to displace the resident, and possibly inhibitory, apoC.

Using a solid phase ligand binding assay, it was demonstrated that LRP can bind all three of the major isoforms of apoE<sup>147</sup>. There was even an isoform-specific effect in which apoE2 bound less readily than apoE3 or apoE4. ApoE2 was approximately 1/2 to 1/3 as effective at LRP binding which is considerably higher than that observed for binding to the LDLr. The authors speculated that the diminished isoform-specific differential in LDLr versus LRP binding may be due to the greater number of potential binding opportunities in the ligand binding region of this much larger receptor. Rabbit  $\beta$ VLDL was able to readily bind LDLr derived from rat liver membranes, but, reminiscent of their previous work, in order for LRP binding to occur, the addition of exogenous apoE was required. The authors suggested that resident apoE is capable of binding but is present in an inactive conformation. This contention was supported by the fact that when apoE was purified from  $\beta$ VLDL and then added back to this lipoprotein, it was able to bind to LRP. *In vivo*, these particles may acquire newly synthesized apoE which are able to adopt a receptor competent conformation upon lipoprotein association.

#### **d) ApoER2**

Human apoE receptor 2 (apoER2) has a domain structure similar to other members of the LDLr family and binds apoE-rich particles with high affinity<sup>148</sup>. LDL had a much lower binding affinity for this protein suggesting significant structural differences in comparison to LDLr. Of note is the predominance of this protein's mRNA in the brain, indicating the potential of a key role in neuronal functioning.



### e) VLDLr

This receptor was identified in 1992 by screening a rabbit heart cDNA library depleted of LDLr mRNA by subtractive hybridization<sup>149</sup>. Northern blot analysis of rabbit tissues indicated that VLDLr was expressed most abundantly in heart, muscle, and adipose tissue with minor amounts in spleen, lung, brain, kidney, adrenal, testis, and small intestine. Only a barely detectable amount was expressed in the liver. This protein bound VLDL,  $\beta$ VLDL, IDL and apoE-containing liposomes, but not LDL, suggesting that it was specific for the apoE component of lipoproteins. There is a high degree of structural similarity to the LDLr with a notable difference being the presence of an additional cysteine-rich repeat in the LBD which the authors hypothesized may inhibit LDL binding.

Using receptor null mice, it has been demonstrated that this receptor, along with apoER2, is an obligate component in cell signaling events that dictate neuronal migration in the brain<sup>150</sup>. The lack of VLDLr manifested itself primarily in the cerebellum while apoER2 affected neocortical development. There also was some degree of coordination and overlap in their functioning. Thus, members of the LDLr family have the capacity to transmit extracellular signals to the interior probably with the aid of adapter or accessory proteins.

## 1.4 Interactions of ApoE With Other Apolipoproteins

---

The association of apoE with other apolipoproteins on the surface of lipoprotein particles can have numerous consequences including steric hindrance, which can prevent other, more productive, interactions from occurring, and competition for lipid, ECM, or receptor binding.

In an aqueous environment, apoE is a stable tetramer although only a small percentage of this protein is in the lipid-free form in plasma<sup>151</sup>. This protein readily associates with lipid surfaces as a monomer as suggested by molecular weight calculations of this protein determined from surface pressure changes at

the air-water interface of an apoE monolayer<sup>39</sup> and on spherical particles by chemical cross-linking of protein complexed with lipid microemulsions<sup>128</sup>.

### 1.4.1 ApoA

ApoA-I is a 28 kDa, 243 amino acid protein that is found primarily associated with HDL and is a mediator of reverse cholesterol transport<sup>152</sup>. It has been speculated that this apolipoprotein can microsolubilize cholesterol and phospholipid from the surface of cells to create new HDL particles which can then acquire plasma lipids and remove them from circulation<sup>153</sup>. It was recently demonstrated *in vitro* that apoA-I can stimulate the production of apoE in foam cell macrophages (more markedly when cholesterol loaded), supporting an additional anti-atherogenic role for this apolipoprotein which differs from its effects on cholesterol removal<sup>154</sup>. ApoA-I may stimulate the release of apoE in and around atherosclerotic lesions so that an increased number of apoE molecules are available to mediate lipoprotein clearance.

The recent determination of the X-ray crystal structure of an N-terminal deletion mutant of this protein has provided some insight into the conformational alternatives for the association of exchangeable apolipoproteins with lipoprotein particles<sup>110</sup>.

A complex of apoE with apoA-II was originally identified in HDL-I (a minor subclass) of normal subjects and d <1.006 fraction of normal and type II hyperlipoproteinemic subjects<sup>155</sup>. In the isolated HDL-I, apoE was present primarily as a dimer with apoA-II with only a minor component being a monomer. HDL-I was able to bind to LDLr in an apoE-dependent manner, and this binding was markedly enhanced when the apoE/apoA-II complex was disrupted by treatment with a reducing agent<sup>156</sup>. This finding indicated that apoE is the primary ligand for LDLr binding of HDL and suggests that apoA-II may mask receptor binding sites on apoE. Chemical reduction, followed by apoA-II dissociation, may induce a conformational alteration in apoE that then permits receptor interaction. It is uncertain whether disulfide reduction occurs

to a significant extent *in vivo*, representing a possible means to modulate receptor binding.

subsequently, Weisgraber and Shinto quantified apoE-containing disulfide-linked dimers present in plasma isolated from subjects homozygous for the apoE3 gene<sup>157</sup>. Immunoblotting indicated that approximately 26% of apoE was homodimer, 28% apoE3-apoA-II heterodimer, and the remainder was monomeric. When complexed with DMPC, the homodimer exhibited a reduced ability to compete with LDL for binding to LDLr and did not appear to have as high a lipid binding affinity as the monomer. Reduced receptor interaction may have been due to the masking of the receptor binding site as a result of disulfide bond formation. The prevalence of these dimers could have a pronounced effect on lipoprotein clearance in apoE3 homozygotes. The reduced lipid binding ability of these multimers may ensure that their prevalence does not adversely affect receptor binding.

### 1.4.2 ApoB

There are primarily two forms of this protein found in normal plasma, apoB-100 and apoB-48. ApoB-100 is a 513 kDa protein of hepatic origin which, in addition to its dependence on lipid for structural stability, presents considerable challenges for the elucidation of its tertiary structure. ApoB is approximately 45%  $\alpha$ -helical, some of which has amphiphilic potential<sup>158</sup>. ApoB-48 contains the amino terminal 48 % of apoB-100 and, in humans, is produced in the intestines where a single copy is incorporated into chylomicrons. ApoB-100 is the primary protein component of VLDL and its derivatives, IDL and LDL. ApoB-100 is the only other apolipoprotein (next to apoE) that is able to bind to the LDLr. Lipoproteins containing apoB-48 are devoid of receptor binding potential and, thus, rely on apoE for their cellular uptake. Binding of apoB-100 to the LDLr requires repeats 3 to 7, in contrast to apoE, which can tolerate deletion of any repeat but the fifth<sup>137</sup>, suggesting a difference in the precise mode (or at least the location) of receptor interaction. Additional differences were suggested by the finding that deletion of the EGF-precursor domain of

LDLr prevents LDL binding but still allows lipoproteins containing apoE to bind<sup>133</sup>.

Young et al. identified a monoclonal antibody isolated from several mammalian species that bound apoB-100, but not apoB-48, with a 1:1 stoichiometry and was able to inhibit the binding, internalization and degradation of LDL by fibroblast cells<sup>159</sup>. This finding suggested that there was only one receptor binding site. However, the epitope may not be at the receptor binding site but, rather, may sterically hinder interaction with this region or it may induce a conformational change. Additionally, in support of the contention that apoB and apoE have differing sites/mechanism of interaction with LDLr, neither apoE nor apoE•DMPC complexes could compete with LDL for binding to this antibody.

The lack of receptor binding by apoB-48 implicates the C-terminal half of apoB-100 in mediating this activity. The primary regions in apoB that are critical for LDLr interaction have been further defined to amino acids 3147-3157 and 3357-3367<sup>160</sup>.

ApoB is dependent upon lipoprotein surface characteristics for binding to the LDLr. Reminiscent of apoE, chemical modification of lysine residues suggested that electrostatic interactions are important for receptor binding<sup>129</sup>. However, this association is probably multifactorial since reductive methylation of lysines, which preserves the positive charge on the  $\epsilon$  amino group, resulted in binding inhibition<sup>161,162</sup>. Additionally, apoB has heparin binding sites which, as with apoE, may facilitate receptor interactions<sup>123</sup>.

As with other apolipoproteins, apoB conformation and, as a consequence, lipoprotein particle surface charge, are modulated by the lipoprotein dynamics. Alterations in particle size result in changes to the ionization state of side chains, modifying the charge profile that is presented to the receptor and, thereby, modulating binding<sup>163</sup>.

### 1.4.3 ApoC

Members of the apolipoprotein C family are exchangeable apoproteins that are a component of all of the commonly found lipoproteins except LDL. These proteins can have a significant influence on the ability of apoE to clear lipoproteins from circulation. ApoC-III has a pronounced inhibitory effect on uptake of apoE-containing synthetic lipid emulsions or chylomicrons from perfused rat livers<sup>164</sup>. The ability of remnant particles to bind receptors is likely enhanced by a decreased ratio of apoC relative to apoE as chylomicrons are lipolysed<sup>165</sup>. Shelburne et al. speculated that the initial excess of apoC relative to apoE on lipoprotein particles may deny their immediate uptake by the liver, prolonging their presence in circulation, allowing removal of lipid components by peripheral tissues prior to hepatic uptake<sup>164</sup>.

The ease of displacement of apoE by apoC-III in the competition binding experiments of Yokoyama and colleagues suggested that there is a relatively small change in the free energy of apoE upon transition from a lipid-associated to a lipid-free state, emphasizing the readily reversible nature of lipoprotein association<sup>39</sup>.

ApoC-II is present on the surface of VLDL and activates lipoprotein lipase. While apoE may not be in a receptor active state on VLDL, one role may be to anchor particles to the cell surface via HSPG, bringing apoC-II into close proximity with the surface-associated lipases resulting in lipid catabolism.

ApoC has also been implicated in the modulation of apoE binding to LRP. Kowal et al. showed that the addition of plasma-derived apoC to ligand blots prevented the binding of apoE-enriched  $\beta$ VLDL to LRP on the surface of LDLr-deficient fibroblast cells<sup>147</sup>. Weisgraber and colleagues found a similar dependence on apoC concentration for LRP binding wherein apoC-I had the most pronounced effect followed by apoC-II. ApoC-III had no effect<sup>166</sup>. Binding inhibition appeared to be primarily due to displacement of apoE from the lipoprotein surface by apoC-I (which had a greater effect than apoC-II) although masking or conformational alterations of apoE could not be ruled out. Some investigators have shown that there can be a reduction in receptor

binding with increasing apoC concentration without apoE displacement<sup>165,167</sup>. In such situations, the N-terminal fragment of apoE may be displaced from the surface while the C-terminus acts as an anchor to retain surface association. ApoC may also prevent the clustering of apoE's, inhibiting the interaction of multiple copies of apoE on the same particle with cell surface receptors, a requisite for high affinity binding.

## 1.5 Model Systems

---

A number of model systems have been utilized to investigate the role that apoE plays in lipid homeostasis and other processes that are critical for normal functioning.

### 1.5.1 Peptide Analogs

There have been a number of attempts to mimic the receptor binding activity of apoE by creating *de novo* designed synthetic peptides. One of the hopes of these endeavors is to create a molecule that is able to simulate the ability of full-length apoE to reduce plasma cholesterol<sup>168</sup>. Such an achievement might also provide insight into the conformational requirements (both secondary and tertiary) of a receptor competent molecule.

One of the first attempts at producing a synthetic peptide of a segment of apoE was by Sparrow et al.<sup>169</sup> To confirm the predicted amphipathic, lipid binding character of the  $\alpha$ -helix in the putative receptor binding region, the authors synthesized four peptides of varying lengths containing the amino acid residues between positions 129 and 169. Following incubation of the peptides with DMPC, only the longest peptide (129-169) formed high MW complexes and demonstrated a significant increase in  $\alpha$ -helical structure as determined by CD (to 56%), indicating that the putative helix formed between residues 130-150 does indeed possess amphipathic properties as demonstrated by its lipid binding activity.

In 1991, Dyer and Curtiss presented data on the ability of a peptide corresponding to residues 141-155 to prevent the binding, internalization (endocytosis) and degradation of  $^{125}\text{I}$ -LDL to the surface of fibroblasts and a human monocytic cell line (THP-1)<sup>170</sup>. The monomer was unable to prevent degradation of LDL by THP-1 cells while a linear tandem repeat of these residues could, although a 200-fold molar excess was required to obtain the same level of inhibition as LDL. However, it was not apparent whether inhibition was due to the free protein or to LDL-associated species since, at the concentrations used, significant lipoprotein binding occurred. Similar results were found with fibroblast cells although the difference between LDL and dimer was only 100-fold. The authors also provided support for the contention that the high affinity binding is due to the presence of multiple copies of the receptor binding region, in close proximity. In comparison to the dimer, a linear trimer of the residues 141-155 was able to prevent fibroblast  $^{125}\text{I}$ -LDL degradation 20 times more potently, further supporting the requirement of multiple copies of the receptor binding region for high affinity binding to occur. This group extended these findings and defined in greater detail some of the structural requirements for the binding of protein to the LDLr<sup>171</sup>. CD analysis indicated that the monomer had essentially random secondary structure while the dimer was 70 %  $\alpha$ -helix, suggesting that this secondary structure may be a critical feature for receptor binding. However, when a longer linear peptide (129-162) was analyzed, despite having helical content similar to the dimer, receptor binding activity was minimal. Thus,  $\alpha$ -helicity alone is not sufficient for binding. The authors also demonstrated that the amino terminal residues Leu-Arg-Lys in the 141-155 peptide were required for receptor interaction. Helical net diagrams suggested that, in the dimer, these residues contribute to the formation of 2 clusters of approximately 6 positive charges on the hydrophilic face of these amphipathic helical segments. A critical density of positive charge(s) over a specific area may be a key component of binding. For these molecules to have a significant amount of receptor binding activity, it was required that there be at least two helices in a sequence or a dimer of one<sup>170,171</sup>. It was proposed that the dimer may be able to bind to LDLr because the two

patches of positive charge mimics the interaction of multiple copies of apoE with the ligand binding domain of a single LDLr protein.

Despite the apparent success of these studies, the receptor binding affinity of synthetic constructs were an order of magnitude lower than that of apoE, suggesting that there are components of this process that have yet to be incorporated.

A peptide containing the amino acid residues from 129-169 of apoE has been demonstrated to have receptor binding activity comparable to that of the full-length protein<sup>172</sup>. The peptide lipophilicity was increased by introducing an acyl or up to 2 alkyl groups onto the N-terminus resulting in these molecules becoming nontransferable and increasing their  $\alpha$ -helicity when lipid-bound. The dialkyl peptide had the most dramatic effect, enhancing the uptake and degradation of <sup>125</sup>I-LDL by human skin fibroblasts approximately 6-fold, suggesting that the affinity of this peptide for the LDLr is in the same range as native apoE.

While the fourth helix of the N-terminal domain has captured most of the attention in the development of synthetic peptides which mimic receptor binding activity, Meredith et al. have explored the highly conserved anionic region in helix 2 between amino acid residues 41 and 60<sup>173-176</sup>. This region encompasses the very end of helix 1 and the beginning of helix 2. Notably, it contains the small helix between residues 44 and 53 (H') whose function so far remains unknown. This group has attempted to constrain these residues to form a stable  $\alpha$ -helix by introducing lactam cross-links between the *i* and *i* + 3 side chains<sup>173,175</sup>. Subsequent cell surface binding appears to be associated with binding to a receptor other than the LDLr, while HSPG was excluded as a participant since heparinase treatment did not diminish binding. LRP is a likely candidate since the addition of RAP (known to associate with LRP *in vivo*) in binding assays was able to block this association. The relevance of this interaction *in vivo* is unclear.



### 1.5.2 ApoLp-III

There is a remarkable structural similarity between the N-terminal fragment of apoE and another exchangeable apolipoprotein, apoLp-III. The X-ray structure of this 166-amino acid insect exchangeable apolipoprotein revealed that it is a globular bundle of five amphipathic  $\alpha$ -helices<sup>177</sup>. Based on structural similarity, it can be proposed that both of these proteins may interact with lipid in a similar manner and, thus, structure/function studies on apoLp-III may provide insight into how the N-terminal domain of apoE is able to adapt to perform its various functions. As with apoE(1-183), bacterial expression results in the accumulation of this protein in the culture media in a relatively pure form, further supporting conformational similarity<sup>178</sup>. It has been proposed to interact with lipids via an opening of the bundle at a “hinge” region, such that helices 1, 2 and 5 move away from helices 3 and 4, exposing its hydrophobic interior for interaction with lipid<sup>179</sup>. To test this hypothesis, Narayanaswami and colleagues created a disulfide bond which tethered the loop regions between helices 1 & 2 and helices 3 & 4 by introducing Cys residues into the loop midpoints<sup>180</sup>. It was anticipated that, as a result of this potential conformational constraint, interaction with lipid surfaces would be prevented. Under oxidizing conditions, the disulfide-bonded apoLp-III was unable to associate with lipoprotein particles while the reduced form bound in a manner comparable to wild-type, suggesting that a conformational opening is essential for interaction with lipoprotein surfaces. However, there was no difference in the ability of wild-type or double mutant protein to transform phospholipid multilamellar vesicles into bilayer disc-like particles under either oxidizing or reducing conditions. This latter finding suggested that there is some fundamental difference in the conformational alterations necessary for interaction of this protein with spherical versus discoidal complexes. Based upon the structural similarity of this protein with that of apoE, it can be postulated that a similar difference in the molecular dynamics of interaction with various lipid surfaces may also occur. Such an apparent conformational flexibility attests to the versatility of the architecture of these proteins.

Further insight into the conformational alterations of apoLp-III upon lipid interaction was provided by the NMR studies of Wang et al. in which complexes of  $^{15}\text{N}$  labeled protein were formed with dodecylphosphocholine (DPC)<sup>181</sup>. It was found that the chemical shift of the hydrophobic residues, Leu and Val, remained unchanged with increasing concentrations of DPC below the critical micellar concentration (CMC), the point at which micelles actually form. At the CMC, there was an abrupt alteration in the chemical shift indicating a significant change in the chemical environment of these residues. This sharp change was suggestive of the swapping of interhelical hydrophobic interactions on the interior of the bundle for helix-lipid interactions, and thus, opening of the helix bundle. In contrast, the hydrophilic residues monitored, Lys and Gly, demonstrated a gradual change in their chemical shift as the lipid concentration increased, remaining at a constant position once the CMC was reached, suggesting that these residues are accessible to DPC prior to lipoprotein complex formation.

As mentioned above, apoLp-III is able to form discoidal particles from phospholipid vesicles. Utilizing specific labeling by the fluorophore pyrene maleimide in combination with fatty acids containing spin labels at different locations along their acyl chains, Sahoo et al. were able to demonstrate that association of apoLp-III with spherical lipoproteins was superficial, explaining the ease with which it is able to dissociate from the surface and adopt its lipid-free state<sup>182</sup>.

### 1.5.3 Mice

As a complement to *in vitro* studies and to supplement the human cases of hyperlipidemia, mouse models have proven to be a powerful tool to test hypotheses that describe the contribution of apoE to mammalian homeostasis.

#### i) Transgenic Mice

To investigate the potential effects that apoE may have on lipoprotein metabolism, Shimano et al. established a line of transgenic mice which overexpressed rat apoE<sup>183</sup>. The authors integrated rat apoE into the mouse

genome and identified a high expressing strain in which the protein was expressed primarily in liver and was associated almost exclusively with plasma lipoproteins. It was noted that, on a normal chow diet, plasma cholesterol and triglyceride levels were reduced by 43% and 68%, respectively, when compared to normal mice. This reduction appeared to be primarily due to a reduction in the amounts of VLDL and LDL, consistent with heightened clearance of TG-rich particles by apoE. Accelerated clearance would result in there being little intermediate particles remaining for conversion to LDL particles. When fed a high cholesterol diet these mice did not develop hypercholesterolemia, in contrast to control mice. Since a high level of cholesterol causes suppression of the expression of the LDLr, clearance of this molecule is probably primarily via remnant receptors such as LRP. One caveat with this study is that rat, rather than human apoE, was used and this form of the protein is more akin to apoE4 than apoE3. Thus, clearance of TG-rich particles might not happen to quite the same extent if human apoE3 was overexpressed. Support for this suggestion was provided by overexpression of human apoE3 in apoE knockout mice<sup>184</sup>. ApoE3-overexpressing mice were hypertriglyceridemic having elevated VLDL and decreased low and high density lipoproteins. ApoE3-enriched VLDL had markedly lower apoC-II concentrations which was reflected in significantly reduced lipoprotein lipase activity. Additionally, there was an increase in hepatic VLDL triglyceride production. Thus, excess apoE can stimulate VLDL triglyceride production and inhibit VLDL lipolysis, emphasizing the importance of maintaining moderate concentrations of plasma apoE for normal lipoprotein metabolism.

Further supporting a role for apoE in lipoprotein metabolism, transgenic mice were created which expressed a receptor binding deficient form of the human protein (apoE(Arg112, Cys142))<sup>185</sup>. Mutant apoE was found associated primarily with  $\alpha$  migrating lipoproteins (HDL<sub>1</sub>) which appeared to retard the clearance of these molecules. When fed a high fat diet, apoE associated primarily with apoB-containing lipoproteins leading to significantly increased plasma and VLDL cholesterol levels. These studies highlight the importance of apoE for the metabolism of both HDL<sub>1</sub> and VLDL sized particles.

Human apoE3 has a characteristic preference for lipoprotein particles which can differ substantially from proteins which are highly similar such as mouse apoE (70 % sequence identity). Sullivan et al. used gene replacement to substitute the mouse apoE gene with that of the human and analyzed differences in lipoprotein preference and plasma lipid levels<sup>186</sup>. In mice, apoE is normally associated with HDL sized particles. In human apoE3 expressing mice (3/3), apoE distribution was shifted from HDL to larger particles and there was a decrease in  $\beta$ -migrating particles and those containing apoA-I. When mice were fed a high fat diet, 3/3 mice had a five-fold increase in total cholesterol versus 1.5-fold for wild-type. ApoE replacement mice had a 13-fold larger atherosclerotic plaque size after 3 months. It was postulated that these differences may have been due to slight differences between the mouse and human LDLr although there is a high degree of homology in the receptor binding region suggesting that differences may be due to regions outside of this area. There also may be differences in the interaction with HSPG which may have a different composition in mice. Finally, there may be altered interactions with other proteins such as hepatic lipase. These findings emphasize the importance of a fully functioning apoE for lipoprotein clearance and lipid homeostasis as well as species-specific differences in lipoprotein metabolism.

## ii) Knockout Mice

A very informative way of determining the importance of a protein in cellular development and whole-organism homeostasis is to create a laboratory animal that does not express this protein. A number of groups have created apoE null mice and have been able to gain insights into the role that apoE may be playing. Zhang et al. disrupted the mouse apoE gene and found that the resultant mice appeared physically and behaviorally normal<sup>79</sup>. There was, however, a total plasma cholesterol level 5 times that of wild-type litter mates<sup>187</sup>. HDL cholesterol was 45% that of normal, while triglyceride levels were 68% higher. These trends paralleled those found in human patients with apoE deficiency. It was suggested that the reduction in HDL cholesterol may have been due to the sequestration of apoA-I (along with apoA-IV) by VLDL and IDL sized particles

leaving less apoA-I available for creation and maintenance of HDL particles. There was a shift in lipoprotein distribution levels away from the normally predominant HDL towards larger particles which floated in the LDL or VLDL range. Such an alteration suggests that apoE may not only aid the solubilization of lipoproteins, but also participates in their remodeling. The authors also examined the apolipoprotein composition of lipoproteins in the apoE null mice. Most significant was the great increase in the ratio of apoB-48 to apoB-100 from 1:1 to 20:1. This finding emphasizes the importance of apoE in the clearance of chylomicron remnants which are dependent upon apoE for receptor binding. Histological analysis of the homozygotes revealed fatty streaks in the aorta and foam cell deposits were noticed in this area in 5-month-old mice. Lesions progressed with age until near occlusion of this area in an 8-month-old female. The presence of preatherosclerotic lesions were enough for the authors to conclude that the lack of apoE is sufficient for atherosclerosis to be initiated.

## **1.6 Specific Aims**

---

ApoE is an exchangeable apolipoprotein that plays a key role in lipoprotein metabolism. The primary contribution apoE makes to this process is the ability to bind to cell surface receptors, and, thus, promote the clearance of lipoprotein particles from circulation. While apoE is a highly soluble protein, an obligate requirement of its receptor binding activity is lipid association, suggesting that a significant structural reorganization must occur prior to the adoption of this bioactive state. Elucidation of the lipid-bound structure of apoE, particularly the amino terminal domain in which the receptor binding potential resides, should provide insight into the repertoire of structures that exchangeable apolipoproteins are capable of adopting and delineate the molecular profile that is presented by the solvent exposed face for receptor interaction.

The steps taken to achieve the objectives outlined above are described in the chapters of this thesis as noted below:

1. Designed a bacterial expression system for the N-terminal domain of apoE and developed a purification protocol. Protein was subsequently characterized both physically and functionally to confirm that its properties were native-like and to establish its suitability for more detailed structural studies.
2. Determined the relative lipid affinity of apoE in comparison to apoA-I and apoLp-III on the surface of spherical lipoprotein particles and developed a receptor binding competent spherical lipoprotein particle containing recombinant protein.
3. Used Fourier transform infrared spectroscopy to determine the orientation of the helices of the N-terminal domain of apoE in relation to the acyl chains of phospholipid when present around the periphery of discoidal particles.
4. Established the suitability of the spectroscopic technique, fluorescence resonance energy transfer (FRET), for monitoring the conformational alterations of the N-terminal domain of apoE upon adoption of the lipid-bound, receptor competent state.
5. Refined FRET analysis by producing mutants containing single energy donors located on different helices and minimized the potential for intermolecular energy transfer. Mapped the relative position of helices in the lipid-associated protein and presented a model based on this data.

## 1.7 Bibliography

---

1. Okuizumi, K., Onodera, O., Tanaka, H., Kobayashi, H., Tsuji, S., Takahashi, H., Oyanagi, K., Seki, K., Tanaka, M., Naruse, S., Miyatake, T., Mizusawa, H. & Kanazawa, I. ApoE- $\epsilon$ 4 and early onset Alzheimer's. *Nature Genet.* **7**, 10-11 (1994).
2. Davis, R.A. & Vance, J.E. Structure, assembly and secretion of lipoproteins. in *Biochemistry of lipids, lipoproteins and membranes*, Vol. 31 (eds. Vance, D.E. & Vance, J.) 473-493 (Elsevier Sci. B.V., Amsterdam, 1996).
3. Mahley, R.W. & Rall, S.C.J. Type III hyperlipoproteinemia (Dysbetalipoproteinemia): the role of apolipoprotein E in normal and abnormal lipoprotein metabolism. in *The metabolic and molecular bases of inherited disease*, Vol. 2 (eds. Scriver, C.R., Beaudet, A.L., Sly, W.S. & Valle, D.) 1953-1980 (McGraw-Hill, Inc., New York, 1995).
4. Havel, R.J. & Kane, J.P. Primary dysbetalipoproteinemia: predominance of a specific apoprotein species in triglyceride-rich lipoproteins. *Proc. Natl. Acad. Sci. USA* **70**, 2015-2019 (1973).
5. Mahley, R.W. & Huang, Y. Apolipoprotein E: from atherosclerosis to Alzheimer's disease and beyond. *Current Opinion in Lipidology* **10**, 207-217 (1999).
6. Goldstein, J.L., Hobbs, H.H. & Brown, M.S. Familial hypercholesterolemia. in *The metabolic and molecular bases of inherited disease*, Vol. 2 (eds. Scriver, C.R., Beaudet, A.L., Sly, W.S. & Valle, D.) 1981-2030 (McGraw-Hill, Inc., New York, 1995).
7. Hobbs, H.H., Russell, D.W., Brown, M.S. & Goldstein, J.L. The LDL receptor locus and familial hypercholesterolemia: mutational analysis of a membrane protein. *Ann. Rev. Genet.* **24**, 133-170 (1990).
8. Brown, M.S. & Goldstein, J.L. A receptor-mediated pathway for cholesterol homeostasis. *Science* **232**, 34 (1986).
9. Brown, M.S. & Goldstein, J.L. Familial hypercholesterolemia: defective binding of lipoproteins to cultured fibroblasts associated with impaired regulation of 3-hydroxy-3-methylglutaryl coenzyme A reductase activity. *Proc. Nat. Acad. Sci. USA* **71**, 788-792 (1974).
10. Goldstein, J.L. & Brown, M.S. Binding and degradation of low density lipoproteins by cultured human fibroblasts. *J. Biol. Chem.* **249**, 5153-5162 (1974).
11. Rall, S.C.J., Weisgraber, K.H. & Mahley, R.W. Human apolipoprotein E. The complete amino acid sequence. *J. Biol. Chem.* **257**, 4171-4178 (1982).

12. McLean, J.W., Elshourbagy, N.A., Chang, D.J., Mahley, R.W. & Taylor, J.M. Human apolipoprotein E mRNA. cDNA cloning and nucleotide sequencing of a new variant. *J. Biol. Chem.* **259**, 6498-6504 (1984).
13. Zannis, V.I., McPherson, J., Goldberger, G., Karathanasis, S.K. & Breslow, J.L. Synthesis, intracellular processing, and signal peptide of human apolipoprotein E. *J. Biol. Chem.* **259**, 5495-5499 (1984).
14. Olaisen, B., Teisberg, P. & Gedde-Dahl, T.J. The locus for apolipoprotein E (apoE) is linked to the complement component C3 (C3) locus on chromosome 19 in man. *Hum. Genet.* **62**, 233-236 (1982).
15. Paik, Y., Chang, D.J., Reardon, C.A., Davies, G.E., Mahley, R.W. & Taylor, J.M. Nucleotide sequence and structure of the human apolipoprotein E gene. *Proc. Natl. Acad. Sci. USA* **82**, 3445-3449 (1985).
16. Mahley, R.W. Apolipoprotein E: cholesterol transport protein with expanding role in cell biology. *Science* **240**, 622-630 (1988).
17. Utermann, U., Langenbeck, U., Beisiegel, U. & Weber, W. Genetics of the apolipoprotein E system in man. *Am. J. Hum. Genet.* **32**, 339- (1980).
18. Utermann, A., Steinmetz, A. & Weber, W. Genetic control of human apolipoprotein E polymorphism: comparison of one- and two-dimensional techniques of isoprotein analysis. *Hum. Genet.* **60**, 344 (1982).
19. Zannis, V.I. & Breslow, J.L. Human very low density lipoprotein apolipoprotein E isoprotein polymorphism is explained by genetic variation and posttranslational modification. *Biochemistry* **20**, 1033-1041 (1981).
20. Jain, R.S. & Quarfordt, S.H. The carbohydrate content of apolipoprotein E from human very low density lipoprotein. *Life Sci.* **25**, 1315-1323 (1979).
21. Wernette-Hammond, M.E., Lauer, S.J., Corsini, A., Walker, D., Taylor, J.M. & Rall, S.C., Jr. Glycosylation of human apolipoprotein E. The carbohydrate attachment site is threonine 194. *J. Biol. Chem.* **264**, 9094-9101 (1989).
22. Ji, Z.-S., Fazio, S. & Mahley, R.W. Variable heparan sulfate proteoglycan binding of apolipoprotein E variants may modulate the expression of type III hyperlipoproteinemia. *J. Biol. Chem.* **269**, 13421-13428 (1994).
23. Shore, V.G. & Shore, B. Heterogeneity of human plasma very low density lipoproteins. Separation of species differing in protein components. *Biochemistry* **12**, 502-507 (1973).



24. Zannis, V.I. & Breslow, J.L. Characterization of a unique human apolipoprotein E variant associated with type III hyperlipoproteinemia. *J. Biol. Chem.* **255**, 1759-1762 (1980).
25. Utermann, G., Pruin, N. & Steinmetz, A. Apolipoprotein E polymorphism in health and disease. *Clin. Genet.* **15**, 37-62 (1982).
26. Weisgraber, K.H., Rall, S.C.J. & Mahley, R.W. Human E apoprotein heterogeneity. Cysteine-arginine interchanges in the amino acid sequence of the apo-E isoforms. *J. Biol. Chem.* **256**(1981).
27. Davignon, J., Gregg, R.E. & Sing, C.F. Apolipoprotein E polymorphism and atherosclerosis. *Arteriosclerosis* **8**, 1-21 (1988).
28. Weisgraber, K.H., Innerarity, T.L. & Mahley, R.W. Abnormal lipoprotein receptor-binding activity of the human E apoprotein due to cysteine-arginine interchange at a single site. *J. Biol. Chem.* **257**, 2518-2521 (1982).
29. Innerarity, T.L., Weisgraber, K.H., Arnold, K.S., Rall, S.C.J. & Mahley, R.O. Normalization of receptor binding of apolipoprotein E3: evidence for modulation of the binding site conformation. *J. Biol. Chem.* **259**, 7261-7267 (1984).
30. Dong, L.M., Parkin, S., Trakhanov, S.D., Rupp, B., Simmons, T., Arnold, K.S., Newhouse, Y.M., Innerarity, T.L. & Weisgraber, K.H. Novel mechanism for defective receptor binding of apolipoprotein E2 in type III hyperlipoproteinemia. *Nature Struct. Biol.* **3**, 718-722 (1996).
31. Lalazar, A., Weisgraber, K.H., Rall, S.C., Jr, Giladi, H., Innerarity, T.L., Levanon, A.Z., Boyles, J.K., Amit, B., Gorecki, M. & Mahley, R.W. Site-specific mutagenesis of human apolipoprotein E. Receptor binding activity of variants with single amino acid substitutions. *J. Biol. Chem.* **263**, 3542-3545 (1988).
32. Huang, Y., Liu, X.Q., Rall, S.C.J. & Mahley, R.W. Apolipoprotein E2 reduces the low density lipoprotein level in transgenic mice by impairing lipoprotein lipase-mediated lipolysis of triglyceride-rich lipoproteins. *J. Biol. Chem.* **273**, 17483-17490 (1998).
33. Wilson, P.W.F. Relation of high-density lipoprotein subfractions and apolipoprotein E isoforms to coronary disease. *Clin. Chem.* **41**, 165-169 (1995).
34. Gregg, R.E., Zech, L.A., Schaefer, E.J., Stark, D., Wilson, D. & Brewer, H.B.J. Abnormal in vivo metabolism of apolipoprotein E4 in humans. *J. Clin. Invest.* **78**, 815-821 (1986).

35. Weisgraber, K.H. Apolipoprotein E distribution among human plasma lipoproteins: role of the cysteine-arginine interchange at residue 112. *J. Lipid Res.* **31**, 1503-1511 (1990).
36. Dong, L.M., Wilson, C., Wardell, M.R., Simmons, T., Mahley, R.W., Weisgraber, K.H. & Agard, D.A. Human apolipoprotein E. Role of arginine 61 in mediating the lipoprotein preferences of the E3 and E4 isoforms. *J. Biol. Chem.* **269**, 22358-22365 (1994).
37. Dong, L.M. & Weisgraber, K.H. Human apolipoprotein E4 domain interaction. Arginine 61 and glutamic acid 255 interact to direct the preference for very low density lipoproteins. *J. Biol. Chem.* **271**, 19053-19057 (1996).
38. Wetterau, J.R., Aggerbeck, L.P., Rall, S.C., Jr. & Weisgraber, K.H. Human apolipoprotein E3 in aqueous solution: I. Evidence for two structural domains. *J. Biol. Chem.* **263**, 6240-6248 (1988).
39. Yokoyama, S., Kawai, Y., Tajima, S. & Yamamoto, A. Behavior of human apolipoprotein E in aqueous solutions and at interfaces. *J. Biol. Chem.* **260**, 16375-16382 (1985).
40. Aggerbeck, L.P., Wetterau, J.R., Weisgraber, K.H., Wu, C.C. & Lindgren, F.T. Human apolipoprotein E3 in aqueous solution: II. Properties of the amino- and carboxyl-terminal domains. *J. Biol. Chem.* **263**, 6249-6258 (1988).
41. Gianturco, S.H., Gotto, A.M.J., Hwang, S.-H.C., Karlin, J.B., Lin, A.H.Y., Prasad, S.C. & Bradley, W.A. Apolipoprotein E mediates uptake of Sf 100-400 hypertriglyceridemic very low density lipoproteins by the low density lipoprotein receptor pathway in normal human fibroblasts. *J. Biol. Chem.* **258**, 4526-4533 (1983).
42. Innerarity, T.L., Friedlander, E.J., Rall Jr., S.C., Weisgraber, K.H. & Mahley, R.W. The receptor-binding domain of human apolipoprotein E: Binding of apolipoprotein E fragments. *J. Biol. Chem.* **258**, 12341-12347 (1983).
43. Segrest, J.P., Jones, M.K., De Loof, H., Brouillette, C.G., Venkatachalapathi, Y.V. & Anantharamaiah, G.M. The amphipathic helix in the exchangeable apolipoprotein: a review of secondary structure and function. *J. Lipid Res.* **33**, 141-166 (1992).
44. Chou, P.Y. & Fasman, G.D. Prediction of protein conformation. *Biochemistry* **13**, 222-245 (1974).
45. Chou, P.Y. & Fasman, G.D. Conformational parameters for amino acids in helical, beta-sheet, and random coil regions calculated from proteins. *Biochemistry* **13**, 211-222 (1974).

46. De Pauw, M., Vanloo, B., Weisgraber, K. & Rosseneu, M. Comparison of lipid-binding and lecithin:cholesterol acyltransferase activation of the amino- and carboxyl-terminal domains of human apolipoprotein E3. *Biochemistry* **34**, 10953-10960 (1995).
47. Wilson, C., Wardell, M.R., Weisgraber, K.H., Mahley, R.W. & Agard, D.A. Three-dimensional structure of the LDL receptor-binding domain of human apolipoprotein E. *Science* **252**, 1817-1822 (1991).
48. Rall, S.C., Jr, Weisgraber, K.H. & Mahley, R.W. Isolation and characterization of apolipoprotein E. *Methods in Enzymology* **128**, 273-287 (1986).
49. Gretch, D.G., Sturley, S.L. & Antie, A.D. Human apolipoprotein E mediates processive buoyant lipoprotein formation in insect larvae. *Biochemistry* **34**, 545-552 (1995).
50. Koo, C., Innerarity, T.L. & Mahley, R.W. Obligatory role of cholesterol and apolipoprotein E in the formation of large cholesterol-enriched and receptor-active high density lipoproteins. *J. Biol. Chem.* **260**, 11934-11943 (1985).
51. Huang, Y., Von Eckardstein, A., Wu, S., Maeda, N. & Assmann, G. A plasma lipoprotein containing only apolipoprotein E and with  $\gamma$  mobility on electrophoresis releases cholesterol from cells. *Proc. Natl. Acad. Sci. USA* **91**, 1834-1838 (1994).
52. Zhang, W.-Y., Gaynor, P.M. & Kruth, H.S. Apolipoprotein E produced by human monocyte-derived macrophages mediates cholesterol efflux that occurs in the absence of added cholesterol acceptors. *J. Biol. Chem.* **271**, 28641-28646 (1996).
53. Thuren, T., Wilcox, R.W., Sisson, P. & Waite, M. Hepatic lipase hydrolysis of lipid monolayers: regulation by apolipoproteins. *J. Biol. Chem.* **266**, 84853-84861 (1991).
54. Thuren, T., Weisgraber, K.H., Sisson, P. & Waite, M. Role of apolipoprotein E in hepatic lipase catalyzed hydrolysis of phospholipid in high-density lipoproteins. *Biochemistry* **31**, 2332-2338 (1992).
55. Blue, M.-L., Williams, D.L., Zucker, S., Khan, S.A. & Blum, C.B. Apolipoprotein E synthesis in human kidney, adrenal gland, and liver. *Proc. Natl. Acad. Sci. USA* **80**, 283-287 (1983).
56. Prack, M.M., Nicosia, M., Williams, D.L. & Gwynne, J. Relationship between apolipoprotein E mRNA expression and tissue cholesterol content in rat adrenal gland. *J. Lipid Res.* **32**, 1611-1618 (1991).

57. Williams, D.L., Wong, J.S., Wissig, S.L. & Hamilton, R.L. Cell surface "blanket" of apolipoprotein E on rat adrenocortical cells. *J. Lipid Res.* **36**, 745-758 (1995).
58. Bamberger, M., Glick, J.M. & Rothblat, G.H. Hepatic lipase stimulates the uptake of high density lipoprotein cholesterol by hepatoma cells. *J. Lipid Res.* **24**, 869-876 (1983).
59. Swarnakar, S., Reyland, M.E., Deng, J., Azhar, S. & Williams, D.L. Selective uptake of low density lipoprotein-cholesteryl ester is enhanced by inducible apolipoprotein E expression in cultured mouse adrenocortical cells. *J. Biol. Chem.* **273**, 12140-12147 (1998).
60. Riddell, D.R., Graham, A. & Owen, J.S. Apolipoprotein E inhibits platelet aggregation through the L-arginine:nitric oxide pathway. *J. Biol. Chem.* **272**, 89-95 (1997).
61. Thaulow, E., Erikssen, J., Sandvik, L., Stormorken, H. & Cohn, P.F. Blood platelet count and function are related to total and cardiovascular death in apparently healthy men. *Circulation* **84**, 613-617 (1991).
62. Elwood, P.C., S., R., Sharp, D., Beswick, A.D., O'Brien, J.R. & Yarnell, J.W.G. Ischemic heart disease and platelet aggregation: the caerphilly collaborative heart disease study. *Circulation* **83**, 38-44 (1991).
63. Rawlins, F.A., Villegas, G.M., Hedley-Whyte, E.T. & Uzman, B.G. Fine structural localization of cholesterol-1,2-<sup>3</sup>H in degenerating and regenerating mouse sciatic nerve. *J. Cell. Biol.* **52**, 615-625 (1972).
64. Poirier, J., Hess, M., May, P.C. & Finch, C.E. Astrocytic apolipoprotein E mRNA and GFAP mRNA in hippocampus after entorhinal cortex lesioning. *Brain Res.* **11**, 97-106 (1994).
65. Leblanc, A.C. & Podusio, J.F. Regulation of apolipoprotein E gene expression after injury of the rat sciatic nerve. *J. Neurosci. Res.* **25**, 162-171 (1990).
66. Rawlins, F.A., Hedley-Whyte, E.T., Villegas, G. & Uzman, B.G. Reutilization of 1,2-<sup>3</sup>H-cholesterol in the regeneration of peripheral nerve. *Lab. Invest.* **22**, 237-240 (1970).
67. Poirier, J., Baccichet, A., Dea, D. & Gauthier, S. Cholesterol synthesis and lipoprotein reuptake during synaptic remodelling in hippocampus in adult rats. *Neuroscience* **55**, 81-90 (1993).
68. Boyles, J.K., Notterpek, L.M. & Anderson, L.J. Accumulation of apolipoproteins in the regeneration and remyelinating mammalian peripheral nerve. *J. Biol. Chem.* **265**, 17802-17815 (1990).

69. Masliah, E. Synaptic integrity in apoE knockout mice. in *Research advances in Alzheimer's disease and related disorders* (eds. Iqbal, K., Mortimer, J.A., Winblad, B. & Winiewski, H.) (Wiley and Sons Ltd., London, 1994).
70. Masliah, E., Mallory, M., Ge, N., Alford, M., Veinbergs, I. & Roses, A.D. Neurodegeneration in the central nervous system of apoE-deficient mice. *Exp. Neurol.* **136**(1995).
71. Corder, E.H., Robertson, K., Lannfelt, L., Bogdanovic, N., Eggertsen, G., Wilkins, J. & Hall, C. HIV-infected subjects with the E4 allele for apoE have excess dementia and peripheral neuropathy. *Nature Medicine* **4**, 1182-1184 (1998).
72. Ignatius, M.J., Gebicke-Harter, P.J., Skene, J.H., Schilling, J.W., Weisgraber, K.H., Mahley, R.W. & Shooter, E.M. Expression of apolipoprotein E during nerve degeneration and regeneration. *Proc. Natl. Acad. Sci. USA* **83**, 1125-1129 (1986).
73. Nathan, B.P., Bellosta, S., Sanan, D.A., Weisgraber, K.H., Mahley, R.W. & Pitas, R.E. Differential effects of apolipoproteins E3 and E4 on neuronal growth in vitro. *Science* **264**, 850-852 (1994).
74. Nathan, B.P., Chang, K.-C., Bellosta, S., Brisch, E., Ge, N., Mahley, R.W. & Pitas, R.E. The inhibitory effect of apolipoprotein E4 on neurite outgrowth is associated with microtubule depolymerization. *J. Biol. Chem.* **270**, 19791-19799 (1995).
75. Perry, G. *Alterations in the neuronal cytoskeleton in Alzheimer's disease*, (Plenum Press, New York, 1987).
76. Fagan, A.M., Bu, G., Sun, Y., Daugherty, A. & Holtzman, D.M. Apolipoprotein E-containing high density lipoprotein promotes neurite outgrowth and is a ligand for the low density lipoprotein receptor-related protein. *J. Biol. Chem.* **271**, 30121-30125 (1996).
77. DeMattos, R.B., Curtiss, L.K. & Williams, D.L. A minimally lipidated form of cell-derived apolipoprotein E exhibits isoform-specific stimulation of neurite outgrowth in the absence of exogenous lipids or lipoproteins. *J. Biol. Chem.* **273**, 4206-4212 (1998).
78. Raber, J., Wong, D., Buttini, M., Orth, M., Bellosta, S., Pitas, R.E., Mahley, R.W. & Mucke, L. Isoform-specific effects of human apolipoprotein E on brain function revealed in apoE knockout mice: increased susceptibility of females. *Proc. Natl. Acad. Sci. USA* **95**, 10914-10919 (1998).
79. Piedrahita, J.A., Zhang, S.H., Hagan, J.R., Oliver, P.M. & Maeda, N. Generation of mice carrying a mutant apolipoprotein E gene inactivated by

- gene targeting in embryonic stem cells. *Proc. Natl. Acad. Sci. USA* **89**, 4471-4475 (1992).
80. Van Duijn, C.M., de Knijff, P., Cruts, M., Wehnert, A., Havekes, L.M., Hofman, A. & Van Broeckhoven, C. Apolipoprotein E4 allele in a population-based study of early onset Alzheimer's disease. *Nature Genet.* **7**, 74-78 (1994).
  81. Saunders, A.M., Strittmatter, W.J., Schmechel, D., St. George-Hyslop, P.H., Pericak-Vance, M.A., Joo, S.H., Rosi, B.L., Gusella, J.F., Crapper-MacLachlan, D.R., Alberts, M.J., Hulette, C., Crain, B., Goldgaber, D. & Roses, A.D. Association of apolipoprotein E allele  $\epsilon$ 4 with late-onset familial and sporadic Alzheimer's disease. *Neurology* **43**, 1467-1472 (1993).
  82. Rebeck, G.W., Reiter, J.S., Stickland, D.K. & Hyman, B.T. Apolipoprotein E in sporadic Alzheimer's disease: allelic variation and receptor interactions. *Neuron* **11**, 575-580 (1993).
  83. Corder, E.H., Saunders, A.M., Strittmatter, W.J., Schmechel, D., Gaskell, P.C., Small, G.W., Roses, A.D., Haines, J.L. & Pericak-Vance, M.A. Gene dose of apolipoprotein E type 4 allele and the risk of Alzheimer's disease in late onset families. *Science* **261**, 921-923 (1993).
  84. Poirier, J. Apolipoprotein E in animal models of CNS injury and in Alzheimer's disease. *Trends in Neuro. Sci.* **17**, 525-530 (1994).
  85. Schachter, F., Faure-Delanef, L., Guénot, F., Rouger, H., Froguel, P., Lesueur-Ginot, L. & Cohen, D. Genetic associations with human longevity at the APOE and ACE loci. *Nature Genet.* **6**, 29-31 (1994).
  86. Corder, E.H., Saunders, A.M., Risch, N.J., Strittmatter, W.J., Schmechel, D.E., Gaskell, P.C.J., Rimmler, J.B., Locke, P.A., Conneally, P.M., Schmechel, K.E., Small, G.W., Roses, A.D., Haines, J.L. & Pericak-Vance, M.A. Protective effect of apolipoprotein E type 2 allele for late onset Alzheimer's disease. *Nature Genet.* **7**, 180-184 (1994).
  87. West, H.L., Rebeck, G.W. & Hyman, B.T. Frequency of the apolipoprotein E  $\epsilon$ 2 allele is diminished in sporadic Alzheimer's disease. *Neurosci. Lett.* **175**, 46-48 (1994).
  88. Wisniewski, T. & Frangione, B. Apolipoprotein E: a pathological chaperone protein in patients with cerebral and systemic amyloid. *Neurosci. Lett.* **135**, 235-238 (1992).
  89. Sanan, D.A., Weisgraber, K.H., Russell, R.W., Mahley, W., Huang, D., Saunders, A., Schmechel, D., Wisniewski, T., Frangione, B., Roses, A.D. & Strittmatter, W.J. Apolipoprotein E associates with  $\beta$  amyloid peptide of

- Alzheimer's disease to form novel monofibrils. *J. Clin. Invest.* **94**, 860-869 (1994).
90. Strittmatter, W.J., Saunders, A.M., Schmechel, D., Pericak-Vance, M., Enghild, J., Salvesen, G.S. & Roses, A.D. Apolipoprotein E: high-avidity binding to beta-amyloid and increased frequency of type 4 allele in late-onset familial Alzheimer disease. *Proc. Natl. Acad. Sci. USA* **90**, 1977-1981 (1993).
  91. Wisniewski, T., Golabek, A., Matsubara, E., Ghiso, J. & Frangione, B. Apolipoprotein E: binding to soluble Alzheimer's  $\beta$ -amyloid. *Biochem. Biophys. Res. Commun.* **192**, 359-365 (1993).
  92. Castaño, E.M., Prelli, F., Wisniewski, T., Golabek, A., Kumar, R.A., Soto, C. & Frangione, B. Fibrillogenesis in Alzheimer's disease of amyloid  $\beta$  peptide and apolipoprotein E. *Biochem. J.* **306**, 599-604 (1995).
  93. LaDu, M.J., Pederson, T.M., Frail, D.E., Reardon, C.A., Getz, G.S. & Falduto, M.T. Purification of apolipoprotein E attenuates isoform-specific binding to  $\beta$ -amyloid. *J. Biol. Chem.* **270**, 9039-9042 (1995).
  94. Winkler, K., Scharnagl, H., Tisljar, U., Hoschützky, H., Friedrich, I., Hoffmann, M.M., Hüttinger, M., Wieland, H. & Marz, W. Competition of A $\beta$  amyloid peptide and apolipoprotein E for receptor-mediated endocytosis. *J. Lipid Res.* **40**, 447-455 (1999).
  95. Strittmatter, W.J., Weisgraber, K.H., Huang, D.Y., Dong, L.M., Salvesen, G.S., Pericak-Vance, M., Schmechel, D., Saunders, A.M., Goldgaber, D. & Roses, A.D. Binding of human apolipoprotein E to synthetic amyloid beta peptide isoform-specific effects implications for late-onset Alzheimer disease. *Proc. Natl. Acad. Sci. U.S.A.* **90**, 8098-8102 (1993).
  96. Strittmatter, W.J., Weisgraber, K.H., Goedert, M., Saunders, A.M., Huang, D., Corder, E.H., Dong, L.-M., Jakes, R., Alberts, M.J., Gilbert, J.R., Han, S.-H., Hulette, C., Eistein, G., Schmechel, D.E., Pericak-Vance, M.A. & Roses, A.D. Hypothesis: Microtubule instability and paired helical filament formation in the Alzheimer's disease brain are related to apolipoprotein E genotype. *Exp. Neurol.* **125**, 163-171 (1994).
  97. Kopke, E., Tung, Y.-C., Shaikh, S., Alonso, A.C., Iqbal, K. & Grundke-Iqbal, I. Microtubule-associated protein tau. Abnormal phosphorylation of a non-paired helical filament pool in Alzheimer disease. *J. Biol. Chem.* **268**, 24374-24384 (1993).
  98. Goedert, M., Spillantini, M.G. & Jakes, R. Multiple isoforms of human microtubule-associated protein tau: sequences and localisation in neurofibrillary tangles. *Neuron* **3**, 519-526 (1989).

99. Wille, H., Drewes, G. & Biernat, J. Alzheimer-like paired helical filaments and antiparallel dimers formed from microtubule-associated protein tau in vitro. *J. Cell Biol.* **116**, 573-584 (1992).
100. Corder, E.H., Saunders, A.M. & Risch, N.J. Apolipoprotein E type 2 allele decreases the risk of late-onset Alzheimer disease. *Nature Genet.* (1993).
101. Ohm, T.G., Kirca, M., Bohl, J., Scharnagl, H., Gross, W. & Marz, W. Apolipoprotein E polymorphism influences not only cerebral senile plaque load but also Alzheimer-type neurofibrillary tangle formation. *Neuroscience* **66**(1995).
102. Innerarity, T.L. & Mahley, R.W. Enhanced binding by cultured human fibroblasts of apo-E-containing lipoproteins as compared with low density lipoproteins. *Biochemistry* **17**, 1440-1447 (1978).
103. Innerarity, T.L., Pitas, R.E. & Mahley, R.W. Binding of arginine-rich (E) apoprotein after recombination with phospholipid vesicles to the low density lipoprotein receptors of fibroblasts. *J. Biol. Chem.* **254**, 4186-4190 (1979).
104. Lund-Katz, S., Weisgraber, K.H., Mahley, R.W. & Phillips, M.C. Conformation of apolipoprotein E in lipoproteins. *J. Biol. Chem.* **268**, 23008-23015 (1993).
105. Prévost, M. & Kocher, J.-P. Structural characterization by computer experiments of the lipid-free LDL-receptor-binding domain of apolipoprotein E. *Protein Eng.* **12**, 475-483 (1999).
106. Gursky, O. & Atkinson, D. Thermal unfolding of human high-density apolipoprotein A-I: implications for a lipid-free molten globular state. *Proc. Natl. Acad. Sci. USA* **93**, 2991-2995 (1996).
107. Soulages, J.L. & Bendavid, O.J. The lipid binding activity of the exchangeable apolipoprotein apolipoprotein III correlates with the formation of a partially folded conformation. *Biochemistry* **37**, 10203-10210 (1998).
108. Raussens, V., Fisher, C.A., Goormaghtigh, E., Ryan, R.O. & Ruyschaert, J.-M. The low density lipoprotein receptor active conformation of apolipoprotein E. Helix organization in N-terminal domain-phospholipid disc particles. *J. Biol. Chem.* **273**, 25825-25830 (1998).
109. Weisgraber, K.H. Apolipoprotein E: structure-function relationships. *Ad. Protein Chem.* **45**, 249-302 (1994).
110. Borhani, D.W., Rogers, D.P., Engler, J.A. & Brouillette, C.G. Crystal structure of truncated human apolipoprotein A-I suggests a lipid-bound conformation. *Proc. Natl. Acad. Sci. U.S.A.* **94**(1997).



111. Borensztajn, J., Kotlar, T.J. & McNeill, B.J. Uptake of phospholipid-depleted chylomicrons by the perfused rat liver. *Biochem. J.* **192**, 845-851 (1980).
112. Borensztajn, J. & Kotlar, T.J. Hepatic uptake of phospholipid-depleted chylomicrons *in vivo*. Comparison with the uptake of chylomicron remnants. *Biochem. J.* **200**, 547-553 (1981).
113. Borensztajn, J., Getz, G.S. & Kotlar, T.J. Uptake of chylomicron remnants by the liver: further evidence for the modulating role of phospholipids. *J. Lipid Res.* **29**, 1087-1096 (1988).
114. Linga, V., Leight, M.A., Curtiss, L.K., Marcel, Y.L., St. Clair, R.W. & Parks, J.S. Dietary fish oil-induced decrease in low density lipoprotein binding to fibroblasts is mediated by apolipoprotein E. *J. Lipid Res.* **35**, 491-500 (1994).
115. Jonas, A., Steinmetz, A. & Churgay, L. The number of amphipathic  $\alpha$ -helical segments of apolipoproteins A-I, E, and A-IV determines the size and functional properties of their reconstituted lipoprotein particles. *J. Biol. Chem.* **268**, 1596-1602 (1993).
116. Gianturco, S.H., Brown, F.B., Gotto, A.M.J. & Bradley, W.A. Receptor-mediated uptake of hypertriglyceridemic very low density lipoproteins by normal human fibroblasts. *J. Lipid Res.* **23**, 984-993 (1982).
117. Bradley, W.A., Hwang, S.-H.C., Karlin, J.B., Lin, A.H., Prasad, S.C., Gotto, A.M.J. & Gianturco, S.H. Low-density lipoprotein receptor binding determinants switch from apolipoprotein E to apolipoprotein B during conversion of hypertriglyceridemic very-low-density lipoprotein to low-density lipoproteins. *J. Biol. Chem.* **259**, 14728-14735 (1984).
118. Sehayek, E., Lewin-Velvert, U., Chajek-Shaul, T. & Eisenberg, S. Lipolysis exposes unreactive endogenous apolipoprotein E-3 in human and rat plasma very low density lipoprotein. *J. Clin. Invest.* **88**, 553-560 (1991).
119. Granot, E., Schwiegelshohn, B., Tabas, I., Gorecki, M., Vogel, T., Carpentier, Y.A. & Deckelbaum, R.J. Effects of particle size on cell uptake of model triglyceride-rich particles with and without apoprotein E. *Biochemistry* **33**, 15190-151997 (1994).
120. Mims, M.P., Soma, M.R. & Morrisett, J.D. Effect of particle size and temperature on the conformation and physiological behavior of apolipoprotein E bound to model lipoprotein particles. *Biochemistry* **29**, 6639-6647 (1990).

121. Parks, J.S. & Gebre, A.K. Studies on the effects of dietary fish oil on the physical and chemical properties of low density lipoproteins in cynomolgus monkeys. *J. Lipid Res.* **32**, 305-315 (1991).
122. Braschi, S., Neville, T.A.-M., Vohl, M.-C. & Sparks, D.L. Apolipoprotein A-I charge and conformation regulate the clearance of reconstituted high density lipoprotein in vivo. *J. Lipid Res.* **40**, 522-532 (1999).
123. Mahley, R.W., Weisgraber, K.H. & Innerarity, T.L. Interaction of plasma lipoproteins containing apolipoproteins B and E with heparin and cell surface receptors. *Biochim. Biophys. Acta* **575**, 81-91 (1979).
124. Weisgraber, K.H., Rall, S.C., Jr, Mahley, R.W., Milne, R.W., Marcel, Y.L. & Sparrow, J.T. Human apolipoprotein E: determination of the heparin binding sites of apolipoprotein E3. *J. Biol. Chem.* **261**, 2068-2076 (1986).
125. Lucas, M. & Mazzone, T. Cell surface proteoglycans modulate net synthesis and secretion of macrophage apolipoprotein E. *J. Biol. Chem.* **271**, 13454-13460 (1996).
126. Burgess, J.W., Gould, D.R. & Marcel, Y.L. The HepG2 extracellular matrix contains separate heparinase- and lipid-releasable pools of apoE. *J. Biol. Chem.* **273**, 5645-5654 (1998).
127. Pitas, R.E., Innerarity, T.L. & Mahley, R.W. Cell surface receptor binding of phospholipid/protein complexes containing different ratios of receptor-active and -inactive E apoprotein. *J. Biol. Chem.* **255**, 5454-5460 (1980).
128. Funahashi, T., Yokoyama, S. & Yamamoto, A. Association of apolipoprotein E with the low density lipoprotein receptor: demonstration of its co-operativity on lipid microemulsion particles. *J. Biochem.* **105**, 582-587 (1989).
129. Mahley, R.W., Innerarity, T.L., Pitas, R.E., Weisgraber, K.H., Brown, J.H. & Gross, E. Inhibition of lipoprotein binding to cell surface receptors of fibroblasts following selective modification of arginyl residues in arginine-rich an B apoproteins. *J. Biol. Chem.* **252**, 7279-7287 (1977).
130. Weisgraber, K.H., Innerarity, T.L., Harder, K.J., Mahley, R.W., Milne, R., Marcel, Y.L. & Sparrow, J.T. The receptor-binding domain of human apolipoprotein E: monoclonal antibody inhibition of binding. *J. Biol. Chem.* **258**, 12348-12354 (1983).
131. Lalazar, A., Ou, S.I. & Mahley, R.W. Human Apolipoprotein E: Receptor binding activity of truncated variants with carboxyl-terminal deletions. *J. Biol. Chem.* **264**, 8447-8450 (1989).

132. Hofmann, S.L., Russell, D.W., Brown, M.S., Goldstein, J.L. & Hammer, R.E. Overexpression of low density lipoprotein (LDL) receptor eliminates LDL from plasma in transgenic mice. *Science* **239**, 1279-1281 (1988).
133. Davis, C.G. Acid-dependent ligand dissociation and recycling of LDL receptor mediated by growth factor homology region. *Nature* **326**, 760-765 (1987).
134. Daly, N.L., Scanlon, M.J., Djordjevic, J.T., Kroon, P.A. & Smith, R. Three-dimensional structure of a cysteine-rich repeat from the low-density lipoprotein receptor. *Proc. Natl. Acad. Sci. USA* **92**, 6334-6338 (1995).
135. Daly, N.L., Djordjevic, J.T., Kroon, P.A. & Smith, R. Three-dimensional structure of the second cysteine-rich repeat from the human low-density lipoprotein receptor. *Biochemistry* **34**, 14474-14481 (1995).
136. Yamamoto, T., Davis, C.G., Brown, M.S., Schneider, W.J., Casey, M.L., Goldstein, J.L. & Russell, D.W. The human LDL receptor: a cysteine-rich protein with multiple Alu sequences in its mRNA. *Cell* **39**, 27-38 (1984).
137. Russell, D.W., Brown, M.S. & Goldstein, J.L. Different combinations of cysteine-rich repeats mediate binding of low density lipoprotein receptor to two different proteins. *J. Biol. Chem.* **264**, 21682-21688 (1989).
138. Fass, D.F., Blacklow, S., Kim, P.S. & Berger, J.M. Molecular basis of familial hypercholesterolaemia from structure of LDL receptor module. *Nature* **388**, 691-693 (1997).
139. Trakhanov, S., Parkin, S., Raffai, R., Milne, R., Newhouse, Y.M., Weisgraber, K.H. & Rupp, B. Structure of a monoclonal 2E8 fab antibody fragment specific for the low-density lipoprotein-receptor binding region of apolipoprotein E refined at 1.9 Å. *Acta Cryst.* **D55**, 122-128 (1999).
140. Zhao, Y. & Mazzone, T. LDL receptor binds newly synthesized apoE in macrophages: a precursor pool for apoE secretion. *J. Lipid Res.* **40**, 1029-1035 (1999).
141. Kita, T., Goldstein, J.L., Brown, M.S., Watanabe, Y., Hornick, C.A. & Havel, R.J. Hepatic uptake of chylomicron remnants in WHHL rabbits: a mechanism genetically distinct from the low density lipoprotein receptor. *Proc. Natl. Acad. Sci. USA* **79**, 3623-3627 (1982).
142. Hui, D.Y., Innerarity, T.L. & Mahley, R.W. Lipoprotein binding to canine hepatic membranes. Metabolically distinct apo-E and apo-B, E receptors. *J. Biol. Chem.* **256**, 5646-5655 (1981).
143. Mahley, R.W., Hui, D.Y., Innerarity, T.L. & Weisgraber, K.H. Two independent lipoprotein receptors on hepatic membranes of dog, swine,

- and man. Apo-B,E and apo-E receptors. *J. Clin. Invest.* **68**, 1197-1206 (1981).
144. Herz, J. Surface location and high affinity for calcium of a 500-kd liver membrane protein closely related to the LDL-receptor suggest a physiological role as lipoprotein receptor. *EMBO J.* **7**(1988).
  145. Beisiegel, U., Weber, W., Ihrke, G., Herz, J. & Stanley, K.K. The LDL-receptor related protein, LRP, is an apolipoprotein E-binding protein. *Nature* **341**, 162-164 (1989).
  146. Kowal, R.C., Herz, J., Goldstein, J.L., Esser, V. & Brown, M.S. Low density lipoprotein receptor-related protein mediates uptake of cholesteryl esters derived from apoprotein E-enriched lipoproteins. *Biochemistry* **86**, 5810-5814 (1989).
  147. Kowal, R.C., Herz, J., Weisgraber, K.H., Mahley, R.W., Brown, M.S. & Goldstein, J.L. Opposing effects of apolipoproteins E and C on lipoprotein binding to low density lipoprotein receptor-related protein. *J. Biol. Chem* **265**, 10771-10779 (1990).
  148. Kim, D.-H., Iijima, H., Goto, K., Sakai, J., Ishii, H., Kim, H.-J., Suzuki, H., Kondo, H., Saeki, S. & Yamamoto, T. Human apolipoprotein E receptor 2. A novel lipoprotein receptor of the low density lipoprotein family predominantly expressed in brain. *J. Biol. Chem.* **271**, 8373-8380 (1996).
  149. Takahashi, S., Kawarabayasi, Y., Nakai, T., Sakai, J. & Yamamoto, T. Rabbit very low density lipoprotein receptor: a low density lipoprotein receptor-like protein with distinct ligand specificity. *Proc. Natl. Acad. Sci. USA* **89**, 9252-9256 (1992).
  150. Trommsdorff, M., Gotthardt, M., Hiesberger, T., Shelton, J., Stockinger, W., Nimpf, J., Hammer, R.E., Richardson, J.A. & Herz, J. Reeler/disabled-like disruption of neuronal migration in knockout mice lacking the VLDL receptor and apoE receptor 2. *Cell* **97**, 689-701 (1999).
  151. van't Hooft, F. & Havel, R.J. Metabolism of apolipoprotein E in plasma high density lipoproteins from normal and cholesterol-fed rats. *J. Biol. Chem.* **257**, 10996-11001 (1982).
  152. Fielding, C.J. & Fielding, P.E. Evidence for a lipoprotein carrier in human plasma catalyzing sterol efflux from cultured fibroblasts and its relationship to lecithin:cholesterol acyltransferase. *Proc. Natl. Acad. Sci. USA* **78**, 3911-3914 (1981).
  153. Gillotte, K.L., Zaiou, M., Lund-Katz, S., Anantharamaiah, G.M., Holvoet, P., Dhoest, A., Palgunachari, M.N., Segrest, J.P., Weisgraber, K.H., Rothblat, G.H. & Phillips, M.C. Apolipoprotein-mediated plasma membrane microsolvubilization. Role of lipid affinity and membrane penetration in the

- efflux of cellular cholesterol and phospholipid. *J. Biol. Chem.* **274**, 2021-2028 (1999).
154. Rees, D., Sloane, T., Jessup, W., Dean, R.T. & Kritharides, L. Apolipoprotein A-I stimulates secretion of apolipoprotein E by foam cell macrophages. *J. Biol. Chem.* **274**, 27925-27933 (1999).
  155. Weisgraber, K.H. & Mahley, R.W. Apoprotein (E-A-II) complex of human plasma lipoproteins: I. Characterization of this mixed disulfide and its identification in a high density lipoprotein subfraction. *J. Biol. Chem.* **253**, 6281-6288 (1978).
  156. Innerarity, T.L., Mahley, R.W., Weisgraber, K.H. & Bersot, T.P. Apoprotein (E-A-II) complex of human plasma lipoproteins: II. Receptor binding activity of a high density lipoprotein subfraction modulated by the apo(E-A-II) complex. *J. Biol. Chem.* **253**, 6289-6295 (1978).
  157. Weisgraber, K.H. & Shinto, L.H. Identification of the disulfide-linked homodimer of apolipoprotein E3 in plasma. *J. Biol. Chem.* **266**, 12029-12034 (1991).
  158. Cladaras, C., Hadzopoulou-Cladaras, M., Nolte, R.T., Atkinson, R.T. & Zannis, V.I. The complete sequence and structural analysis of human apolipoprotein B-100: relationship between apoB-100 and apoB-48 forms. *EMBO J.* **5**, 3495-3507 (1986).
  159. Young, S.G., Witztum, J.L., Casal, D.C., Curtiss, L.K. & Bernstein, S. Conservation of the low density lipoprotein receptor-binding domain of apoprotein B. Demonstration by a new monoclonal antibody, MB47. *Arteriosclerosis* **6**, 178-188 (1986).
  160. Innerarity, T.L., Weisgraber, K.H., Rall, S.C., Jr & Mahley, R.W. Functional domains of apolipoprotein E and apolipoprotein B. *Acta Med. Scand. Suppl.* **715**, 51-59 (1987).
  161. Weisgraber, K.H., Innerarity, T.L. & Mahley, R.W. Role of lysine residues of plasma lipoproteins in high affinity binding to cell surface receptors on human fibroblasts. *J. Biol. Chem.* **253**, 9053-9062 (1978).
  162. Lund-Katz, S., Ibdah, J.A., Letizia, J.Y., Thomas, M.T. & Phillips, M.C. A <sup>13</sup>C NMR characterization of lysine residues in apolipoprotein B and their role in binding to the low density lipoprotein receptor. *J. Biol. Chem.* **263**, 13831-13838 (1988).
  163. Lund-Katz, S., Lapland, P.M., Phillips, M.C. & Chapman, M.J. Apolipoprotein B-100 conformation and particle surface charge in human LDL subspecies: Implication for LDL receptor interaction. *Biochemistry* **37**, 12867-12874 (1998).

164. Shelburne, F., Hanks, J., Meyers, W. & Quarfordt, S. Effect of apoproteins on hepatic uptake of triglyceride emulsions in the rat. *J. Clin. Invest.* **65**, 652-658 (1980).
165. Mjos, O.D., Faergeman, O., Hamilton, R.L. & Havel, R.S. Characterization of remnants produced during the metabolism of triglyceride-rich lipoproteins of blood plasma and intestinal lymph in the rat. *J. Clin. Invest.* **56**, 603-615 (1975).
166. Weisgraber, K.H., Mahley, R.W., Kowal, R.C., Herz, J., Goldstein, J.L. & Brown, M.S. Apolipoprotein C-I modulates the interaction of apolipoprotein E with  $\beta$ -migrating very low density lipoproteins ( $\beta$ -VLDL) and inhibits binding of  $\beta$ -VLDL to low density lipoprotein receptor-related protein. *J. Biol. Chem.* **265**, 22453-22459 (1990).
167. Windler, E. & Havel, R.J. Inhibitory effects of C apolipoproteins from rats and humans on the uptake of triglyceride-rich lipoproteins and their remnants by the perfused rat liver. *J. Lipid Res.* **26**, 556-565 (1985).
168. Mahley, R.W., Weisgraber, K.H., Hussain, M.M., Greenman, B., Fisher, M., Vogel, T. & Gorecki, M. Intravenous infusion of apolipoprotein E accelerates clearance of plasma lipoproteins in rabbits. *J. Clin. Invest.* **83**, 2125-2130 (1989).
169. Sparrow, J.T., Sparrow, D.A., Culwell, A.R. & Gotto, A.M.J. Apolipoprotein E: phospholipid binding studies with synthetic peptides containing the putative receptor binding region. *Biochemistry* **24**, 6984-6988 (1985).
170. Dyer, C.A. & Curtiss, L.K. A synthetic peptide mimic of plasma apolipoprotein E that binds the LDL receptor. *J. Biol. Chem.* **266**, 22803-22806 (1991).
171. Dyer, C.A., Cistola, D.P., Parry, G.C. & Curtiss, L.K. Structural features of synthetic peptides of apolipoprotein E that bind the LDL receptor. *J. Lipid Res.* **36**, 80-88 (1995).
172. Mims, M.P., Darnule, A.T., Tovar, R.W., Pownall, H.J., Sparrow, D.A., Sparrow, J.T., Via, D.P. & Smith, L.C. A nonexchangeable apolipoprotein E peptide that mediates binding to the low density lipoprotein receptor. *J. Biol. Chem.* **269**, 20539-20547 (1994).
173. Benzinger, T.L.S., Braddock, D.T., Dominguez, S.R., Burkoth, T.S., Miller-Auer, H., Subramanian, R.M., Fless, G.M., Jones, D.N.M., Lynn, D.G. & Meredith, S.C. Structure-function relationships in side chain lactam cross-linked peptide models of a conserved N-terminal domain of apolipoprotein E. *Biochemistry* **37**, 13222-13229 (1998).
174. Braddock, D.T., Mercurius, K.O., Subramanian, R.M., Dominguez, S.R., Davies, P.F. & Meredith, S.C. Conformationally specific enhancement of

- receptor-mediated LDL binding and internalization by peptide models of a conserved anionic N-terminal domain of human apolipoprotein E. *Biochemistry* **35**, 13975-13984 (1996).
175. Dominguez, S.R., Miller-Auer, H., Reardon, C.A. & Meredith, S.C. Peptide model of a highly conserved, N-terminal domain of apolipoprotein E is able to modulate lipoprotein binding to a member of the class A scavenger receptor family. *J. Lipid Res.* **40**, 753-763 (1999).
  176. Luo, P., Braddock, D.T., Subramanian, R.M., Meredith, S.C. & Lynn, D.G. Structural and thermodynamic characterization of a bioactive peptide model of apolipoprotein E: side-chain lactam bridges to constrain the conformation. *Biochemistry* **33**, 12367-12377 (1994).
  177. Breiter, D.R., Kanost, M.R., Benning, M.M., Wesenberg, G., Law, J.H., Wells, M.A., Rayment, I. & Holden, H.M. Molecular structure of an apolipoprotein determined at 2.5-Å resolution. *Biochemistry* **30**, 603-608 (1991).
  178. Ryan, R.O., Schieve, D., Wientzek, M., Narayanaswami, V., Oikawa, K., Kay, C.M. & Agellon, L.B. Bacterial expression and site directed mutagenesis of a functional recombinant apolipoprotein. *J. Lipid Res.* **36**, 1066-1072 (1995).
  179. Wientzek, M., Kay, C.M., Oikawa, K. & Ryan, R.O. Binding of insect apolipoprotein III to dimyristoylphosphatidylcholine vesicles. Evidence for a conformational change. *J. Biol. Chem.* **269**, 4605-4612 (1994).
  180. Narayanaswami, V., Wang, J., Kay, C.M., Scraba, D.G. & Ryan, R.O. Disulfide bond engineering to monitor conformational opening of apolipoprotein III during lipid binding. *J. Biol. Chem.* **271**, 26855-26862 (1996).
  181. Wang, J., Sahoo, D., Sykes, B.D. & Ryan, R.O. NMR evidence for a conformational adaptation of apolipoprotein III upon lipid association. *Biochem. Cell Biol.* **76**, 276-283 (1998).
  182. Sahoo, D., Narayanaswami, V., Kay, C.M. & Ryan, R.O. Fluorescence studies of exchangeable apolipoprotein-lipid interactions. Superficial association of apolipoprotein III with lipoprotein surfaces. *J. Biol. Chem.* **273**, 1403-1408 (1998).
  183. Shimano, H., Yamada, N., Katsuki, M., Shimada, M., Gotoda, T., Harada, K., Murase, T., Fukazawa, C., Takaku, F. & Yazaki, Y. Overexpression of apolipoprotein E in transgenic mice: marked reduction in plasma lipoproteins except high density lipoprotein and resistance against diet-induced hypercholesterolemia. *Proc. Natl. Acad. Sci. USA* **89**, 1750-1754 (1992).

184. Huang, Y., Liu, X.Q., Rall, S.C.J., Taylor, J.M., von Eckardstein, A., Assmann, G. & Mahley, R.W. Overexpression and accumulation of apolipoprotein E as a cause of hypertriglyceridemia. *J. Biol. Chem.* **273**, 26388-26393 (1998).
185. Fazio, S., Horie, Y., Simonet, W.S., Weisgraber, K.H., Taylor, J.M. & Rall, S.C., Jr. Altered lipoprotein metabolism in transgenic mice expressing low levels of a human receptor-binding-defective apolipoprotein E variant. *J. of Lipid Res.* **35**, 408-416 (1994).
186. Sullivan, P.M., Mezdour, H., Aratani, Y., Knouff, C., Najib, J., Reddick, R.L., Quarfordt, S.H. & Maeda, N. Targeted replacement of the mouse apolipoprotein E gene with the common human apoE3 allele enhances diet-induced hypercholesterolemia and atherosclerosis. *J. Biol. Chem.* **272**, 17972-17980 (1997).
187. Zhang, S.H., Reddick, R.L., Piedrahita, J.A. & Maeda, N. Spontaneous hypercholesterolemia and arterial lesions in mice lacking apolipoprotein E. *Science* **258**, 468-471 (1992).



## Chapter 2

### **Bacterial Overexpression, Isotope Enrichment and NMR Analysis of the N-terminal Domain of Human Apolipoprotein E\***

---

\*A version of this chapter has been published.

Fisher, C.A., Wang, J., Francis, G., Sykes, B.D., Kay, C.M. and Ryan, R.O. (1997) Bacterial overexpression, isotope enrichment and NMR analysis of the N-terminal domain of human apolipoprotein E. *Biochem. Cell. Biol.* **75**: 45-53.

## **2.1 Introduction**

---

The structural properties of the N-terminal fragment of apoE resemble insect apolipoprotein III (apoLp-III), a five helix bundle amphipathic, water soluble apolipoprotein, that reversibly associates with hemolymph lipoproteins<sup>1,2</sup>. In order to investigate the structural properties of apoLp-III and questions related to its conformational adaptability, we designed a bacterial expression vector for high level expression of this protein<sup>3</sup>. Upon transformation of this plasmid vector into *E. coli*, we found that recombinant apoLp-III could be produced in large quantities. Optimization of expression parameters has resulted in routine production of 200 mg/litre cell culture. In addition, apoLp-III was recovered in the cell culture supernatant, greatly facilitating isolation of the recombinant protein. Given their overall similar molecular architecture, we hypothesized that the N-terminal domain of human apoE may behave in a similar manner, permitting overexpression of recombinant protein. Such an expression system would allow for production of sufficient quantities of protein to permit the use of heteronuclear multidimensional NMR spectroscopy to investigate the solution conformation of this protein in the presence and absence of lipid. In the present study we show that the N-terminal domain of human apoE (residues 1-183) can be efficiently produced in large quantities in bacteria and that the recombinant protein is properly folded and possesses functional properties similar to those observed for its natural counterpart. Two dimensional heteronuclear NMR spectroscopy of isotopically labeled recombinant apoE3(1-183) indicates the feasibility of using this spectroscopic technique to probe apoE solution structures.

## **2.2 Materials and Methods**

---

### **Materials**

LDL was isolated from human plasma between the density limits of 1.006 and 1.063 g/ml by sequential density centrifugation<sup>4</sup>. The prepupal subspecies of

high density lipoprotein (HDLp) was isolated from hemolymph of 7-day-old *Manduca sexta* prepupal larvae by density gradient ultracentrifugation<sup>5</sup>. Lipid transfer particle (LTP) was prepared from prepupal hemolymph as described by Ryan et al.<sup>6</sup> LDL was radiolabeled using 100 µg Iodo-Gen iodination reagent (Pierce) and 5 mCi Na<sup>125</sup>I (Amersham) per mg protein. Dimyristoylphosphatidylcholine (DMPC) was from Sigma Chemical Co. (St Louis, MO.). Recombinant human apoE3(1-299) was a gift of Dr. Shinji Yokoyama (University of Alberta). [<sup>15</sup>N]valine and [<sup>15</sup>N]glycine were obtained from Isotech Inc. and <sup>15</sup>NH<sub>4</sub>Cl was from Cambridge Isotope Laboratories.

### **Expression Vector Construction**

Plasmid pHE53 containing the cDNA encoding human apoE3<sup>7</sup> (a kind gift of Dr. Alan Attie, University of Wisconsin) was amplified using a synthetic 23mer oligonucleotide comprising the nucleotide sequence encoding amino acid residues 1-4 of apoE (and a non-annealing overhang containing an *Msc* I restriction site) and a 27mer corresponding to residues 178-183 followed by a stop codon and a non-annealing *Hind* III restriction site. DNA amplification was carried out in a 50 µl reaction volume containing 50 ng of DNA template, 10 pmol of each oligonucleotide primer, 250 µM dNTPs, and 2.5 U Taq DNA polymerase (Promega). Following 5 min denaturation at 95°C, 25 cycles of 1 min at 95°C, 2 min at 56°C, and 3 min at 71°C were completed in a thermal cycler. Appropriately sized amplification products were confirmed by agarose gel electrophoresis, the DNA was ligated into the TA cloning vector pCRII (Invitrogen), transformed into One Shot™ INVαF competent cells (Invitrogen), and transformants were screened for the appropriate insert. Digestion of the plasmid with *Msc* I and *Hind* III was followed by ligation of the isolated 550 bp fragment into a similarly digested pET22b vector (Novagen) to generate the apoE3(1-183)/pET construct. The apoE3(1-183)/pET plasmid was transformed into *E. coli* BL21 cells, cloned and sequenced.

### **Bacterial Expression and Purification of Recombinant ApoE3(1-183)**

Saturated overnight cultures of *E. coli* harboring apoE3(1-183)/pET grown in 2xYT media were transferred into M9 minimal media at a 1:30 dilution and grown at 30°C to an OD<sub>600</sub> = 0.6. Isopropyl β-D thiogalactopyranoside (IPTG) was then added to a final concentration of 1 mM and the culture continued for an additional 4 h. Cells were pelleted by centrifugation for 10 min at 10,000 x g, 4°C, the supernatant concentrated by ultrafiltration, dialyzed against 20 mM NaPO<sub>4</sub> pH 7.0, 150 mM NaCl and subjected to heparin Sepharose CL-6B (Pharmacia Biotech) column chromatography. Protein eluted with 1 M NaCl was desalted on a column of Bio-Gel P-6DG (Bio-Rad), flash frozen and lyophilized. As a final purification step, protein was dissolved in 20 mM NaPO<sub>4</sub>, pH 7.0 and subjected to HPLC on a Zorbax RX-C8 (Dupont) column. Fractions were analyzed using SDS-PAGE and analytical HPLC, and those possessing the most homogeneous protein profiles pooled, lyophilized and stored at -20°C until use.

### **Preparation and Isolation of DMPC Discs**

Recombinant apoE3(1-183), in phosphate buffered saline (PBS; 150 mM NaCl, 3.4 mM EDTA, 50 mM Na<sub>2</sub>PO<sub>4</sub>, and 50 mM NaH<sub>2</sub>PO<sub>4</sub>, pH 7.0), was added to a test tube containing a thin film of DMPC at a lipid to protein ratio of 3:1 (w/w). The DMPC/protein mixture was dissolved by brief heating at 42°C, bath sonicated until clear, and then incubated for 18 h at 24°C. The sample was adjusted to a density = 1.21 g/ml with KBr (final volume 2.5 ml), transferred to a 5 ml quick seal ultracentrifuge tube, overlaid with 0.9% saline and centrifuged at 416,000 x g for 3 h at 4°C. Five hundred μl fractions were collected from the top and assayed for protein and phospholipid using the bicinchoninic acid assay (Pierce Chemical Co., Rockford IL.) using bovine serum albumin as standard and an enzyme-based colorimetric assay (Wako Pure Chemical Industries, Ltd., Osaka, Japan), respectively. Fractions containing coincident peaks of protein and phospholipid were pooled, dialyzed against PBS and stored at 4°C.

### **Lipoprotein Binding Assay**

The ability of recombinant apoE3(1-183) to prevent aggregation of human LDL upon incubation with HDLp and LTP was determined as described by Singh et al.<sup>8</sup>. Assays were performed in a total volume of 200  $\mu$ l containing 250  $\mu$ g HDLp protein, 50  $\mu$ g LDL protein, 2  $\mu$ g LTP, and 25 to 125  $\mu$ g rApoE3(1-183) at 37°C for 1.5 h. Sample turbidity was determined by measuring absorbance at 340 nm in a microplate reader.

### **LDL Receptor Binding Assay**

Normal human skin fibroblasts (EB91-290) were grown to 60% confluence in Dulbecco's Modified Eagle Media (DMEM) containing 10% fetal bovine serum (FBS). Subsequently, cells were switched to media containing 10% delipidated FBS. At confluence, cells were cooled on ice 30 min, washed twice with PBS/fatty acid free albumin (FAFA) and incubated for 2 h at 4°C in DMEM containing 25 mM Hepes, 1 mg/ml FAFA, 2  $\mu$ g/ml <sup>125</sup>I-labeled LDL, and 0.12 - 10  $\mu$ g of receptor binding competitor (4°C). The media was removed and the cells washed five times with PBS/FAFA, and two times with PBS alone. Following this, the cells were released from dishes by incubation with 0.1 N NaOH for 1 h at 24°C. The relative ability of DMPC/apolipoprotein complexes to compete for LDL receptor binding sites was determined by measuring cell-associated <sup>125</sup>I. Radioactivity was quantitated on a Beckman LS 6000 TA liquid scintillation spectrometer.

### **Circular Dichroism Spectroscopy**

Circular dichroism (CD) spectroscopy was performed on a Jasco J-720 spectropolarimeter (Jasco Inc.) as previously described<sup>9</sup>.

### **Electron Microscopy**

Electron microscopy of rApoE3(1-183)-DMPC disc complexes was performed in a Philips EM420 as previously described<sup>10</sup>.

### **NMR Spectroscopy**

NMR experiments were carried out at 30°C on a Varian Unity INOVA 500 spectrometer equipped with four channels, a pulsed-field gradient triple resonance probe with an actively shielded z gradient, and a gradient amplifier unit. The sensitivity-enhanced 2D  $^{15}\text{N}$ - $^1\text{H}$  heteronuclear single quantum correlation (HSQC) spectra<sup>11,12</sup> were acquired with the following number of complex points and acquisition times: F1( $^{15}\text{N}$ ) 128, 91.5 ms, F2( $^1\text{H}$ ) 512, 73 ms, 8-16 transients. The spectral widths were 1500 Hz in F1 ( $^{15}\text{N}$ ) and 8000 Hz in the F2 ( $^1\text{H}$ ) dimension. Samples with 0.3-0.4 mM  $^{15}\text{N}$ -uniformly labeled or  $^{15}\text{N}$ -Gly labeled rApoE(1-183) in 100 mM acetate buffer were used. Carrier positions used in the HSQC experiments were:  $^{15}\text{N}$ , 119.0 ppm;  $^1\text{H}$ , 4.7 ppm.

### **Electrospray Ionization Mass Spectrometry**

Molecular weight determinations for control and isotope enriched rApoE3(1-183) were made using a VG quattro electrospray mass spectrometer (Fisons Instruments, Manchester, UK). Molecular weights were determined as the mean value calculated for several multiply charged ions within a coherent series. The instrument was calibrated using the series of ion peaks from horse heart myoglobin with a molecular mass of 16,951 daltons. Calculated masses were derived from the amino acid sequence using the program MacPro Mass (Terry Lee, City of Hope, Duarte, CA).

### **Analytical Procedures**

Sodium dodecyl sulfate polyacrylamide gel electrophoresis (SDS-PAGE) was performed according to Laemmli<sup>13</sup> and stained with Coomassie Brilliant Blue R-250. For immunoblot analyses, protein was transferred to a polyvinylidene difluoride (PVDF) membrane (Millipore Corp.) and probed with monoclonal antibody 1D7 (a gift of Dr. Ross Milne, University of Ottawa) at a dilution of 1:2500. Peroxidase-linked anti-mouse IgG and chemiluminescence (ECL) reagents (Amersham) were used to detect antigen-antibody complexes.

Analytical ultracentrifugation was performed on a Beckman model E ultracentrifuge as previously described<sup>10</sup>.

## 2.3 Results

---

### Expression and Isolation of Recombinant ApoE3(1-183)

The amino terminal domain of human apoE3 is both water soluble and possesses no post-translational modifications, making it an ideal candidate for expression in a bacterial system. The apoE3(1-183)/pET construct codes for a protein containing an 18 amino acid bacterial pel B leader sequence which directs newly synthesized proteins to the periplasmic space. Based on previous experience with a similar construct, we hypothesized that, following endogenous signal peptidase cleavage of the leader sequence, rApoE3(1-183) would escape the bacteria and accumulate in the medium, resulting in overexpression of the recombinant protein. As seen in **Fig. 2-1**, a major protein of approximately 25 kDa was present in the pellet fraction of induced *E. coli* cultures, with a slightly faster migrating protein specifically accumulating in the supernatant fraction. The slower migrating protein was tentatively identified as unprocessed recombinant apoE3(1-183) (i.e. with the pel B leader sequence attached). The identity of the induced proteins was confirmed by immunoblot analysis (**Fig. 2-2**) wherein anti-apoE3 mAb 1D7 specifically bound to both polypeptides. Thus, we conclude that the slower migrating immunoreactive band corresponds to unprocessed rApoE3(1-183). In contrast to previous bacterial expression systems for apoE and its truncated variants, the supernatant fraction of the induced cell culture contained large amounts of nearly pure recombinant protein.

Further purification was achieved by heparin Sepharose column chromatography and reversed phase HPLC yielding a preparation of  $\geq 95\%$  purity (**Fig. 2-3**).

### Physical Characterization of Recombinant ApoE3(1-183)

Electrospray mass spectrometry yielded a molecular weight of 21,191 Da. This value agrees well with the calculated mass of 21,193 Da for this fragment of human apoE3, and confirms that the pel B leader sequence has been properly cleaved.

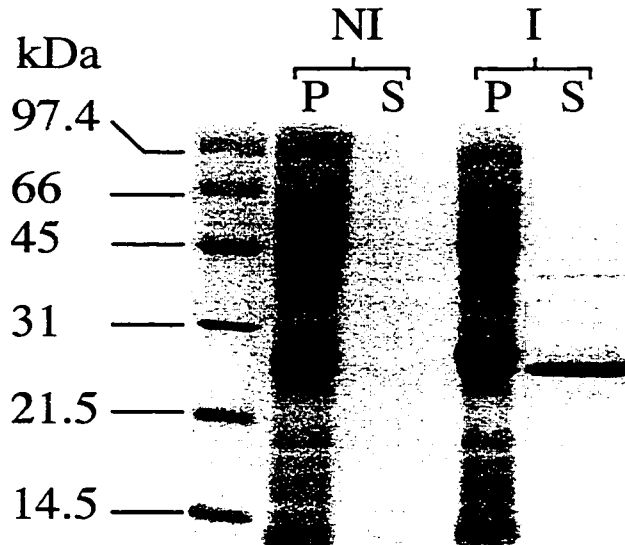


**Fig. 2-1** Electrophoresis of protein recovered in the pellet (P) and supernatant (S) fractions of bacterial cultures transformed with the apoE3(1-183)/pET vector. I = induced with 1mM IPTG; NI = non-induced. Bacteria were grown at 37°C in 2xYT media for 4 h. Proteins were separated on a 12 % acrylamide SDS slab gel and stained with Coomassie blue.



**Fig. 2-2** Immunoblot of rApoE3(1-183). Pellet and supernatant fractions obtained from IPTG induced bacterial cell cultures harboring the apoE3(1-183)/pET vector were separated by SDS-PAGE, electrophoretically transferred to a PVDF membrane and probed with anti-apoE mAb (1D7). Lane 1) bacterial cell pellet; lane 2) cell culture supernatant.



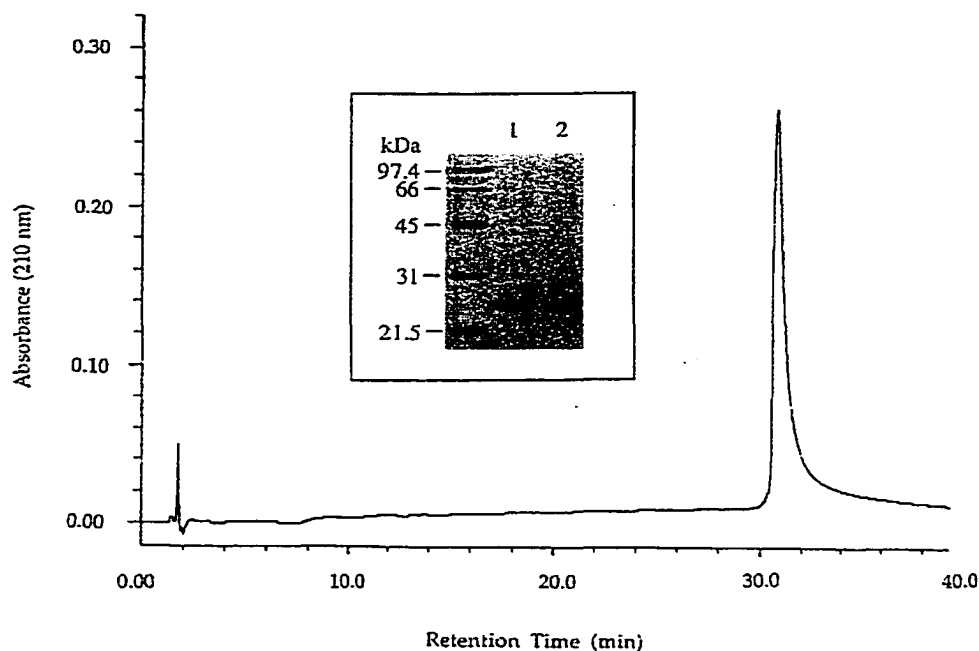


**Fig. 2-3** Reversed phase HPLC profile of purified rApoE3(1-183). Protein was purified by chromatography of induced bacterial cell culture supernatant on a heparin Sepharose column followed by HPLC on a Zorbax C8 reversed phase column. **Inset:** SDS-PAGE of rApoE3(1-183) at various stages of purification. Lane 1) induced bacterial culture supernatant; lane 2) HPLC purified protein.

To confirm that the recombinant protein adopts the expected secondary structure, CD spectroscopy was performed. The N-terminus of apoE is predominantly  $\alpha$ -helical as determined by both secondary structure analysis and X-ray crystallography<sup>14</sup>. The spectra depicted in **Fig. 2-4** reveals dual minima of ellipticity at 208 and 222 nm, a characteristic of proteins with a high  $\alpha$ -helix content. Addition of the helix inducing solvent, trifluoroethanol, increased the negative ellipticity values approximately 20% while the profile shape was unaltered, further confirming a helical secondary structure. Analysis of the far U.V. spectra by the Convex Constraint Analysis program of Perczel et al.<sup>15</sup> indicated 58%  $\alpha$ -helical content which increased to 73% in the presence of 50% trifluoroethanol.

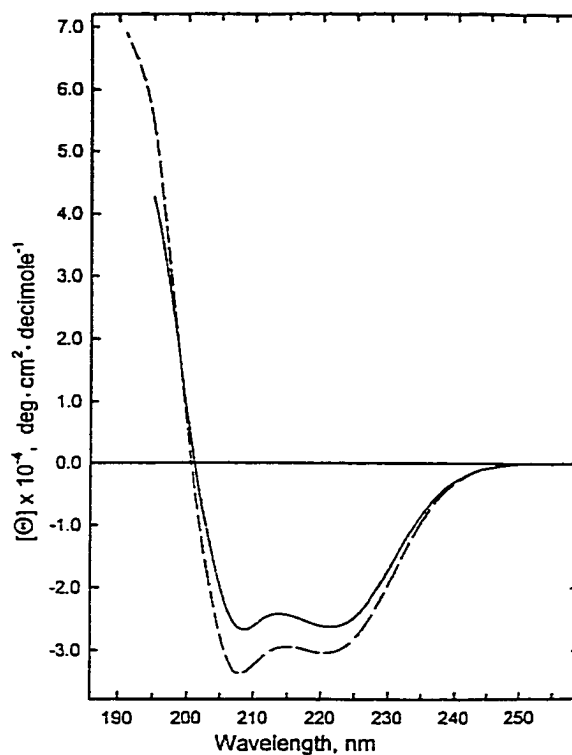


**Fig. 2-4** Circular dichroism spectra of rApoE3(1-183). Far U.V. (190-255 nm) spectra of protein in the presence (-----) or absence (——) of 50 % trifluoroethanol in 50 mM KCl, 25 mM KPO<sub>4</sub>, pH 7.0 or 100 mM KCl, 50 mM KPO<sub>4</sub>, pH 7.0, respectively.

### **Functional Characterization of Recombinant ApoE3(1-183)**

A characteristic of the N-terminal domain of apoE is the ability to generate lipid bilayer discs upon incubation with phospholipids<sup>16</sup>. Co-sonication of the protein with DMPC produced disc-like structures when mixed at a 1:3 protein to phospholipid ratio (w/w). Flotation equilibrium centrifugation experiments yielded an apparent molecular mass of 611,400 Da which was in agreement with the value obtained from electrophoresis in a non-denaturing gradient polyacrylamide gel and comparison with protein standards. Stacked discs, comparable to those generated with other exchangeable apolipoproteins, are shown in the electron micrograph depicted in **Fig. 2-5**. Heterogeneity was observed in the diameters of discs which tended to form rouleaux composed of several to approximately 20 individual disc complexes.

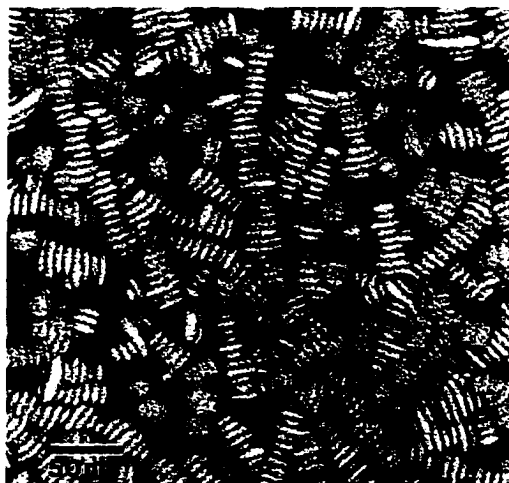


**Fig. 2-5** Electron micrograph of rApoE3(1-183)/DMPC complexes. Disc complexes isolated by density gradient ultracentrifugation were stained with 2% sodium phosphotungstate and photographed in a Philips EM420 operated at 100 kV.

To assess the ability of recombinant apoE3(1-183) to associate with the surface of lipoprotein particles, we employed an assay of apolipoprotein function based on *in vitro* facilitated enrichment of the neutral lipid content of human LDL. Catalytic amounts of insect hemolymph LTP facilitates net vectorial transfer of diacylglycerol from HDLp to human LDL<sup>17</sup>. As a consequence of lipid loading, hydrophobic patches on the LDL particle surface become exposed as the capacity of resident surface protein and phospholipid to cover the surface is exceeded. As a result, particle aggregation ensues, which is manifest by an increase in sample turbidity. Aggregation can be prevented, however, by inclusion of amphipathic exchangeable apolipoproteins in the incubation mixture. These associate with the modified lipoprotein surface retaining particle integrity<sup>8</sup>. As seen in **Fig. 2-6**, rApoE3(1-183) effectively prevented lipid-enrichment-induced LDL particle aggregation in a concentration dependent manner.

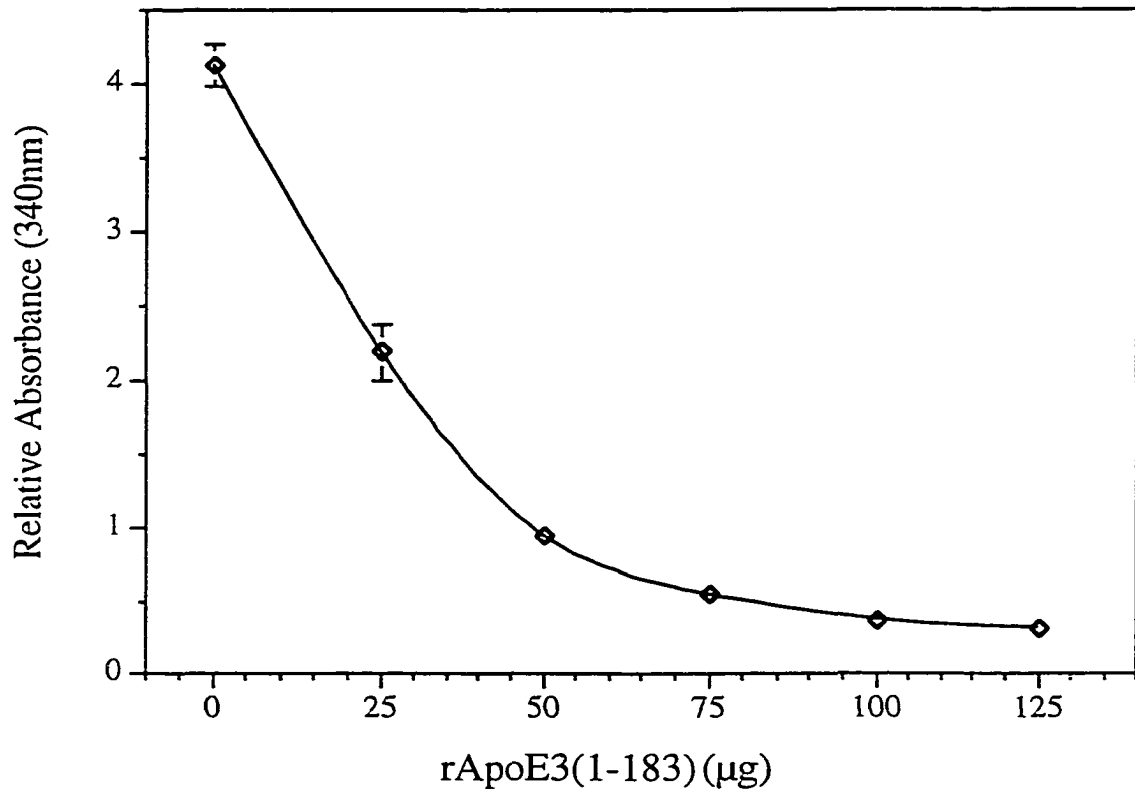


**Fig. 2-6.** The effect of rApoE3(1-183) on the turbidity of lipid-enriched LDL. HDLp (250 µg protein) and LDL (50 µg protein) were incubated in the presence of 2 µg LTP in a 200 µl volume for 1.5 h at 37°C in the absence or presence of indicated amounts of rApoE3(1-183). The absorbance was determined at 340 nm using a microplate reader. The values reported are the mean  $\pm$  standard deviation ( $n = 3$ ).

An important function of the amino terminal domain of apoE is its role as a ligand for receptor interactions. When isolated, this domain retains this binding ability, but only when lipid associated<sup>16</sup>. Recombinant apoE3(1-183), when complexed with DMPC, effectively competed with <sup>125</sup>I-LDL for binding sites on the surface of cultured human skin fibroblasts as evidenced by a concentration dependent reduction in bound <sup>125</sup>I-labeled LDL (**Fig. 2-7**). A comparable reduction in cell associated radioactivity was also observed in experiments employing full length apoE3 and unlabeled LDL as competitors.

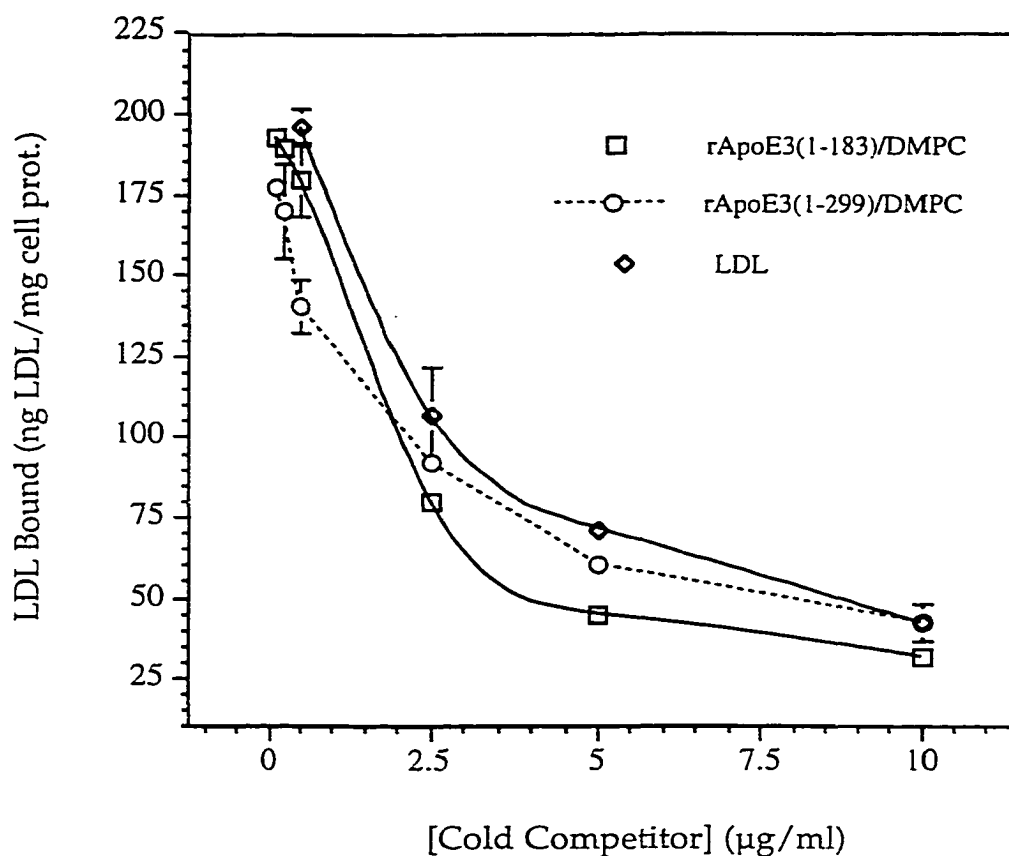


**Fig. 2-7.** The ability of LDL, rApoE3(1-183) and rApoE3(1-299) to compete with  $^{125}\text{I}$ -labeled LDL for binding to cultured human skin fibroblasts. Two  $\mu\text{g/ml}$   $^{125}\text{I}$ -labeled LDL and 0.12-10  $\mu\text{g/ml}$  of receptor binding competitor were added per dish of cells. Incubations were carried out at  $4^\circ\text{C}$  for 2 h followed by determination of cell associated radioactivity and protein.

### NMR Studies of Recombinant ApoE3(1-183)

In experiments designed to optimize experimental conditions for NMR studies, the effect of pH on the secondary structure content of rApoE3(1-183) was determined by circular dichroism spectroscopy. A plot of  $[\theta]_{222}$  as a function of pH for rApoE3(1-183) is shown in **Fig. 2-8**. At pH values around the pI (4.6 to 6.4) the protein displayed a tendency to precipitate, precluding use of this pH range for NMR studies. Otherwise, high  $\alpha$ -helicity is retained down to pH 3.5 and up to pH 10.

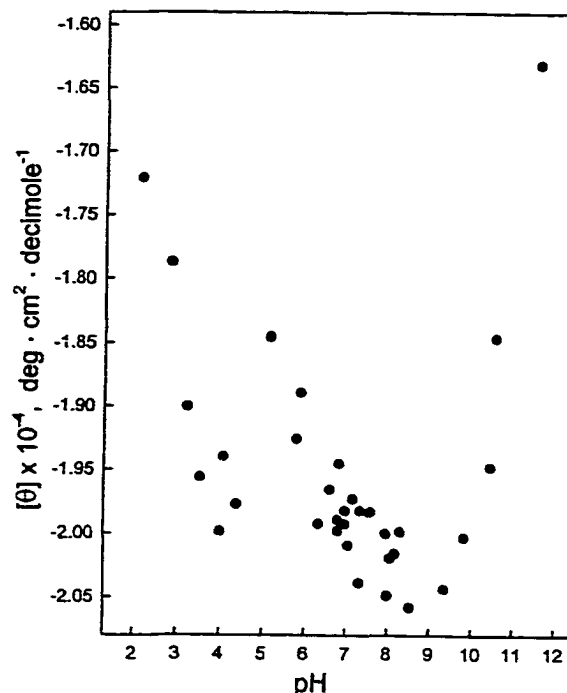


**Fig. 2-8.** Effect of pH on ellipticity of rApoE3(1-183) at 222 nm. A sample containing 0.8 mg/ml protein was adjusted with respect to pH over a range of 2.1-11.6. At each interval, a CD spectrum was obtained and  $[\theta]_{222}$  determined. Data for pH 5.0 - 6.0 were not included due to precipitate formation in the sample.

At pH 7.0, however, preliminary NMR experiments revealed poor chemical shift dispersion indicating studies at this pH may not be feasible. Since the protein retains a high helix content down to pH 3.5, we evaluated the self association properties of rApoE3(1-183) in this pH range by sedimentation equilibrium experiments conducted in the analytical ultracentrifuge (data not shown). Consistent with its predominant existence as a monomer, at pH 3.7 an apparent molecular weight (MW) = 23,490 was obtained in the presence of 10 mM dithiothreitol.

In spite of the relatively large size of rApoE(1-183), the present protein preparation meets several essential criteria for multidimensional NMR characterization: i) the protein is monomeric in solution at concentrations up to 15 mg/ml<sup>18</sup>; ii) recombinant protein is available in large quantities and iii) the protein retains its secondary structure content over a broad pH range. The ability

to express recombinant protein in bacteria facilitates enrichment of the protein with  $^{15}\text{N}$  or  $^{13}\text{C}$  labeled amino acids, which is necessary for multi-dimensional heteronuclear NMR. Enrichment of apoE3(1-183) with  $^{15}\text{N}$  was accomplished by culturing bacteria harboring the apoE3(1-183)/pET plasmid construct in M9 minimal media containing  $^{15}\text{NH}_4\text{Cl}$  as the sole nitrogen source. **Figure 2-9** (panel A) shows the  $^1\text{H}$ - $^{15}\text{N}$  HSQC spectrum of a 0.3 mM solution of lipid-free uniformly  $^{15}\text{N}$ -labeled apoE3(1-183) obtained at pH 3.8. The spectral pattern obtained indicates a uniform distribution of  $^{15}\text{N}$  into the protein backbone amide and side chain amine positions consistent with electrospray mass spectrometry data which revealed an  $^{15}\text{N}$  incorporation  $\sim 90\%$ , on average. The peaks observed correlate the chemical shifts of amide protons with the amide nitrogens of the same amino acid. Thus, when cultured in  $^{15}\text{NH}_4\text{Cl}$ , all peptide backbone amide groups (with the exception of proline, which lacks a backbone amide proton) will give rise to a crosspeak. Furthermore, the upper right hand region of the spectra contains crosspeaks from  $^{15}\text{N}$ -labeled amine groups of Gln and Asn side chains. Figure 2-9 also indicates that the resonance peaks are generally shifted upfield, consistent with the fact that the protein secondary structure is predominantly  $\alpha$ -helix. The chemical shift in the  $^{15}\text{N}$ -dimension is well dispersed which results in good separation of the overall crosspeaks. The strong crosspeaks observed in the lower left hand corner of the spectrum arise from Trp residues. Finally, as expected for a protein of this size possessing  $\alpha$ -helical structure, the central region of the spectrum is crowded and will require 3D/4D NMR methods to resolve individual resonances for the purpose of complete spectral assignment.

Enrichment of specific amino acids of rApoE3(1-183) with  $^{15}\text{N}$  was performed by supplementing M9 media (lacking  $\text{NH}_4\text{Cl}$ ) with a given  $^{15}\text{N}$  labeled amino acid and the 19 other unlabeled amino acids. In this case, we chose glycine for  $^{15}\text{N}$ -specific labeling since they resonate in a unique region of the HSQC spectra and thus, are easier to identify. There are 10 Gly in apoE3(1-183).

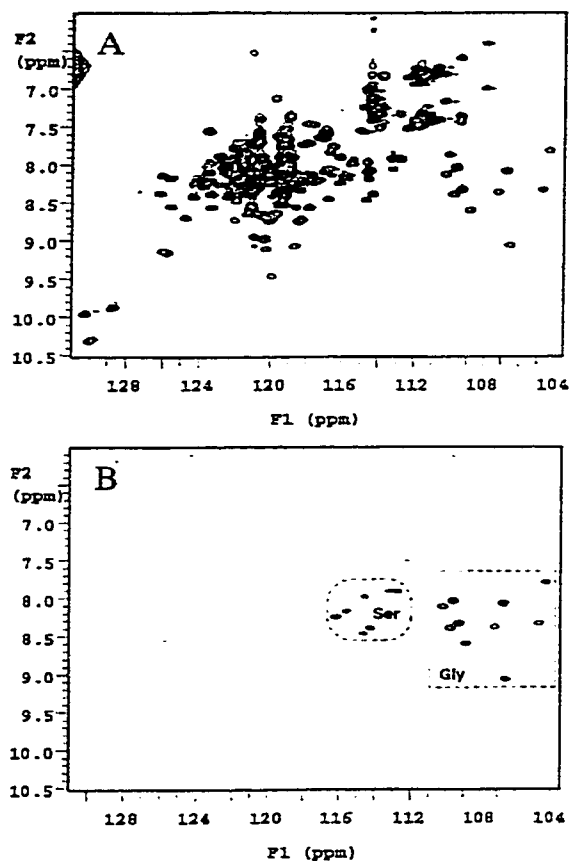


**Fig. 2-9.** Two dimensional  $^1\text{H}$ - $^{15}\text{N}$  heteronuclear single quantum correlation (HSQC) spectrum of rApoE3(1-183) obtained from bacterial cell cultures grown in **A**) M9 minimal medium containing  $^{15}\text{NH}_4\text{Cl}$  as the sole nitrogen source or **B**) M9 minimal medium containing  $^{15}\text{N}$ -glycine supplemented with other unlabeled amino acids. Samples were dissolved in 100 mM acetate buffer, pH 3.8 containing 95%  $\text{H}_2\text{O}$ /5%  $\text{D}_2\text{O}$ . The spectrum was obtained at 30°C.

Figure 2-9 (**panel B**) reveals a spectrum consisting of 10 distinct strong crosspeaks, with chemical shifts in the range normally seen for glycine in HSQC spectra, together with several less intense crosspeaks, tentatively assigned to serine residues. This latter observation is not unexpected since the bacterial aminotransferase responsible for serine production from hydroxypyruvate employs glycine as the nitrogen donor.



## 2.4 Discussion

---

Vogel et al.<sup>19</sup> first reported expression of recombinant apoE in bacteria. These workers demonstrated that bacterially expressed apoE is indistinguishable from natural apoE by several criteria, including lipid interaction and receptor binding. The expression system employed resulted in recovery of recombinant apoE in the cells at levels in the range of 1% of total soluble cellular protein. Longer induction periods, however, led to cell lysis and proteolysis. Subsequently, Lalazar et al.<sup>20</sup> reported expression of C-terminally truncated forms of apoE in *E. coli*. These truncated variants formed complexes with model phospholipids and the variant corresponding to residues 1-183 possessed nearly full receptor binding activity. The recombinant variants were purified from the soluble fraction of the bacterial cell pellet. Subsequently, Dong et al.<sup>21</sup> used a glutathione S-transferase (GST) fusion expression vector to produce a GST-apoE fusion protein in *E. coli*. Recombinant protein was isolated from bacterial cell culture pellets and, following complexation with DMPC, the apoE (or corresponding variant), was liberated by treatment with Factor Xa. In all these systems the cells were permitted to grow between 0.3 and 0.75 h following induction of recombinant protein synthesis. In the present report we have established a bacterial expression system for production of the N-terminal domain of human apoE that is not hampered by intracellular accumulation of recombinant protein. Thus, cell toxicity is greatly diminished and it is possible to grow cells for longer periods of time after induction. This results in very high yields of recombinant protein. Using the apoE3(1-183)/pET vector construct, a steady increase in mature recombinant apoE3(1-183) accumulated in the culture supernatant over the course of 4 h following induction. At an incubation temperature of 37°C, the intracellular content of recombinant protein contained both unprocessed material that still retained the pel B leader sequence and mature rApoE3(1-183). At this temperature, cell growth appeared to be too rapid for the signal peptidase to keep pace with recombinant protein production resulting in increased quantities of unprocessed protein in the pellet. At 30°C, cell growth (and protein production) was sufficiently slow that the peptidase was able to efficiently catalyze cleavage

of the signal sequence, resulting in recovery of the bulk of recombinant protein within cells in the processed form. In the medium, only mature rApoE3(1-183) accumulated. It appears from the results obtained, and those reported earlier for apoLp-III<sup>3</sup>, that upon cleavage of the leader sequence by the endogenous bacterial leader peptidase, the recombinant protein escapes the bacteria and accumulates in the medium. As such, any toxic effects of overproduction of recombinant apolipoprotein are alleviated, increasing the potential yield. In the present study, we routinely produced > 100 mg rApoE3(1-183) per litre cell culture. In addition to an increased yield of recombinant protein, the present method is advantageous because the protein of interest accumulates in the culture medium. In practice, therefore, the cell pellet is discarded and the recombinant protein isolated by a convenient two step protocol from the culture supernatant. It is unclear at present how the protein escapes the bacteria. It is known that the pel B leader sequence directs newly synthesized proteins to the periplasmic space where the signal peptidase resides. Thus, it may be some property of this protein (and apoLp-III as well) which allows it to escape the bacteria.

Following isolation of rApoE3(1-183), we verified that the protein mass was that expected from the known sequence of this protein. In addition, immunoblot analysis confirmed the identity of the recombinant protein as apoE. Circular dichroism spectroscopy revealed that rApoE3(1-183) adopted the expected  $\alpha$ -helical secondary structure. In addition, we showed that rApoE3(1-183) was capable of associating with lipoprotein surfaces. For this we employed a novel general assay for apolipoprotein function adapted from Singh et al.<sup>8</sup>. From previous studies it is known that facilitated vectorial net lipid transfer occurs from insect lipophorin to human LDL when incubated in the presence of catalytic amounts of LTP<sup>17</sup>. In the presence of an excess of potential donor lipoprotein (e.g. lipophorin), LDL accepts lipid beyond its capacity to retain a stable particle structure and irreversibly aggregates, causing development of sample turbidity<sup>8</sup>. It should be noted that co-incubation of apoLp-III in such a system does not alter the extent of facilitated lipid transfer but does prevent aggregation of LDL. The mechanism whereby exogenous exchangeable

apolipoproteins prevent lipid transfer-induced aggregation of LDL involves formation of a stable binding interaction between the apolipoprotein and the modified surface of LDL<sup>8</sup>. In the case of rApoE3(1-183), this result is the first report, to our knowledge, of binding of the N-terminal domain to a spherical lipoprotein particle. In a previous study, Weisgraber<sup>22</sup> investigated the ability of the N-terminal domain of apoE to associate with lipoprotein particles and found that it was recovered exclusively in the lipoprotein free fraction following incubation with plasma and subsequent chromatographic separation. These data, however, are not inconsistent with the present results. It is likely that the N-terminal domain is unable to displace other apolipoproteins from the surface of lipoproteins and, thus, in the absence of creation of new hydrophobic lipoprotein surface, the N-terminal domain of apoE remains in the lipid-free state. By contrast, the high lipid binding affinity of the C-terminal domain of apoE facilitates lipoprotein interaction which can be observed upon incubation of intact apoE with plasma. In the present study we have employed a highly efficient lipid transfer particle to redistribute lipids among isolated lipoproteins *in vitro*, thereby creating new hydrophobic surface which has been shown to attract apolipoproteins. This assay is simplified by the fact that apolipoprotein association prevents lipid transfer-induced LDL aggregation and this effect is readily quantitated turbidimetrically. In addition to an ability to associate with lipid surfaces, from receptor binding assays it is concluded that recombinant apoE3(1-183) possesses the ability to serve as a ligand for the LDL receptor on cultured human skin fibroblasts. This result is in concordance with an earlier report by Innerarity et al.<sup>16</sup>

In order to optimize experimental conditions for NMR studies of rApoE3(1-183), we examined the effect of pH on the secondary structure content and self association of this protein using CD spectroscopy and sedimentation equilibrium ultracentrifugation. Figure 2-8 shows that rApoE3(1-183) retains high  $\alpha$ -helicity within the pH range 3.5-10. Protein aggregation occurred near the pI (5.4) with formation of a precipitate in the sample solution. This property precludes NMR studies within this pH range. Furthermore, since poor chemical shift dispersion was observed around neutral pH, this range was also eliminated.

However, sedimentation equilibrium results indicated that rApoE3(1-183) retains a predominantly monomeric state at  $\text{pH} < 4.0$ . Since it is critical that the protein exist as a monomer in solution, we selected  $\text{pH} 3.8$  for NMR studies.

Preliminary NMR results shown in Fig. 2-9 indicate the feasibility of multinuclear multidimensional NMR for the study of rApoE3(1-183). Chemical shifts in both dimensions of the HSQC spectrum are well dispersed, indicating the protein maintains its secondary and tertiary structure under the conditions of the experiment. For the  $^1\text{H}$  dimension, amide proton chemical shifts range from 6.3 ppm to 9.5 ppm, similar to the corresponding chemical shift dispersion seen for apoLp-III<sup>23</sup>, a 166-residue, structurally related exchangeable apolipoprotein. In the  $^{15}\text{N}$  dimension, amide proton chemical shift ranges from 104 ppm to 126 ppm. Taken together, these results suggest that complete assignment of this protein by multinuclear multidimensional NMR techniques is feasible. Hence, it should be possible to generate a solution structure for rApoE3(1-183) and investigate conformational changes and dynamic interactions which occur upon lipid-binding. It is noteworthy that such investigations are not possible using X-ray crystallography since, to date, crystallization of apoE in complex with lipid has not been reported.

## 2.5 Bibliography

---

1. Breiter, D.R., Kanost, M.R., Benning, M.M., Wesenberg, G., Law, J.H., Wells, M.A., Rayment, I. & Holden, H.M. Molecular structure of an apolipoprotein determined at 2.5-Å resolution. *Biochemistry* **30**, 603-608 (1991).
2. Blacklock, B.J. & Ryan, R.O. Hemolymph lipid transport. *Insect Biochem. Mol. Biol.* **24**, 855-873 (1994).
3. Ryan, R.O., Schieve, D., Wientzek, M., Narayanaswami, V., Oikawa, K., Kay, C.M. & Agellon, L.B. Bacterial expression and site directed mutagenesis of a functional recombinant apolipoprotein. *J. Lipid Res.* **36**, 1066-1072 (1995).
4. Schumaker, V.N. & Puppione, D.L. Sequential floatation ultracentrifugation. *Methods Enzymol.* **128**, 155-170 (1986).
5. Prasad, S.V., Ryan, R.O., Law, J.H. & Wells, M.A. Changes in lipoprotein composition during larval-pupal metamorphosis of an insect, *Manduca sexta*. *J. Biol. Chem.* **261**, 558-562 (1986).
6. Ryan, R.O., Senthilathipan, K.R., Wells, M.A. & Law, J.H. Facilitated diacylglycerol exchange between insect hemolymph lipophorins. Properties of *Manduca sexta* lipid transfer particle. *J. Biol. Chem.* **263**, 14410-14415 (1988).
7. Wernette-Hammond, M.E., Lauer, S.J., Corsini, A., Walker, D., Taylor, J.M. & Rall, S.C., Jr. Glycosylation of human apolipoprotein E. The carbohydrate attachment site is threonine 194. *J. Biol. Chem.* **264**, 9094-9101 (1989).
8. Singh, T.K.A., Scraba, D.G. & Ryan, R.O. Conversion of human low density lipoprotein into a very low density lipoprotein-like particle in vitro. *J. Biol. Chem.* **267**, 9275-9280 (1992).
9. Ryan, R.O., Oikawa, K. & Kay, C.M. Conformational, thermodynamic, and stability properties of *Manduca sexta* apolipoprotein III. *J. Biol. Chem.* **268**, 1525-1530 (1993).
10. Wientzek, M., Kay, C.M., Oikawa, K. & Ryan, R.O. Binding of insect apolipoprotein III to dimyristoylphosphatidylcholine vesicles. Evidence for a conformational change. *J. Biol. Chem.* **269**, 4605-4612 (1994).
11. Kay, L.E., Keifer, P. & Saarinen, T. Pure absorption gradient enhanced heteronuclear single quantum correlation spectroscopy with improved sensitivity. *J. Am. Chem. Soc.* **114**, 10663-10665 (1992).
12. Zhang, O., Kay, L.E., Olivier, J.P. & Forman-Kay, J.D. Backbone <sup>1</sup>H and <sup>15</sup>N resonances of the N-terminal SH3 domain of drk in folded and unfolded

- states using enhanced-sensitivity pulsed field gradient NMR techniques. *J. Biomol. NMR* **4**, 845-858 (1994).
13. Laemmli, U.K. Cleavage of structural proteins during the assembly of the head of bacteriophage T4. *Nature* **227**, 680-685 (1970).
  14. Wilson, C., Wardell, M.R., Weisgraber, K.H., Mahley, R.W. & Agard, D.A. Three-dimensional structure of the LDL receptor-binding domain of human apolipoprotein E. *Science* **252**, 1817-1822 (1991).
  15. Perczel, A., Hollosi, M., Tusnady, G. & Fasman, G.D. Convex constraint analysis: a natural deconvolution of circular dichroism curves of proteins. *Prot. Engineering* **4**, 669-679 (1991).
  16. Innerarity, T.L., Friedlander, E.J., Rall Jr., S.C., Weisgraber, K.H. & Mahley, R.W. The receptor-binding domain of human apolipoprotein E: Binding of apolipoprotein E fragments. *J. Biol. Chem.* **258**, 12341-12347 (1983).
  17. Ryan, R.O., Wessler, A.N., Price, H.M., Ando, S. & Yokoyama, S. Insect lipid transfer particle catalyzes bidirectional vectorial transfer of diacylglycerol from lipophorin to human low density lipoprotein. *J. Biol. Chem.* **265**, 10551-10555 (1990).
  18. Aggerbeck, L.P., Wetterau, J.R., Weisgraber, K.H., Wu, C.C. & Lindgren, F.T. Human apolipoprotein E3 in aqueous solution: II. Properties of the amino- and carboxyl-terminal domains. *J. Biol. Chem.* **263**, 6249-6258 (1988).
  19. Vogel, T., Weisgraber, K.H., Zeevi, M.I., Ben-Artzi, H., Levanon, A.Z., Rall, S.C., Jr, Innerarity, T.L., Hui, D.Y., Taylor, J.M. & Kanner, D. Human apolipoprotein E expression in *Escherichia coli*: structural and functional identity of the bacterially produced protein with plasma apolipoprotein E. *Proc. Natl. Acad. Sci. USA* **82**, 8696-8700 (1985).
  20. Lalazar, A., Ou, S.I. & Mahley, R.W. Human Apolipoprotein E: Receptor binding activity of truncated variants with carboxyl-terminal deletions. *J. Biol. Chem.* **264**, 8447-8450 (1989).
  21. Dong, L.M., Wilson, C., Wardell, M.R., Simmons, T., Mahley, R.W., Weisgraber, K.H. & Agard, D.A. Human apolipoprotein E. Role of arginine 61 in mediating the lipoprotein preferences of the E3 and E4 isoforms. *J. Biol. Chem.* **269**, 22358-22365 (1994).
  22. Weisgraber, K.H. Apolipoprotein E distribution among human plasma lipoproteins: role of the cysteine-arginine interchange at residue 112. *J. Lipid Res.* **31**, 1503-1511 (1990).
  23. Wang, J., Gagné, S., Sykes, B.D. & Ryan, R.O. Insight into lipid surface recognition and reversible conformational adaptation of an exchangeable

apolipoprotein by multidimensional heteronuclear NMR techniques. *J. Biol. Chem.* **272**, 17912-17920 (1997).

## Chapter 3

### **Human Apolipoprotein E N-terminal Domain Displacement of Apolipoprotein III from Insect Low Density Lipoprotein Creates a Receptor-Competent Hybrid Lipoprotein\***

---

\*A version of this chapter has been published.

Fisher, C.A., Kiss, R.S., Francis, G.A., Gao, P., and Ryan, R.O. (1999) Human apolipoprotein E N-terminal domain displacement of apolipoprotein III from insect low density lipoprotein creates a receptor-competent hybrid lipoprotein. *Biochem. Cell. Biol.* 75: 45-53.



### **3.1 Introduction**

---

The fact that neither full length apoE nor the isolated N-terminal domain is active as a receptor ligand in the absence of lipid suggests that lipoprotein binding induces a conformational change in the protein that confers receptor binding competence<sup>1</sup>. Upon incubation with isolated human plasma lipoproteins, however, the isolated apoE3 N-terminal domain does not form a stable binding interaction<sup>2</sup>. By contrast, the apoE N-terminal domain does associate with dimyristoylphosphatidylcholine, forming bilayer disc particles which function as an effective ligand for the LDL receptor (LDLr) on fibroblasts<sup>3</sup>.

Given the importance of lipid association for manifestation of its biological properties, we investigated the relative lipid binding affinity of the N-terminal domain of apoE3 versus other, well characterized, exchangeable apolipoproteins. To examine this question, we conducted displacement experiments using *Manduca sexta* LDLp as a template. Our results reveal that apoE3 N-terminal domain (residues 1-183) effectively displaces the exchangeable apolipoprotein, apoLp-III, from the surface of LDLp, creating a hybrid lipoprotein which manifests LDLr binding competence.

### **3.2 Material and Methods**

---

#### **Isolation of Lipoproteins and Apolipoproteins**

Recombinant apoE3(1-183) was produced according to Chapter 2. Recombinant apoLp-III was generated as described by Ryan et al.<sup>4</sup> ApoA-I was isolated according to Yokoyama et al.<sup>5</sup> LDLp was isolated from hemolymph of adult *M. sexta* following administration of 20 pmol adipokinetic hormone according to Ryan et al.<sup>6</sup> LDL was isolated from fresh human plasma by sequential ultracentrifugation. Human LDL (5 mg protein in 0.4 M glycine, pH 10) was radioiodinated according to Langer et al.<sup>7</sup> The specific activity of the <sup>125</sup>I-LDL was 100 - 200 cpm/ng LDL protein.

### **Apolipoprotein Displacement Studies**

Two mg isolated LDLp protein were incubated for 1 h at 37° C in the presence of indicated amounts of a given exchangeable apolipoprotein. All incubations were carried out in phosphate buffered saline (PBS; 100 mM sodium phosphate, pH 7.0, 150 mM NaCl, 5 mM EDTA). Following incubation, the sample was adjusted to a density of 1.31 g/ml with KBr (2.5 ml volume), overlaid with 2.5 ml 0.9 % NaCl and subjected to density gradient ultracentrifugation in a Beckman VTi 65. 2 rotor at 65,000 rpm for 70 min at 4° C. The LDLp fraction was collected, dialyzed into PBS and analyzed by SDS-PAGE. Gels were stained with Coomassie Blue R-250 and, following scanning, the intensity of the bands were quantified using the program Image Gauge (Fuji Photo Film Co. Ltd.). The values obtained for each lane were normalized with respect to the intensity of apolipophorin II, one of two non-exchangeable apolipoproteins present on the surface of LDLp.

### **Receptor Binding Assay**

As per Chapter 2.

## **3.3 Results and Discussion**

Insect LDLp is a well characterized lipoprotein particle that contains two nonexchangeable apolipoproteins (one copy of each per particle) termed apolipophorin I ( $M_r \sim 240,000$ ) and apolipophorin II ( $M_r \sim 80,000$ )<sup>8</sup>. In addition, LDLp contains up to 16 copies of the exchangeable apolipoprotein, apoLp-III. It is known that apoLp-III binds reversibly to the surface of LDLp as a function of particle diacylglycerol content<sup>9-11</sup>. Studies of apoLp-III interaction, however, suggest it binds superficially to spherical lipoprotein surfaces<sup>12</sup>. Using a displacement assay, we examined the ability of isolated human apoE3(1-183) to compete for binding sites occupied by apoLp-III on the surface of LDLp.

### Displacement of ApoLp-III from LDLp by ApoE3(1-183)

Incubation of recombinant apoE3(1-183) with LDLp *in vitro* resulted in a concentration dependent, saturable displacement of apoLp-III from the particle surface (Fig. 3-1).

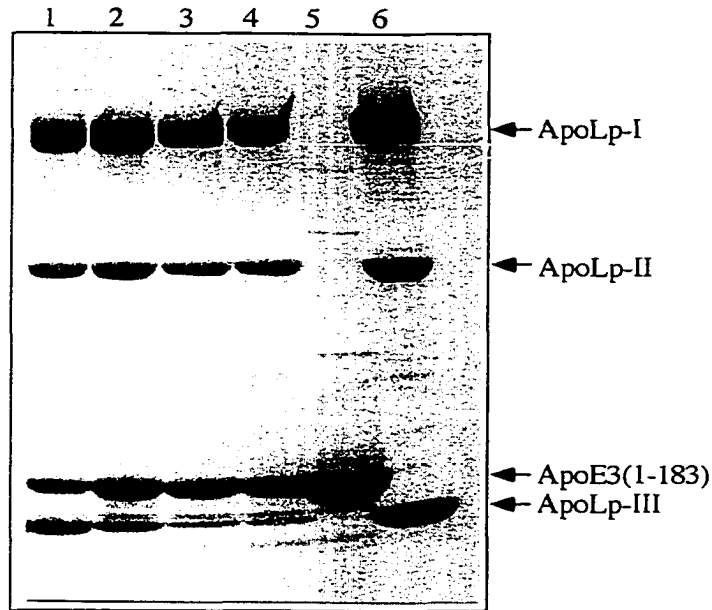


**Fig. 3-1** Effect of exogenous apoE3(1-183) on the apolipoprotein composition of LDLp. LDLp (2 mg protein) was incubated with given amounts of apoE3(1-183) for 1 h at 37 °C (lanes 1 - 4). LDLp was then re-isolated by density gradient ultracentrifugation and its apolipoprotein composition analyzed by electrophoresis under denaturing conditions on a 4 - 20 % acrylamide gradient slab gel. Lane 1) 0.25 mg apoE3(1-183); lane 2) 0.5 mg apoE3(1-183); lane 3) 1.0 mg apoE3(1-183); lane 4) 2.0 mg apoE3(1-183); lane 5) apoE3(1-183) standard, and Lane 6) LDLp control.

At higher concentrations of apoE3(1-183) nearly all apoLp-III was replaced by apoE3(1-183). There was no change in the relative amounts of apoLp-I or apoLp-II. These data suggest that apoE3(1-183) has a higher lipid binding affinity for the surface of LDLp than its natural component, apoLp-III. Control experiments showed that free apolipoproteins do not contaminate the lipoprotein fraction obtained following density gradient ultracentrifugation (data not shown). As the content of apoE3(1-183) bound to LDLp increased, there was a concomitant decrease in the band corresponding to apoLp-III indicating that apoE3(1-183) can compete for binding sites occupied by apoLp-III.

Quantification of the gel bands by densitometry revealed that the amount of apoLp-III associated with LDLp decreased in a linear manner between 0 and 1 mg apoE3(1-183), when normalized against the amount of the non-exchangeable apolipoprotein component, apolipoprotein II. At concentrations above 1 mg, no further displacement of apoLp-III was detected. Following maximum displacement, the apoE3(1-183) band remained relatively constant, consistent with the concept that only a limited number of binding sites are available. Under conditions where excess apoE3(1-183) is present, a small amount of apoLp-III remains associated with LDLp, consistent with the previous finding that two molecules of apoLp-III present on the high density lipoprotein precursor of LDLp are nonexchangeable<sup>11</sup>. To determine if the results obtained above may have been influenced by the experimental design, we isolated apoE3(1-183)-LDLp and determined if bound apoE3(1-183) could be displaced by incubation with increasing amounts of exogenous apoLp-III. ApoE3(1-183)-LDLp was prepared as described above, incubated with increasing amounts of apoLp-III and, following re-isolation, the lipoprotein examined for apolipoprotein exchange. Under all conditions studied, apoLp-III was unable to displace apoE3(1-183) from the particle surface, even in the presence of a large excess of apoLp-III (data not shown). These data corroborate the findings reported in Fig. 3-1 supporting the conclusion that apoE3(1-183) has an intrinsically higher lipid binding affinity than *M. sexta* apoLp-III.

#### **ApoA-I Displacement of ApoE3(1-183) from the Surface of ApoE3(1-183)-LDLp**

In a previous study, we demonstrated that human apoA-I has a higher lipoprotein binding affinity than apoLp-III<sup>13</sup>. To assess the relative lipid binding affinity of human apoA-I versus the N-terminal domain of apoE, apoE3(1-183)-modified LDLp was incubated with exogenous apoA-I, reisolated and the apolipoprotein content assessed by SDS-PAGE (Fig. 3-2).

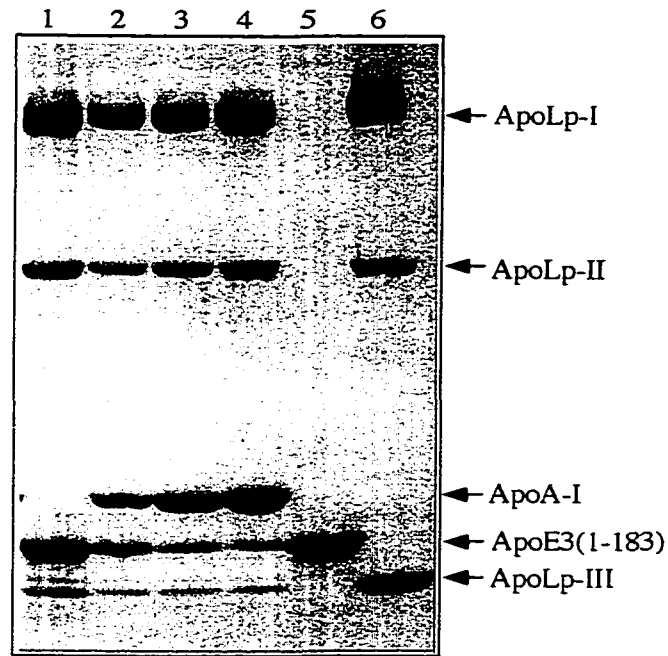


**Fig. 3-2** Effect of exogenous apoA-I on the apolipoprotein composition of apoE3(1-183)-LDLp. ApoE3(1-183)-LDLp (2 mg protein) was incubated with given amounts of apoA-I for 1 h at 37 °C (lanes 2 - 4). The modified LDLp was reisolated by density gradient ultracentrifugation and its apolipoprotein composition analyzed by SDS-PAGE on a 4 - 20 % gradient slab gel. Lane 1) apoE3(1-183)-LDLp control; lane 2) 0.15 mg apoA-I; lane 3) 0.3 mg apoA-I; lane 4) 1.0 mg apoA-I; lane 5) apoE3(1-183) standard and lane 6) LDLp standard.

When increasing amounts of apoA-I were incubated with apoE3(1-183)-modified LDLp, a concentration dependent displacement of apoE3(1-183) from the particle surface occurred. Following incubation and re-isolation, apoA-I was the major exchangeable apolipoprotein on the particle surface, suggesting it has a higher lipid binding affinity than apoE3(1-183). Quantification of the gel bands by densitometry revealed that the amount of apoE3(1-183) associated with LDLp decreased in a linear manner between 0 and 0.3 mg apoA-I, when normalized against the amount of the non-exchangeable apolipoprotein component, apolipoprotein II. At concentrations above 0.3 mg apoA-I, further displacement of apoE was not observed. These results are supported by further experiments wherein an apoA-I-LDLp hybrid lipoprotein was incubated with increasing amounts of exogenous apoE3(1-183). In this experiment, apoE3(1-183) was unable to displace human apoA-I, although a small amount of apoE3(1-183) was

recovered in the LDLp fraction in these experiments. The data indicate that the relative lipid binding affinities of the apolipoproteins investigated in this study are apoA-I > apoE3(1-183) > apoLp-III.

### Competition Binding Assays

Fig. 3-3 shows the results of a competition binding assay in which LDLp was incubated with equal amounts of exogenous apoE3(1-183) and apoA-I. Following incubation, LDLp was re-isolated by density gradient ultracentrifugation and its apolipoprotein composition evaluated by SDS-PAGE. Similar to the results obtained above, apoA-I binds preferentially to the surface of LDLp, out competing apoE3(1-183) for binding sites originally occupied by apoLp-III.

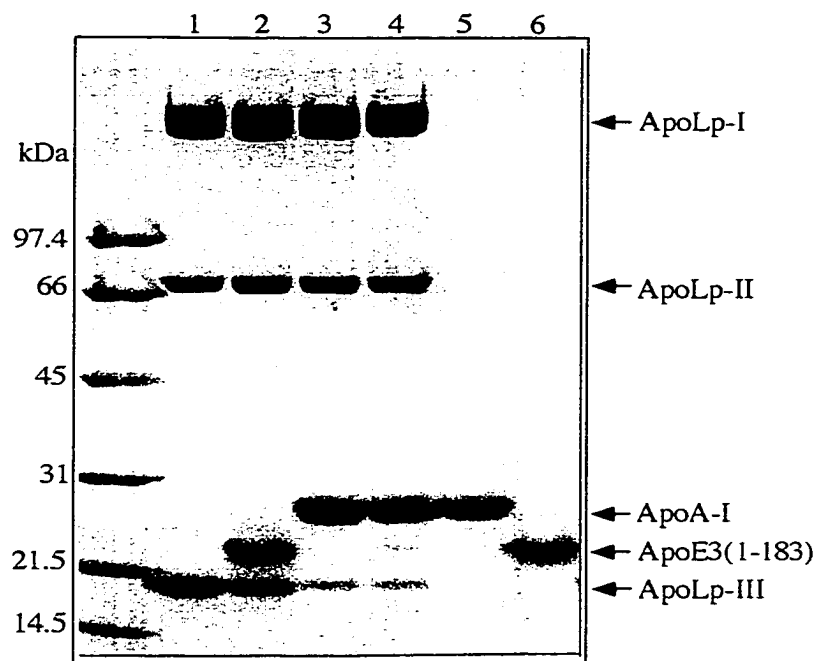


**Fig. 3-3** Effect of exogenous apolipoproteins on the protein composition of LDLp. LDLp (2 mg protein) was incubated with 1.0 mg each of apoE3(1-183) and apoA-I for 1 h at 37 °C. The modified LDLp was reisolated by density gradient ultracentrifugation and its apolipoprotein composition analyzed by SDS-PAGE on a 4 - 20 % gradient slab gel. Lane 1) control LDLp; lane 2) apoE3(1-183)-LDLp standard; lane 3) apoA-I-LDLp standard; lane 4) LDLp plus apoE3(1-183) and apoA-I; lane 5) apoA-I standard and lane 6) apoE3(1-183) standard.

### ApoE3(1-183)-modified LDLp Binding to the LDL Receptor on Cultured Fibroblasts

An important property of apoE3(1-183) is its role as a ligand for cell surface lipoprotein receptors. Since the present system offers a unique opportunity to characterize the receptor binding properties of apoE3(1-183) or mutants bound to a spherical lipoprotein, we investigated the receptor binding properties of hybrid LDLp particles containing apoE3(1-183). The ability of various lipoprotein substrates to compete for binding of  $^{125}\text{I}$ -LDL to receptors on cultured human skin fibroblasts was determined (Fig. 3-4).

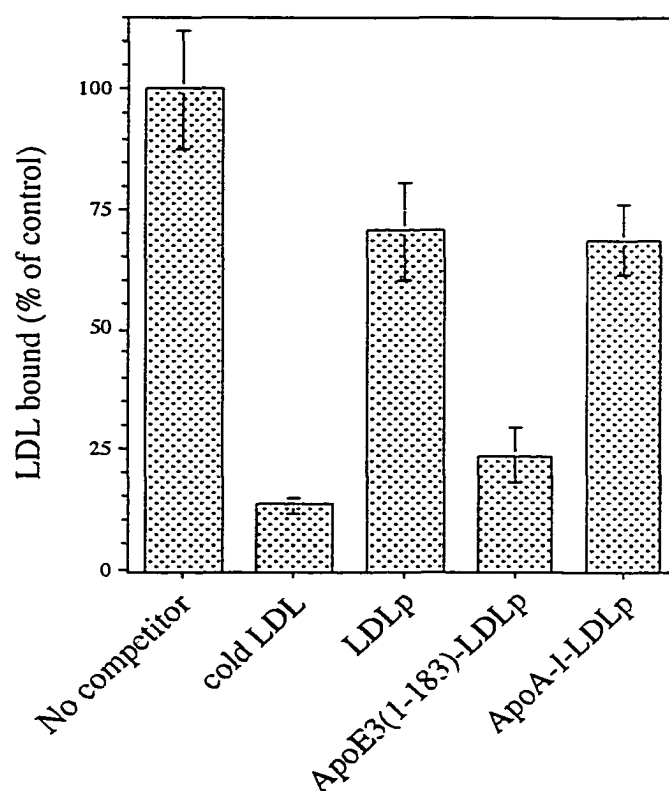


**Fig. 3-4** The ability of natural and hybrid LDLp to compete with  $^{125}\text{I}$ -LDL for binding to cultured human skin fibroblasts.  $^{125}\text{I}$ -LDL (2  $\mu\text{g}/\text{ml}$ ), alone or in the presence of competitor lipoprotein, were added to cell dishes. Incubations were carried out at 4  $^{\circ}\text{C}$  for 2 h followed by determination of cell-associated radioactivity and protein as described in Materials and Methods. Unlabeled competitor LDL concentration was 100  $\mu\text{g}/\text{ml}$  (maximum competition). LDLp and hybrid LDLp competitor lipoprotein concentrations were 25  $\mu\text{g}/\text{ml}$ .

In the absence of competitor lipoprotein, efficient binding of  $^{125}\text{I}$ -LDL was seen. When incubated with an excess of unlabeled LDL, a dramatic decrease in cell-associated radioactivity was observed. While natural LDLp and apoA-I-LDLp were poor competitors for  $^{125}\text{I}$ -LDL binding, apoE3(1-183)-LDLp was an effective competitor in this assay system. In other experiments the ability of apoE3(1-183)-LDLp to compete with  $^{125}\text{I}$ -LDL was found to be concentration dependent and saturable. Also, apoE3(1-183)-LDLp displayed a stronger ability to compete with  $^{125}\text{I}$ -LDL for receptor binding than an equivalent amount of cold LDL (data not shown), indicating that apoE3(1-183)-LDLp was a better ligand. Taken together, these results show that when apoE3(1-183) associates with the surface of LDLp, it adopts a biologically active conformation. Thus, this system can be used to evaluate the receptor binding properties of apoE3(1-183) on the surface of spherical lipoprotein particles.

An advantage of the present system relates to the ability to add apoE3(1-183) units incrementally to the lipoprotein surface. This should allow for investigation of the effect of multiple apoE3(1-183) on a given particle to modulate receptor binding affinity. It is noteworthy that Pitas et al.<sup>14</sup>, using apoE-phospholipid disc complexes, showed that particles containing only one active apoE had a lower binding affinity for the LDL receptor on fibroblasts than discs possessing two, three or four active apoE per particle. Likewise, in studies of LDL receptor-related protein (LRP) binding, Kowal et al.<sup>15,16</sup> found that enrichment of  $\beta$ -VLDL with apoE was required to create an effective ligand. The present study also suggests that an intrinsically higher lipid binding affinity of apoE versus apoLp-III may be responsible for the ability of baculovirus-mediated expression of human apoE in *M. sexta* to generate apoE-containing lipophorin particles which bind to the LDL receptor<sup>17</sup>. Further studies of hybrid LDLp particles containing apoE mutants should reveal additional details of apoE-receptor interactions.



### 3.4 Bibliography

---

1. Weisgraber, K.H. Apolipoprotein E distribution among human plasma lipoproteins: role of the cysteine-arginine interchange at residue 112. *J. Lipid Res.* **31**, 1503-1511 (1990).
2. Innerarity, T.L., Pitas, R.E. & Mahley, R.W. Binding of arginine-rich (E) apoprotein after recombination with phospholipid vesicles to the low density lipoprotein receptors of fibroblasts. *J. Biol. Chem.* **254**, 4186-4190 (1979).
3. Innerarity, T.L., Friedlander, E.J., Rall Jr., S.C., Weisgraber, K.H. & Mahley, R.W. The receptor-binding domain of human apolipoprotein E: Binding of apolipoprotein E fragments. *J. Biol. Chem.* **258**, 12341-12347 (1983).
4. Ryan, R.O., Schieve, D., Wientzek, M., Narayanaswami, V., Oikawa, K., Kay, C.M. & Agellon, L.B. Bacterial expression and site directed mutagenesis of a functional recombinant apolipoprotein. *J. Lipid Res.* **36**, 1066-1072 (1995).
5. Yokoyama, S., Tajima, S. & Yamamoto, A. The process of dissolving apolipoprotein A-I in aqueous buffer. *J. Biochem.* **91**, 1267-1272 (1982).
6. Ryan, R.O., Prasad, S.V., Henriksen, E.J., Wells, M.A. & Law, J.H. Lipoprotein interconversions in an insect, *Manduca sexta*. Evidence for a lipid transfer factor in the hemolymph. *J. Biol. Chem.* **161**, 563-568 (1986).
7. Langer, T., Strober, W. & Levy, R.I. The metabolism of low density lipoprotein in familial Type II hyperlipoproteinemia. *J. Clin. Invest* **51**, 1528-1536 (1972).
8. Blacklock, B.J. & Ryan, R.O. Hemolymph lipid transport. *Insect Biochem. Mol. Biol.* **24**, 855-873 (1994).
9. Wang, J., Liu, H., Sykes, B.D. & Ryan, R.O. Localization of two distant microenvironments for the diacylglycerol component of lipophorin particles by  $^{13}\text{C}$ -NMR. *Biochemistry* **34**, 6755-6761 (1995).
10. Wang, J., Liu, H., Sykes, B.D. & Ryan, R.O.  $^{31}\text{P}$ -NMR study of the phospholipid moiety of lipophorin subspecies. *Biochemistry* **31**, 8706-8712 (1992).
11. Wells, M.A., Ryan, R.O., Kawooya, J.K. & Law, J.H. The role of apolipophorin III in in vivo lipoprotein interconversions in adult *Manduca sexta*. *J. Biol. Chem.* **262**, 4172-4176 (1987).
12. Sahoo, D., Narayanaswami, V., Kay, C.M. & Ryan, R.O. Fluorescence studies of exchangeable apolipoprotein-lipid interactions. Superficial association of

- apolipoprotein III with lipoprotein surfaces. *J. Biol. Chem.* **273**, 1403-1408 (1998).
13. Liu, H., Malhotra, V. & Ryan, R.O. Displacement of apolipoprotein III from the surface of low density lipoprotein by human apolipoprotein A-I. *Biochem. Biophys. Res. Commun.* **179**, 734-740 (1991).
  14. Pitas, R.E., Innerarity, T.L. & Mahley, R.W. Cell surface receptor binding of phospholipid/protein complexes containing different ratios of receptor-active and -inactive E apoprotein. *J. Biol. Chem.* **255**, 5454-5460 (1980).
  15. Kowal, R.C., Herz, J., Goldstein, J.L., Esser, V. & Brown, M.S. Low density lipoprotein receptor-related protein mediates uptake of cholesteryl esters derived from apoprotein E-enriched lipoproteins. *Biochemistry* **86**, 5810-5814 (1989).
  16. Kowal, R.C., Herz, J., Weisgraber, K.H., Mahley, R.W., Brown, M.S. & Goldstein, J.L. Opposing effects of apolipoproteins E and C on lipoprotein binding to low density lipoprotein receptor-related protein. *J. Biol. Chem.* **265**, 10771-10779 (1990).
  17. Gretch, D.G., Sturley, S.L., Friesen, P.D., Beckage, N.E. & Attie, A.D. Baculovirus-mediated expression of human apolipoprotein E in *Manduca sexta* larvae generates particles that bind to the low density lipoprotein receptor. *Proc. Natl. Acad. Sci. USA* **88**, 8530-8533 (1991).

## Chapter 4

### **The LDL Receptor Active Conformation of Apolipoprotein E. Helix Organization in N-terminal Domain-phospholipid Disc Particles\***

---

\*A version of this chapter has been published.

Raussens, V., Fisher, C.A., Goormaghtigh, E., Ryan, R.O., and Ruyschaert, J-M. (1998) The low density lipoprotein receptor active conformation of apolipoprotein E. Helix organization in N-terminal domain-phospholipid disc particles. *J. Biol. Chem.* **273**: 25825-25830.

Note: C. Fisher was involved in the conception of the project, design of the experiments, interpretation of the data and writing of the manuscript.

## **4.1 Introduction**

---

Like most exchangeable apolipoproteins, the N-terminal domain of apoE is capable of transforming multilamellar vesicles of DMPC into uniform size bilayer disc complexes. Interestingly, in the absence of lipid, the receptor binding region (residues 130 – 150)<sup>1</sup> does not interact with the LDL receptor on fibroblasts<sup>2</sup>. Thus, it is postulated that lipid binding induces a conformational change in this domain which confers receptor recognition properties. A description of the structure and association of apoE N-terminal domain DMPC disc complexes, which mimic lipoprotein complexes containing the full length apoE in terms of receptor binding interactions<sup>3</sup>, is of primary importance in terms of understanding the molecular details of this process.

We have used FTIR-ATR spectroscopy to study the N-terminal domain (residues 1-183) of the apoE3 isoform. First, we evaluated the secondary structure of the protein, both free in solution and complexed with DMPC and compared it to previous measurements<sup>4,5</sup> and with the X-ray structure of the lipid-free protein<sup>6</sup>. Second, using linear dichroism, we provide experimental evidence that apoE3 N-terminal domain  $\alpha$ -helices orient perpendicular to the acyl chains of the lipids in discoidal complexes. Based on these dichroism IR data and geometric considerations, we propose a model of association of the apoE3 N-terminal domain in discoidal complexes and discuss possible implications in terms of the apoE3 structure-function relationship.

## **4.2 Materials and Methods**

---

### **Materials**

DMPC was purchased from Sigma Chemical Co. (St. Louis, MO). Phospholipid (choline) enzymatic colorimetric analysis kit was obtained from Wako Pure Chemical Industries, Ltd. (Osaka, Japan).

### **Purification of Apolipoprotein E3 N-terminal Domain**

Recombinant apoE3(1-183) was produced and isolated according to Chapter 2.

### **Preparation of DMPC:apoE3(1-183) Disc Complexes**

DMPC:apoE3(1-183) complexes were prepared by the cholate dialysis method<sup>7</sup>. Briefly, 2 mg DMPC, dissolved in CHCl<sub>3</sub>, was dried under N<sub>2</sub> to form a thin film. Ninety µl prewarmed (37 °C) sodium cholate (30 mg/ml) was added to create a lipid suspension. The contents were incubated at 37 °C with shaking for 30 min, vortexing every 10 min. Subsequently, 0.9 mg recombinant apoE3(1-183) and buffer were added (final buffer concentration 10 mM Tris, pH 7.4, 140 mM NaCl, 150 nM NaN<sub>3</sub>, 250 nM EDTA) and the mixture incubated at 37 °C for 1 h with shaking. The solution was dialyzed against buffer to remove the cholate. Where necessary, free apolipoprotein was removed by gel permeation chromatography on a Sepharose CL-6B (Pharmacia Biotech) column.

### **Disc Particle Characterization**

ApoE3(1-183):DMPC complexes were subjected to non-denaturing gradient gel electrophoresis on a 4-20 % acrylamide slab with Stokes diameter determined by comparison to the mobility of known standards<sup>8</sup>. Samples for electron microscopy were adsorbed to carbon coated grids and negatively stained with 2 % sodium phosphotungstate, pH 7.0 (ref.<sup>9</sup>). Grids were photographed in a Philips EM 420 operated at 100 kV. Protein assays were performed with the bicinchoninic acid assay (Pierce Chemical Co, Rockford, IL) using bovine serum albumin as the standard. Phospholipid analysis was carried out using an enzyme based-colorimetric assay.

### **Analytical Ultracentrifugation**

A Beckman Model E analytical ultracentrifuge was used for hydrodynamic analysis of apoE3(1-183):DMPC complexes. Samples were dialyzed for 24 h

against 100 mM Tris, pH 7.5, 2.5 M KBr to equilibrate the complexes at a density of 1.21 g/ml. The Rayleigh interference optical system was used for flotation equilibrium experiments using the high speed equilibrium technique described by Nelson et al.<sup>10</sup> Runs were performed at 18,000 rpm at 293 K in a double sector, charcoal-filled Epon sample cell equipped with sapphire windows for a minimum of 48 h before equilibrium photographs were taken. Molecular mass calculations were carried out using an APL computer program. The  $\ln Y$  versus  $r^2$  data were fitted to a second order polynomial equation using least squares techniques, and the apparent weight average molecular mass was calculated from the slope of the resulting plot.

### **IR spectroscopy**

Spectra were recorded on a Bruker IFS 55 infrared spectrophotometer equipped with a reflectance accessory and a polarizer mount assembly with a gold wire grid element. The internal reflection element was a germanium ATR plate (50x20x2 mm, Harrick EJ2121) with an aperture angle of 45° yielding 25 internal reflections. 256 accumulations were performed to improve the signal/noise ratio. The spectrophotometer was continuously purged with air dried on a silica gel column (5x130 cm). Spectra were recorded at a nominal resolution of 2 cm<sup>-1</sup>. All the measurements were made at 30° C. Prior to any analysis, the side-chain contributions to the spectra were subtracted according to Goormaghtigh et al.<sup>11</sup>

### **Sample preparation**

Oriented multilayers were formed by slow evaporation of ~ 50 µl of the sample (~2 mg/ml) on one side of the ATR plate. The ATR plate was then sealed in a universal sample holder. The basic FTIR setup is depicted in **Fig. 4-1**.

### Secondary structure determination

Secondary structure quantification was performed on samples subjected to 1 h deuteration as described previously<sup>12</sup>. Briefly, Fourier self-deconvolution was applied to increase the resolution of the spectra in the amide I region. Least squares iterative curve fitting was performed to fit different components of the amide I band revealed by the self-deconvolution to the non deconvolved spectrum between 1700 and 1600  $\text{cm}^{-1}$ . The proportion of various structural elements was computed as reported<sup>12</sup>.

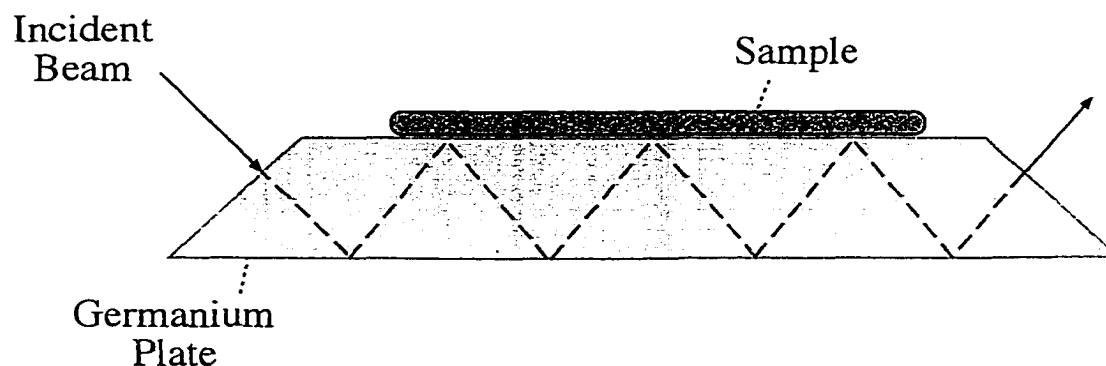


**Fig. 4-1** Basic FTIR setup. An incident beam is depicted entering the crystal in which internal reflection occurs. At the crystal-sample interface, absorption occurs due to interaction with the beam's evanescent field.

### Orientation of the secondary structure

For the amount of material used in the present studies, film thickness remains small when compared to the IR wavelength. This allows the "thin film" approximation to be used for establishment of equations describing the dichroic ratio as a function of the orientational order parameter<sup>13</sup>. In an  $\alpha$ -helix, the main transition dipole moment lies approximately parallel to the helical axis. It is therefore possible to determine the mean orientation of the  $\alpha$ -helix structure from the orientation of the peptide bond C=O group<sup>13</sup>. To obtain this information, additional spectra were recorded with parallel and perpendicular polarized incident light with respect to a normal to the ATR

plate (the plane the incident IR beam makes upon passage through the crystal has the same orientation). Polarization was expressed as the dichroic ratio  $R_{\text{ATR}} = A''/A^\perp$ . The mean angle between the helix axes and a normal to the ATR plate surface was then calculated from  $R_{\text{ATR}}$ . In these calculations, a  $27^\circ$  angle between the long axis of the  $\alpha$ -helix and the C=O dipole moment was considered<sup>13,14</sup>. The  $\gamma_w(\text{CH}_2)$  transition at  $1203 \text{ cm}^{-1}$  whose dipole lies parallel to the all-*trans* hydrocarbon chains was used to characterize the lipid acyl chain orientation<sup>15</sup>.

When two helix populations (or any other structure) with different orientations are present in a sample, both orientations must be considered in the interpretation of the dichroic ratio. We define the dichroic ratios of helix populations a and b as

$$R_a = \frac{A_a''}{A_a^\perp} \quad \text{and} \quad R_b = \frac{A_b''}{A_b^\perp}$$

and the experimental dichroic ratio is given by

$$R_{\text{exp}} = \frac{A_a'' + A_b''}{A_a^\perp + A_b^\perp}$$

Since the total, unpolarized contribution from populations a and b must remain proportional to the fraction of population a ( $x$ ) and b ( $1-x$ ):

$$\frac{x}{1-x} = \frac{A_a'' + 2A_a^\perp}{A_b'' + 2A_b^\perp}$$

Resolving these equations, we find that

$$R_a = \frac{xR(R_b + 2) + 2(1-x)(R - R_b)}{x(R_b + 2) - (1-x)(R - R_b)}$$



$$R_b = \frac{(1-x)R(R_a + 2) + 2x(R - R_a)}{(1-x)(R_a + 2) - x(R - R_a)}$$

$$x = \frac{(R - R_b)(R_a + 2)}{(R_b + 2)(R_a - R) - (R_a + 2)(R_b - R)}$$

### **4.3 Results and Discussion**

---

#### **ApoE3(1-183):DMPC disc particles**

The cholate dialysis method was employed to prepare apoE3(1-183):DMPC disc complexes. Non-denaturing gradient gel electrophoresis indicated the presence of a uniform population of complexes. Comparison of the relative migration of the complexes versus that of known standards yielded a Stokes diameter of ~11 nm. The morphology of the complexes was investigated by negative stain electron microscopy, revealing disc shaped complexes of a similar diameter. Subsequently, flotation equilibrium experiments were conducted to evaluate the molecular mass of the apoE3(1-183):DMPC discs. Plots of  $\ln Y$  versus  $r^2$  yielded a straight line, indicating one species of complex was present with an apparent molecular weight of 468,000. Compositional analysis of the discs revealed a molar ratio of DMPC:apoE3(1-183) of ~ 200:1.

#### **Secondary Structure Characterization**

Fig. 4-2 displays the IR spectra of a lipid-free apoE3(1-183) sample and apoE3(1-183):DMPC discoidal complexes in the region of 1800-1400  $\text{cm}^{-1}$ .

The amide I band (1700-1600  $\text{cm}^{-1}$ ) reveals a sharp peak centered at 1654  $\text{cm}^{-1}$  for lipid-free apoE3(1-183) and at 1653  $\text{cm}^{-1}$  for the apoE3(1-183):DMPC sample. 1654 and 1653  $\text{cm}^{-1}$  are wavenumbers characteristic of  $\alpha$ -helical structures<sup>14,16</sup>. The maximum intensity of the amide II peaks (1600-1500  $\text{cm}^{-1}$ ) are located at 1547  $\text{cm}^{-1}$ , a region normally assigned to helical structures<sup>14,16</sup>. Quantification of secondary structure conformers present was

performed on samples subjected to deuteration for 1h. Partial deuteration of the sample allows for discrimination between the relative contributions of random coil and  $\alpha$ -helix. The percentage of helical secondary structure reaches 65% for lipid-free apoE3(1-183) and 60% for the protein in complex with DMPC (**Table 4-1**).

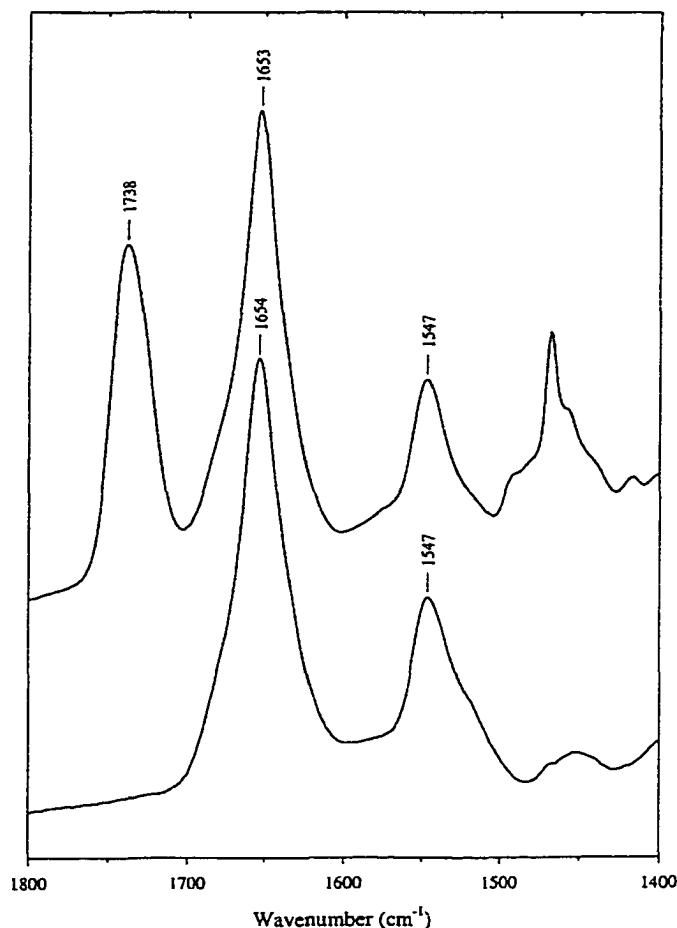


**Fig. 4-2** IR spectra of lipid-free apoE3(1-183) in 10 mM phosphate buffer (pH 7.4) (bottom spectrum) and of apoE3(1-183):DMPC disc complexes (upper spectrum) in the 1800-1400  $\text{cm}^{-1}$  region. Measurements were made at 30°C.

Similar amounts of other secondary structure elements were observed in both lipid-free and DMPC-bound apoE3(1-183). Conceivably these arise from the extreme N- and C-terminal regions which were disordered in the crystal<sup>6</sup>.

**Table 4-1.** Secondary structure components in apoE3(1-183) as determined by self-deconvolution and curve fitting of apoE3(1-183) IR spectra in the DMPC-bound and lipid-free states, as described in Materials and Methods.

	$\alpha$ -helix	$\beta$ -sheet	turn	coil
ApoE3(1-183):DMPC	60%	15%	3%	22%
Lipid-free apoE3(1-183)	65%	14%	5%	16%

The 65%  $\alpha$ -helix content determined for apoE3(1-183) by ATR-FTIR spectroscopy is in good agreement with data obtained by CD and FTIR<sup>4,5</sup>. Using the DSSP algorithm<sup>17</sup> to analyze the X-ray atomic coordinates of the protein in the pdb file (1lpe), five discrete  $\alpha$ -helical segments were identified. Four of these, designated H1 - H4, constitute the bundle and range in length from 17 to 37 residues, while a fifth short helix, H' (residues 45-52) connects H1 and H2 and orients perpendicular to the bundle axis. Thus, 118 of the 183 amino acids present are in a helical conformation (64.5%) and the values derived from FTIR analysis (65%) are in very good agreement with corresponding values determined from the X-ray crystal structure.

ApoE3(1-183) complexed with DMPC was found to possess 60%  $\alpha$ -helical structure. While this value is in agreement with data obtained by CD<sup>4</sup>, it is higher than that reported by De Pauw et al.<sup>5</sup> on the basis of CD and FTIR measurements. Our data suggest that there is no real change in the secondary structure content in the N-terminal domain of apoE3 upon binding to lipid with subtle changes observed likely reflecting a change in tertiary structure.

### **Determination of the Orientation of the Helices**

Spectra of apoE3(1-183):DMPC complexes were recorded with parallel and perpendicular polarized light (**Fig. 4-3A** and **4-3B**, respectively; see ref.<sup>13</sup> for the geometry of the experiment). The dichroic spectrum (**Fig. 4-3C**) was obtained by subtracting the spectrum recorded with perpendicular polarized light from the spectrum recorded with parallel polarized light. Initially, the

orientation of DMPC acyl chains in disc complexes was assessed using characteristic bands associated with lipid molecules. Specific spectral bands, such as  $\nu_{as}(\text{CH}_2)$  at  $2916\text{ cm}^{-1}$ ,  $\nu_s(\text{CH}_2)$  at  $2849\text{ cm}^{-1}$  and  $\delta(\text{CH}_2)$  at  $1467\text{ cm}^{-1}$ , whose dipoles orient perpendicular to the hydrocarbon chains of DMPC<sup>15</sup>, displayed a negative deviation in the dichroic spectrum (Fig. 4-3C).

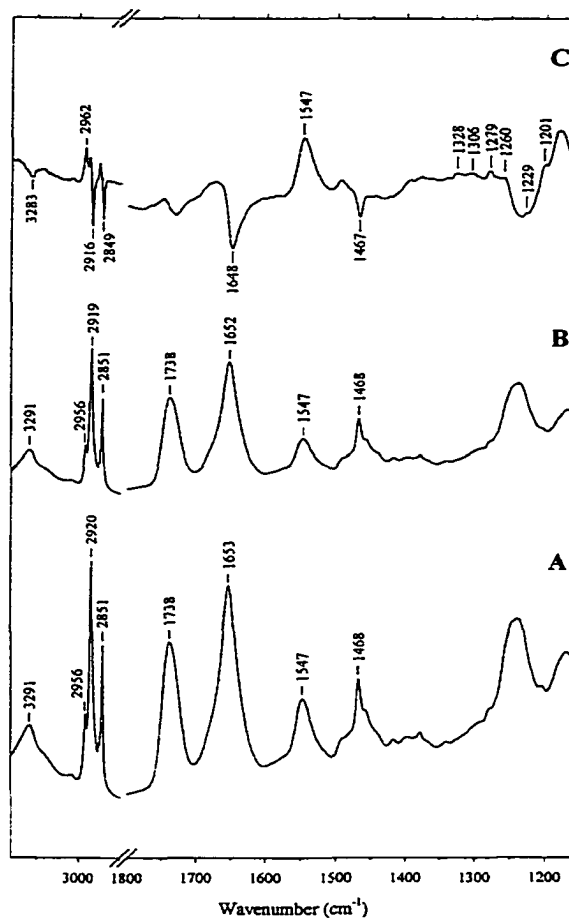


**Fig. 4-3** IR spectra of apoE3(1-183):DMPC complexes. Spectrum A was obtained with parallel polarized light and spectrum B with perpendicular polarized light. Spectrum C is the dichroic spectrum obtained by subtracting spectrum B from spectrum A. The optical density amplitude of spectrum C has been increased five times with respect to spectra A and B. Measurements were made at  $30^\circ\text{C}$ .

This indicates an orientation perpendicular to the normal of the germanium crystal plane. Conversely, bands corresponding to dipoles which orient parallel to the hydrocarbon chains [ $\nu_{as}(\text{CH}_3)$  at  $2962\text{ cm}^{-1}$  and the bands of the  $\gamma_w(\text{CH}_2)$  progression observed for saturated hydrocarbon chains with all-*trans*

configuration at 1328, 1306, 1279, 1260, 1229 and 1201  $\text{cm}^{-1}$ ], had a positive deviation in the dichroic spectrum. Thus, these orient parallel to the normal of the germanium plane. As previously described<sup>18</sup>, we used the last peak in the  $\gamma_w(\text{CH}_2)$  progression peak (1201  $\text{cm}^{-1}$ ) to quantify the lipid chain orientation. The measured dichroic ratio for this band is 4.45 with an isotropic dichroic ratio of 1.67. On the basis of these dichroic ratio measurements we can assume that the maximum tilt between the acyl chains and a normal to the germanium surface is 15 - 20°. Since any additional source of disorder would reduce this tilt<sup>18</sup>, the value of 15 - 20° is a maximum tilt with respect to a normal to the germanium plate. By defining the orientation of a DMPC disc by a normal vector passing through the face of the disc, the results show that the normal vector is oriented parallel to a normal to the germanium plate.

In the case of apoE3(1-183), helix orientation was determined using the amide I band. In the dichroic spectrum (**Fig. 4-3C**), a strong negative deviation at 1648  $\text{cm}^{-1}$  is observed, indicating a parallel orientation of the associated dipole to the surface of the germanium plate and thus, a perpendicular orientation with respect to a vector normal to the face of the disc. From the secondary structure of apoE3(1-183), and the frequency of the negative deviation (1648  $\text{cm}^{-1}$ ), we conclude that the dipole responsible for this deviation is associated with  $\alpha$ -helices which orient in the direction of the helical axes<sup>14</sup>. Thus, the negative deviation observed indicates that the helices are primarily oriented perpendicular to the normal vector of the disc and, therefore, perpendicular to the hydrocarbon chains of the lipids. This helix orientation is confirmed by two additional observations; 1) negative deviation of the amide A band at 3283  $\text{cm}^{-1}$ , for which the dipole orientation is similar to that for the amide I band; and 2) positive deviation of the amide II band (at 1547  $\text{cm}^{-1}$ ), which is oriented in the opposite, perpendicular direction with respect to the helical axes (see refs.<sup>13,14</sup> for a complete discussion of orientation determination in ATR-FTIR).

To quantitatively determine the orientation of the apoE3(1-183) helical segments in the disc complex, we decomposed and curve-fitted the amide I

region of the parallel and perpendicular polarized light spectra (**Fig. 4-3A** and **4-3B**, respectively) with four Lorentzian curves (**Fig.4-4**). Using the main curve associated to the helices (maximum intensity at  $1652\text{ cm}^{-1}$ ), we calculated a dichroic ratio associated with the helical structure in the protein equal to 1.25. With such a dichroic ratio, and assuming that the normal to the disc is parallel to the normal to the plate (see above), the minimum mean tilt between the helical axes and a normal to the face of the DMPC disc is  $60 - 65^\circ$ .

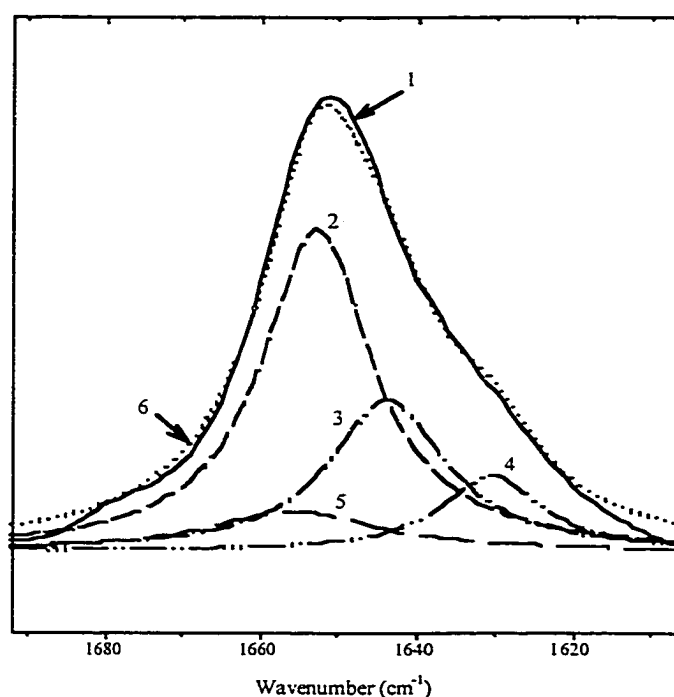


**Fig. 4-4** Decomposition of the amide I region of spectra of apoE3(1-183):DMPC discs obtained with parallel polarized light. Line 1) ATR-FTIR spectrum (Amide I region) of apoE3(1-183):DMPC disc complexes. Curves 2 - 5 correspond to the four components obtained following decomposition of spectrum 1. Curve 6 represents a summation of the four Lorentzian curves showing the goodness of fit of the decomposition procedure. Curve 2, which represents the main helical contribution, was used for the dichroic ratio calculation (see text).

From the X-ray crystal structure of apoE3 N-terminal domain<sup>6</sup> it is recognized that helix H', (the 8 residue helix which connects helix 1 and helix 2 in the bundle) orients perpendicular to the four long helices. Thus, helical

segments in the bundle can be separated into two groups with different orientations. Using the equations described under Materials and Methods, we found that the 1.25 dichroic ratio could also be decomposed into two components with different orientations. A first component representing 92% of the helix content has a 1.11 dichroic ratio while the second, representing the rest of the helix content, has a dichroic ratio of 4.5. It seems reasonable that the 1.11 ratio representing 92% of the helices could be attributed to the four long helices (representing 110 amino acids of a total of 118 in helix conformation), which orient perpendicular to a vector normal to both the face of the disc and the germanium plate (65 - 70° minimum tilt). On the other hand, the dichroic ratio of 4.5 could be attributed to helix H', suggesting this helix orients parallel to the normal vector of the disc, with a maximum tilt of 10 - 15°.

### **Model of Association**

Our results using linear IR dichroism to characterize the orientation of apoE3(1-183) helical segments when bound to DMPC bilayer discs are consistent with a model wherein the four main helices (H1-H4) orient perpendicular with respect to a normal to the face of the discs (and the DMPC acyl chains) while helix H' adopts the opposite orientation. **Fig. 4-5** depicts a model of apoE3(1-183):DMPC discoidal particles in which the helices of the protein align around the periphery of the discoidal phospholipid bilayer, as previously proposed and experimentally demonstrated for insect apoLp-III<sup>18,19</sup>. In solution, the hydrophobic side chains of the amphipathic helices of apoE3(1-183) are oriented toward the interior of the bundle<sup>6</sup>. It has been suggested that, upon lipid interaction, the hydrophobic faces of the helices interact with the hydrophobic acyl chains<sup>1</sup>. This could be accomplished by a conformational change in which the bundle opens, without disruption of the helical boundaries, by pivoting around a hinge region connecting H2 and H3, as proposed by Weisgraber<sup>1</sup>.

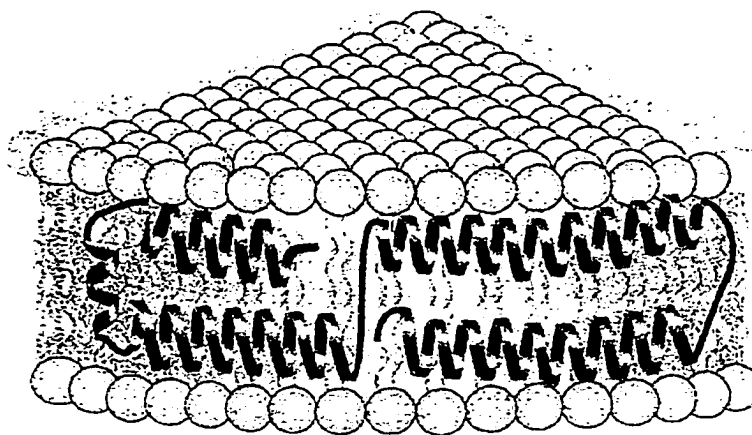


**Fig. 4-5** Model representation of apoE3(1-183) helix orientation and alignment in DMPC disc complexes.

This "open" conformation would expose the hydrophobic faces of individual helices, permitting their direct contact with the lipid surface, specifically phospholipid acyl chains around the perimeter of the disc. In this conformation, the hydrophilic faces of the helices retain contact with the aqueous environment while the hydrophobic faces essentially substitute helix-lipid interactions for the helix-helix interactions which stabilize the bundle<sup>6</sup>.

Our results support this proposed mechanism. First, the absence of a real change in secondary structure content upon lipid binding agrees with the concept that bundle opening occurs without helical disruption. Second, our experimental determination of the orientation of apoE3(1-183)  $\alpha$ -helices in disc complexes agrees with such a model. Even the short helix connecting H1 and H2 seems to adopt the predicted orientation. Third, the following geometric considerations are consistent with this model. The disc particles employed in the present study have a molecular weight of 468,000 and a protein:lipid molar ratio of  $\sim 200:1$ . If each disc particle contained three apoE3(1-183) and 600 DMPC, the calculated molecular mass of the complex would be 470,000, in good agreement with the value determined by flotation equilibrium analysis. In our model, when the bundle opens with helices 1 and 2 on one side and helices 3 and 4 on the other, we estimate that the elongated



structure is about 116 Å long (see figure 4-5). Assuming a helix diameter of 15-17 Å<sup>5</sup>, two helices oriented side by side are large enough to effectively cover the DMPC bilayer thickness. Thus, three elongated, open molecules could cover 348 Å, in agreement with a disc circumference of 345 Å, as derived from gradient gel electrophoresis. In the case of larger diameter discs, it is plausible that additional apoE3(1-183) could be accommodated, adopting a similar orientation.

Recently, De Pauw et al.<sup>5</sup> described the organization of apoE helices in DMPC disc complexes wherein antiparallel 17-residue helices surround the disc, oriented parallel with respect to the lipid chains. Such a model, however, is hard to reconcile with the length of helical segments present in the lipid-free globular conformation of the N-terminal domain (helices 3 and 4 comprise 37 and 32 amino acids, respectively). Indeed, in this case a disruption of the helical segments found in the lipid-free globular conformation, must be imposed. This is likely to be an energetically unfavorable re-orientation and, in the case of helix 4, cannot explain the profound effect of the Arg-Cys interchange (apoE3 and apoE2 isoforms) at position 158 in terms of receptor binding ability<sup>20</sup>. Moreover, using the same geometrical arguments described above, their model is not in agreement with the disc diameter.

The recently reported X-ray crystal structure of a human apolipoprotein A-I N-terminal deletion mutant [(Δ1-43) apoA-I] provides additional support for the model presented in Figure 4-5. Borhani et al.<sup>21</sup> showed that this protein adopts an elongated, horseshoe shape conformation. This structure is predicted to resemble the lipid-associated conformation of apoA-I<sup>22</sup>. Furthermore, the authors suggest that apoA-I may interact with disc particles and spherical high density lipoproteins, forming a "belt" which surrounds the lipid complex. In the case of discs, it is envisaged that two apoA-I molecules could circumscribe the periphery of the disc aligning perpendicular to the phospholipid fatty acyl chains with retention of specific helical pairings observed in the antiparallel dimer seen in the crystal structure of this protein. While our data are consistent with a simple conformational opening of the apoE3(1-183) helix

bundle, they do not exclude a belt configuration wherein paired, extended apoE3(1-183) molecules circumscribe the disc perimeter, as suggested for apoA-I discs<sup>21</sup>.

The model described here represents a first step toward understanding the interactions between apoE3-lipid particles with lipoprotein receptors. Keeping in mind that lipid association is a requirement for high-affinity binding to the LDL receptor<sup>2,3</sup>, the conformational change occurring in the N-terminal, receptor binding domain of apoE3 upon interaction with lipid surfaces is of primary importance. In the absence of modification of the helical structure, we propose that the conformational change is due to a realignment of discrete helical segments, especially the hydrophilic face of helix 4, which contains the amino acids thought to interact with the receptor (amino acids 130-150). Side-chain reorientation could conceivably be attributed to the curvature imposed upon the helices by the disc shape of the particle and/or to the reorientation of the helices with respect to each other when the bundle "opens" and associates with lipid. This rearrangement could modify some of the numerous salt bridges present in the apoE3 N-terminal domain helix bundle conformation<sup>6</sup>. It is noteworthy that the recently determined X-ray crystal structure of the ligand binding repeat 5 of the LDL receptor<sup>23</sup> reveals a concave face which could act as an apoE-lipid particle binding surface. Improved knowledge of the receptor-active conformation of apoE3(1-183) should allow for characterization of the molecular features which modulate receptor-ligand interactions critical to maintenance of plasma lipid homeostasis.

#### 4.4 Bibliography

---

1. Weisgraber, K.H. Apolipoprotein E: structure-function relationships. *Ad. Protein Chem.* **45**, 249-302 (1994).
2. Innerarity, T.L., Pitas, R.E. & Mahley, R.W. Binding of arginine-rich (E) apoprotein after recombination with phospholipid vesicles to the low density lipoprotein receptors of fibroblasts. *J. Biol. Chem.* **254**, 4186-4190 (1979).
3. Innerarity, T.L., Friedlander, E.J., Rall Jr., S.C., Weisgraber, K.H. & Mahley, R.W. The receptor-binding domain of human apolipoprotein E: Binding of apolipoprotein E fragments. *J. Biol. Chem.* **258**, 12341-12347 (1983).
4. Aggerbeck, L.P., Wetterau, J.R., Weisgraber, K.H., Wu, C.C. & Lindgren, F.T. Human apolipoprotein E3 in aqueous solution: II. Properties of the amino- and carboxyl-terminal domains. *J. Biol. Chem.* **263**, 6249-6258 (1988).
5. De Pauw, M., Vanloo, B., Weisgraber, K. & Rosseneu, M. Comparison of lipid-binding and lecithin:cholesterol acyltransferase activation of the amino- and carboxyl-terminal domains of human apolipoprotein E3. *Biochemistry* **34**, 10953-10960 (1995).
6. Wilson, C., Wardell, M.R., Weisgraber, K.H., Mahley, R.W. & Agard, D.A. Three-dimensional structure of the LDL receptor-binding domain of human apolipoprotein E. *Science* **252**, 1817-1822 (1991).
7. Jonas, A. Reconstitution of high-density lipoproteins. *Methods Enzymol.* **258**, 553-582 (1986).
8. Nichols, A.V., Krauss, R.M. & Muslinger, T.A. Nondenaturing polyacrylamide gradient gel electrophoresis. *Methods Enzymol.* **128**, 417-431 (1986).
9. Ryan, R.O., Howe, A. & Scraba, D.G. Studies of the morphology and structure of the plasma lipid transfer particle from the tobacco hornworm, *Manduca sexta*. *J. Lipid Res.* **31**, 871-879 (1990).
10. Nelson, C.A., Lee, J.A., Brewster, M. & Morris, M.D. Flotation equilibrium of serum low density lipoproteins. *Anal. Biochem.* **59**(1974).
11. Goormaghtigh, E., de Jongh, H.H.J. & Ruyschaert, J.-M. Relevance of protein thin films prepared for attenuated total reflection Fourier transform infrared spectroscopy: significance of pH. *Appl. Spectrosc.* **50**, 1519-1527 (1996).

12. Goormaghtigh, E., Cabiaux, V. & Ruyschaert, J.-M. Secondary structure and dosage of soluble and membrane proteins by attenuated total reflection Fourier-transform infrared spectroscopy on hydrated films. *Eur. J. Biochem.* **193**, 409-420 (1990).
13. Goormaghtigh, E. & Ruyschaert, J.-M. in *Molecular description of biological membrane components by computer aided conformational analysis* (ed. Brasseur, R.) 285-329 (CRC Press, Boca Raton, FL, 1990).
14. Goormaghtigh, E., Cabiaux, V. & Ruyschaert, J.-M. Determination of soluble and membrane protein structure by Fourier transform infrared spectroscopy. *Subcell. Biochem.* **23**, 329-362 (1994).
15. Fringeli, U.P. & Gunthard, H.H. Infrared membrane spectroscopy. in *Membrane spectroscopy* (ed. Grell, E.) 270-332 (Springer-Verlag, Berlin, 1981).
16. Goormaghtigh, E., Cabiaux, V. & Ruyschaert, J.-M. Determination of soluble and membrane protein structure by Fourier transform infrared spectroscopy: III. Secondary structures. *Subcell. Biochem.* **23**, 404-450 (1994).
17. Kabsch, W. & Sander, C. Dictionary of protein secondary structure: pattern recognition of hydrogen-bonded and geometrical features. *Biopolymers* **22**, 2577-2637 (1983).
18. Raussens, V., Narayanaswami, V., Goormaghtigh, E., Ryan, R.O. & Ruyschaert, J.-M. Alignment of the apolipoprotein III  $\alpha$ -helices in complex with dimyristoylphosphatidylcholine. A unique spatial orientation. *J. Biol. Chem.* **270**, 12542-12547 (1995).
19. Wientzek, M., Kay, C.M., Oikawa, K. & Ryan, R.O. Binding of insect apolipoprotein III to dimyristoylphosphatidylcholine vesicles. Evidence for a conformational change. *J. Biol. Chem.* **269**, 4605-4612 (1994).
20. Dong, L.M., Parkin, S., Trakhanov, S.D., Rupp, B., Simmons, T., Arnold, K.S., Newhouse, Y.M., Innerarity, T.L. & Weisgraber, K.H. Novel mechanism for defective receptor binding of apolipoprotein E2 in type III hyperlipoproteinemia. *Nature Struct. Biol.* **3**, 718-722 (1996).
21. Borhani, D.W., Rogers, D.P., Engler, J.A. & Brouillette, C.G. Crystal structure of truncated human apolipoprotein A-I suggests a lipid-bound conformation. *Proc. Natl. Acad. Sci. U.S.A.* **94**(1997).
22. Rogers, D.P., Brouillette, C.G., Engler, J.A., Tendian, S.W., Roberts, L., Mishra, V.K., Anantharamaiah, G.M., Lund-Katz, S., Phillips, M.C. & Ray, M.J. Truncation of the amino terminus of human apolipoprotein A-I

substantially alters only the lipid-free conformation. *Biochemistry* **36**, 288-300 (1997).

23. Fass, D.F., Blacklow, S., Kim, P.S. & Berger, J.M. Molecular basis of familial hypercholesterolaemia from structure of LDL receptor module. *Nature* **388**, 691-693 (1997).

## Chapter 5

### **Lipid Binding-induced Conformational Changes in the N-terminal Domain of Human Apolipoprotein E\***

---

\*A version of this chapter has been published.

Fisher, C.A. and Ryan, R.O. (1999) Lipid binding-induced conformational changes in the N-terminal domain of human apolipoprotein E. *J. Lipid Res.* 40: 93-99.

## 5.1 Introduction

In the absence of lipid, the isolated N-terminal domain is not recognized by the LDL receptor. However, complexation with phospholipids to form discoidal structures results in a particle that binds efficiently to the LDL receptor<sup>1</sup>. This behavior is similar to that observed for full length apoE, which binds to LDL receptors on fibroblasts only after complexation with lipid<sup>2</sup>. These data support the view that a lipid binding-induced conformational adaptation of apoE, which can be effectively mimicked by the isolated N-terminal domain, is an essential feature of apoE function as a ligand for receptor-mediated endocytosis of plasma lipoproteins.

In 1991, Wilson et al.<sup>3</sup> reported the X-ray crystal structure of the 22 kDa N-terminal domain of human apoE3 in the lipid-free state. This structure, which is comprised of a bundle of four elongated amphipathic  $\alpha$ -helices, bears a remarkable similarity in molecular architecture to full length apoLp-III from *Locusta migratoria*<sup>4</sup> and *Manduca sexta*<sup>5</sup>. Structural information on these proteins in the absence of lipid has led to the concept that reversible lipid binding is accompanied by a significant conformational change. A model depicting helix bundle apolipoprotein conformational opening is presented in **Fig. 5-1**. In this model, proposed by Weisgraber<sup>6</sup>, the N-terminal domain exposes its hydrophobic interior by “opening” via a putative hinge region located in the loop between helix 2 and helix 3. Inherent in this model is the prediction that helix 1 and 2 move away from helix 3 and 4 as the bundle “opens”. Evidence in support of a major conformational change upon lipid binding has been obtained from surface area measurements at the air-water interface which indicate the protein occupies more area per amino acid than can be accounted for if the protein retained its globular structure<sup>7</sup>. In the present study we have employed fluorescence resonance energy transfer [FRET; see ref.<sup>8</sup> for a review] to characterize helical repositioning which accompanies lipid binding of this protein domain and compared the data obtained with that predicted by the open conformation model.

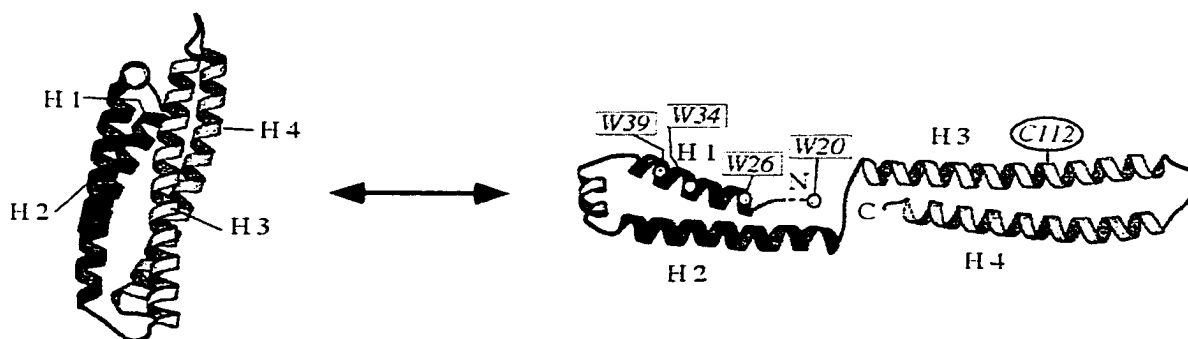


**Fig. 5-1** Model depicting a lipid-association induced conformational change of apoE3 N-terminal domain. The ribbon structure on the left corresponds to the globular lipid-free four helix bundle, established by X-ray crystallography<sup>3</sup>. Conformational opening of the bundle is depicted on the right, with helices 1 and 2 moving away from helix 3 and 4 about a putative hinge region located in the loop between helix 2 and helix 3. Note that the helical boundaries present in the bundle conformation are maintained in the “open” conformation. The position of Trp and Cys residues in the protein are noted. Adapted from Weisgraber<sup>6</sup>.

## 5.2 Materials and methods

### Protein Expression and AEDANS Labeling.

Recombinant apoE3(1-183) was expressed and purified as described in Chapter 2. Isolated protein was stored lyophilized at  $-20^{\circ}\text{C}$ . Five hundred nmoles protein was incubated in 50 mM TrisHCl, pH 8.0, with 0.1 mM dithiothreitol and 500 nmoles N-iodoacetyl-N'-(5-sulfo-1-naphthyl)ethylenediamine (IAEDANS; Molecular Probes, Eugene, OR) at  $37^{\circ}\text{C}$ , 2.5 h in the dark. Unreacted IAEDANS was separated from labeled protein by passage through a Sepharose CL-6B (Pharmacia) column followed by lyophilization. Incorporation of extrinsic fluorophore was confirmed by electro-spray mass spectrometry and/or absorption spectroscopy. That is:

$$\frac{A_{336}}{\epsilon} \times \frac{\text{MW protein}}{[\text{protein}]} = \frac{\text{moles fluorophore}}{\text{moles protein}}$$

where A is the absorbance and  $\epsilon$  is the molar extinction coefficient of the fluorophore. The labeled apoE sample displayed characteristic fluorescence



properties of AEDANS, including an excitation maximum of 336 nm and an emission maximum of 478 nm.

### Fluorescence Measurements

For FRET experiments, protein samples were excited at 295 nm and emission spectra were recorded from 300 nm to 575 nm on a Perkin Elmer Luminescence Spectrometer LS50, using 3-8 nm slit widths for both excitation and emission. Wild-type and AEDANS-apoE3(1-183) samples were dissolved in 50 mM sodium phosphate, pH 7.0. All spectra were recorded at 20 °C. Prior to measurement, samples were allowed to equilibrate to holder temperature for 10 min. Blank spectra were generated from identical solutions lacking protein and were subtracted from spectral data. Corrections for dilutions were made where necessary. Where indicated, AEDANS•apoE3(1-183) was incubated with the appropriate concentration of guanidine HCl, trifluoroethanol (TFE) or detergent for 30 min at room temperature prior to analyses. ApoE3(1-183)-DMPC complexes were formed as described in chapter 2.

### Intramolecular Distance Calculations

The efficiency ( $E$ ) of energy transfer was calculated as follows:

$$E = 1 - \frac{Q_{DA}}{Q_D}$$

where  $Q_D$  and  $Q_{DA}$  is the quantum yield of the donor in the absence and presence of acceptor, respectively.

The distance between energy donor and acceptor ( $R$ ) is,

$$R = R_0 \left( \frac{1}{E} - 1 \right)^{\frac{1}{6}}$$

where  $R_0$  is the distance at which the transfer efficiency is 50%,

$$R_0 = 9.765 \times 10^3 (k^2 J Q_D n^{-4})^{\frac{1}{6}}$$

and  $k^2$  is the orientation factor of the donor and acceptor. In the present case the generally accepted value of 2/3 was used on the basis of the assumption of random rotation of the fluorophores<sup>9</sup> and  $n$  is the refractive index of the medium between donor and acceptor, and was taken to be 1.4<sup>10</sup>.  $J$  is the spectral overlap integral

$$J = \frac{\sum I_D \epsilon_A \lambda^4 \Delta\lambda}{\sum I_D \Delta\lambda}$$

where  $I_D$  is the fluorescence intensity of the donor,  $\epsilon_A$  is the molar extinction coefficient of the acceptor, and  $\lambda$  is the wavelength in cm.

### Other Methods

Circular dichroism spectroscopy, performed as described elsewhere<sup>11</sup>, was employed to monitor protein stability in buffer and during guanidine HCl titration experiments. Electrospray mass spectrometry was performed as described in Chapter 2.

## 5.3 Results

---

### AEDANS Labeling

Recombinant apoE3(1-183) was labeled with AEDANS on Cys112 as described in Materials and Methods. Following removal of unbound chromophore, the labeled protein was subjected to electro-spray mass spectrometry. The spectrum revealed a single mass peak corresponding to apoE3(1-183) plus 1 AEDANS unit with no evidence for incorporation of more than one AEDANS per molecule. Using absorption spectroscopy, the extent of labeling was determined to be between 85 and 95%. Circular dichroism spectroscopy revealed the labeled protein retains its secondary structure content.

### Distance Measurements in the Lipid-free State

Fluorescence emission spectra of unlabeled recombinant apoE3(1-183) and AEDANS•apoE3(1-183) in buffer [excitation 295 nm] are shown in **Fig. 5-2**.

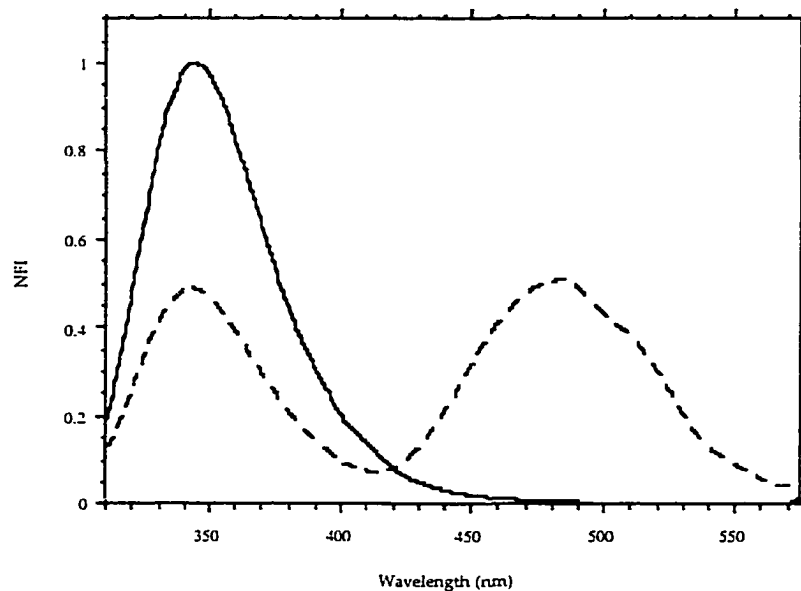


**Fig. 5-2.** Fluorescence emission spectra of apoE3(1-183) in buffer. (—), apoE3(1-183); (---), AEDANS-apoE3(1-183). One  $\mu\text{M}$  protein in 50 mM sodium phosphate, pH 7.0, 20 °C was excited at 295 nm. NFI = normalized fluorescence intensity.

The unlabeled protein sample gave rise to a single emission peak centered around 343 nm, as previously reported by Aggerbeck et al.<sup>12</sup> In the case of AEDANS•apoE3(1-183), the Trp fluorescence emission peak was reduced in intensity and a second peak, of approximately equal intensity, was observed around 480 nm. This corresponds with the known emission properties of AEDANS, whose absorbance spectrum overlaps directly with the emission spectrum of Trp. The appearance of an emission peak at 480 nm, together with the large decrease in Trp emission at 343 nm, suggests that the AEDANS moiety has been excited by energy transfer from Trp residues in helix 1. The magnitude of the spectral changes observed upon AEDANS labeling suggests efficient energy transfer from the donor Trp residues to AEDANS in the helix bundle conformation. Since the relative intensity of the AEDANS emission peak was

unaffected by dilution, it can be concluded that intermolecular energy transfer does not contribute to the results obtained. The resonance energy transfer parameters used for distance determinations are listed in Table 5-1.

**Table 5-1** Parameters for resonance energy transfer in lipid-free and lipid-bound AEDANS labeled apoE3(1-183)<sup>a</sup>

	ApoE3(1-183)	ApoE3(1-183)-DMPC
Quantum Yield, $Q_D^b$	0.20	0.23
Energy transfer efficiency, $E$ (%)	49	2.7
Overlap integral, $\mathcal{J}$ (cm <sup>6</sup> /mol)	$6.3 \times 10^{-15}$	$1.0 \times 10^{-14}$
Distance at 50% efficiency, $R_o$ (Å)	22	24

<sup>a</sup> Values are the average of three independent experiments.

<sup>b</sup> Quantum yield based on a value of 0.20 for 30 mM tryptophan in butanol.

<sup>c</sup> determined as described in Materials & Methods.

Calculations based on the observed energy transfer between Trp and AEDANS moieties in the protein are reported in **Table 5-2** and yield an average distance between the donor Trp residues and the acceptor AEDANS moiety of  $23 \pm 2$  Å.

**Table 5-2** Distance measurements derived from FRET analysis of AEDANS labeled apoE3(1-183) in the presence and absence of lipid.

	R(Å)	
	Measured <sup>a</sup>	Calculated
ApoE3(1-183)	$23 \pm 2$	$21^b$
ApoE3(1-183)-DMPC <sup>c</sup>	$44 \pm 4$	$58^d$

<sup>a</sup> from FRET measurements.

<sup>b</sup> average distance between centres as per PDB co-ordinates of Wilson et al.<sup>3</sup>

<sup>c</sup> DMPC discs were made as per Chapter 2.

<sup>d</sup> derived from the "open conformation" in the orientation depicted in Fig. 5-1; distance calculations determined using the program InsightII (Biosym, San Diego).

### Guanidine HCl Titration of AEDANS•apoE3(1-183)

To evaluate if AEDANS labeling affected protein stability, the effect of increasing guanidine HCl concentrations on energy transfer from Trp to AEDANS was investigated (Fig. 5-3).

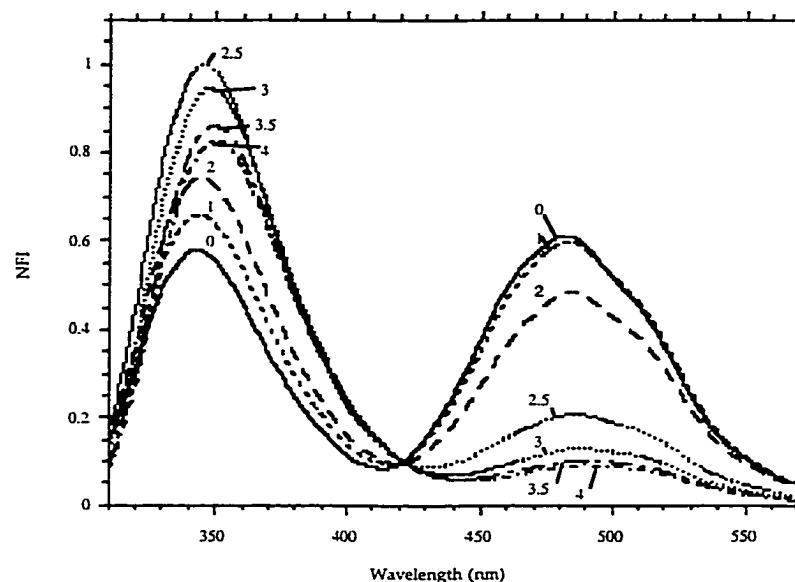


**Fig. 5-3** Effect of guanidine HCl on the efficiency of energy transfer from Trp to AEDANS in AEDANS•apoE3(1-183). Fluorescence emission spectra (excitation 295 nm) obtained from solutions containing 1  $\mu$ M AEDANS•apoE3(1-183) in 50 mM sodium phosphate, pH 7.0. Samples were pre-incubated in the presence of the indicated molarity of guanidine HCl for 30 min prior to analysis. Spectra were recorded at 20°C.

At guanidine HCl concentrations up to 2 M, there was a relatively small decrease in the intensity of the 480 nm emission peak and a corresponding small increase in the 340 nm emission peak. These data suggest that, in 2 M guanidine HCl, apoE3(1-183) retains its globular protein fold, consistent with the work of others<sup>13</sup>. At 2.5 M guanidine HCl and higher, however, a significant decrease in the intensity of the AEDANS emission peak was observed. Likewise, there is a corresponding increase, although less dramatic, in the relative intensity of the Trp emission peak (340 nm). In terms of the Trp fluorescence emission peak, at higher guanidine HCl concentrations, there is a red shift in the emission maximum, indicating the Trp residues are becoming

more solvent exposed as a function of increasing guanidine HCl concentration. Furthermore, the observation that Trp fluorescence emission intensity is highest at 2.5 M indicates that quenching of Trp fluorescence occurs at higher guanidine HCl concentrations. A similar quenching behavior was also evident with unlabeled protein upon titration with guanidine HCl (data not shown).

The large decrease in energy transfer observed between 2 and 2.5 M guanidine HCl fits well with denaturation data on the N-terminal domain of apoE3 reported by others<sup>13</sup> and, thus, provides support for the conclusion that AEDANS modification did not significantly alter the stability properties of the protein. These data also provide validation for the concept that the efficiency of energy transfer seen in buffer is due to the folded state of the protein and that changes in structure or conformation are reflected by changes in energy transfer. In parallel studies using urea as the denaturant, similar results were obtained.

#### **Trifluoroethanol Titration of AEDANS•apoE3(1-183)**

In previous studies of helix bundle exchangeable apolipoprotein conformation<sup>14</sup>, we found that inclusion of 50 % (v/v) TFE as co-solvent induced a conformational change similar to that seen upon lipid binding. This effect was hypothesized to be due to the ability of TFE to provide a lipid mimetic environment, interacting with hydrophobic regions of the protein by displacing helix-helix contacts in the bundle conformation. The effect of TFE on the efficiency of energy transfer in AEDANS•apoE3(1-183) is shown in **Fig. 5-4**. At 10 % (v/v) TFE, an apparent increase in energy transfer was observed, compared to buffer alone, as seen by an increase in AEDANS emission together with a corresponding decrease in Trp fluorescence emission intensity. Based on this information alone it might be concluded that, in the presence of 10 % TFE, the protein structure “tightens”, effectively shortening the distance between the chromophores, and thus, increasing the efficiency of energy transfer. This structural alteration could conceivably arise from the known ability of TFE to induce  $\alpha$ -helical secondary structure in proteins, including apoE3(1-183) (see Chapter 2).

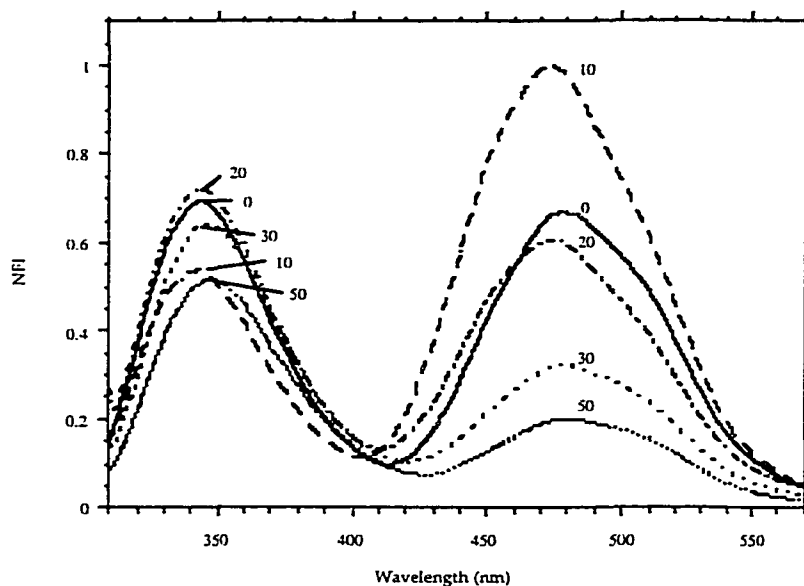


**Fig. 5-4** Effect of trifluoroethanol on energy transfer from Trp to AEDANS in AEDANS•apoE3(1-183). Emission spectra (excitation 295 nm) were obtained on a 1  $\mu$ M sample of AEDANS•apoE3(1-183) in the absence and presence of the indicated percentages of trifluoroethanol (v/v) in 50 mM sodium phosphate, pH 7.0, 20°C.

However, in 10 % TFE, when the AEDANS moiety was excited directly (336 nm), a significant enhancement of the AEDANS emission peak was observed (data not shown). A corresponding enhancement of tryptophan fluorescence emission was not detected in the case of unlabeled apoE3(1-183), which showed a progressive increase in tryptophan fluorescence quenching as a function of TFE concentration. Thus, we conclude that the enhancement in the AEDANS emission peak (excitation 295 nm) observed in 10% TFE may be due to movement of helix 3 (independent of helix 1), positioning the AEDANS moiety toward the hydrophobic interior of the protein. This interpretation is supported by the 6.5 nm blue shift (482 to 475.5 nm) in AEDANS fluorescence emission maximum in 10 % TFE versus buffer alone (excitation 336 nm). At 20 % TFE, a decrease in energy transfer can be seen by the decrease in AEDANS fluorescence emission together with an increase in the tryptophan fluorescence emission peak, versus that seen in 10 % TFE. At 30 % TFE and 50 % TFE, a

significant decrease in the AEDANS emission peak is observed that is not accompanied by a corresponding increase in Trp fluorescence emission.

### Energy Transfer in AEDANS•apoE3(1-183)-DMPC Discs and Detergent Micelles

The experiments described above provide evidence that FRET measurements can provide information about the proximal relationship between helix 1 and helix 3 in AEDANS•apoE3(1-183). On the basis of the “Open Conformation” model of apoE N-terminal domain conformational opening (Fig. 5-1), it can be predicted that such an opening will result in a decreased efficiency of energy transfer between Trp residues in helix 1 and the AEDANS moiety on helix 3. Comparison of AEDANS•apoE3(1-183) energy transfer efficiency in the lipid-free globular conformation and that when the protein is bound to bilayer disc complexes of DMPC (Fig. 5-5 and Table 5-1) suggests a significant change in the relative positions of the donor and acceptor chromophores.

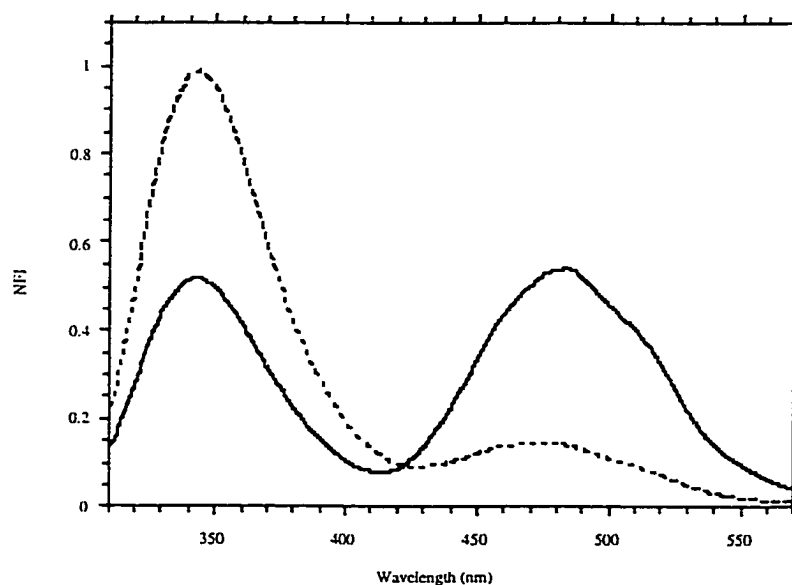


**Fig. 5-5** Effect of interaction with DMPC on the efficiency of energy transfer from Trp to AEDANS in AEDANS•apoE3(1-183). Fluorescence emission spectra (excitation 295 nm) were obtained at 20 °C, protein concentration 1  $\mu$ M; (—), AEDANS•apoE3(1-183) in buffer; (---), AEDANS•apoE3(1-183)-DMPC disc complexes in buffer.



Control spectra of apoE3(1-183)-DMPC disc complexes displayed no fluorescence in the region of AEDANS emission nor was there a significant change in tryptophan fluorescence quantum yield upon binding to DMPC. The average distance between tryptophan residues in helix 1 and the AEDANS moiety in DMPC discs versus that in buffer alone, as well as that predicted on the basis of a simple conformational opening of the helix bundle, are reported in Table 5-2.

Given that each disc possesses multiple copies of apoE3(1-183), a portion of the AEDANS fluorescence emission peak in DMPC disc complexes may arise from intra-molecular or inter-molecular energy transfer. To evaluate the extent to which intermolecular energy transfer may contribute to the results seen for lipid associated apoE3(1-183), experiments were performed using detergent micelles as a model lipid surface, under conditions where a maximum of 1 apoE3(1-183) molecule is bound per micelle. The results obtained (**Fig. 5-6**) showed a similar trend toward less efficient energy transfer when apoE3(1-183) was bound to either SDS or lysophosphatidylcholine micelles.

## **5.4 Discussion**

---

ApoE plays a critical role in plasma cholesterol homeostasis, where it functions as a ligand for cell surface lipoprotein receptors. The receptor binding site of apoE has been localized to residues 130 - 150 in the N-terminal domain of the protein<sup>6</sup>. Importantly, the receptor recognition properties of this protein are manifest only in a lipid-associated state. The availability of detailed structural information in the lipid-free state<sup>3</sup> has allowed for the development of hypotheses about lipid binding-induced conformational changes. In the present study we have employed FRET to investigate helix repositioning of the N-terminal domain four helix bundle upon lipid association, obtaining evidence in favor of a conformational “opening” of the bundle.

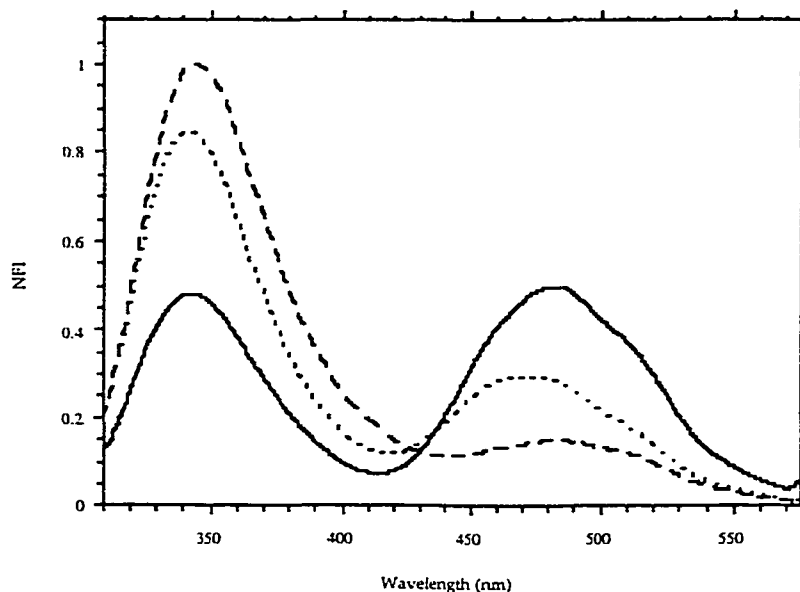


**Fig. 5-6** Effect of detergent micelle interaction on the efficiency of energy transfer in AEDANS•apoE3(1-183). (—), emission spectrum (excitation 295 nm) of 2  $\mu$ M AEDANS•apoE3(1-183) in 50 mM sodium phosphate, pH 7.0; (- - - -), AEDANS•apoE3(1-183) in buffer containing 1% SDS (w/v) and (- · - · - ·), AEDANS•apoE3(1-183) in buffer containing 1 mM lysophosphatidylcholine.

ApoE3(1-183) contains four tryptophan residues (positions 20, 24, 36, 39) and a single cysteine at position 112. From the X-ray structure of this protein it is known that the four tryptophan residues are found in or near helix 1 (residues 23 to 42) of the four helix bundle while Cys112 is located in the C terminal half of helix 3. Tryptophan residues can function as excellent intrinsic energy donors while Cys112 provides a site for specific attachment of an extrinsic energy acceptor. From the work of others, it is recognized that Cys112 is available for covalent modification<sup>15</sup>. In the present study we covalently modified the sulfhydryl group of Cys112 with IAEDANS, a chromophore which has been extensively used in FRET studies<sup>16-19</sup>. AEDANS serves as a suitable energy acceptor in this system because its absorption spectrum overlaps directly with the emission spectrum of tryptophan. The present system is advantageous because the natural locations of tryptophan and cysteine in the folded protein are known from the crystal structure, providing an important reference standard

for FRET studies of lipid binding-induced conformational changes. Indeed, from the X-ray coordinates, the average distance from the compound donor to the acceptor Cys is  $\sim 21$  Å, in good agreement with the value of 23 Å derived from FRET measurements. Furthermore, the helix bundle conformation is monomeric in solution, which minimizes intermolecular contributions to FRET<sup>12</sup>.

Fig. 5-1 depicts a model of a putative “open conformation” of apoE3 N-terminal domain wherein helix 1 and 2 move away from helix 3 and 4 by rotating about a hinge region located in the loop between helix 2 and 3. Such an opening of the molecule would result in exposure of the hydrophobic faces of the amphipathic  $\alpha$ -helices which are otherwise sequestered in the interior of the bundle conformation. These hydrophobic regions are thought to interact with lipid surfaces, creating a stable, yet reversible, binding interaction. An alternate model, presented by de Pauw et al.<sup>20</sup>, suggests that interaction with DMPC to form bilayer disc complexes induces the helical segments in apoE to realign, forming antiparallel 17 residue helices which orient parallel to the phospholipid fatty acyl chains. Considering the width of an  $\alpha$ -helix to be 15 - 16 Å, and introducing “breaks” in helices 2, 3 and 4, the estimated distance between Trp residues in helix 1 and Cys112 would approach 60 Å. While the FRET data reported herein do not exclude this model, this postulated molecular organization is not consistent with recently acquired infrared data on apoE3(1-183)-DMPC disc complexes (see Chapter 4) or the predicted effect that realignment of helix 4 (residues 130-164) into two helices would have on the relative position of Arg150. The orientation of this residue relative to the defined LDL receptor binding region (residues 130-150) has been shown to be an important determinant of marked differences in apoE3/apoE2 isoform specific receptor binding properties<sup>21</sup>.

Guanidine HCl titration experiments revealed important points about this system. Firstly, changes in the efficiency of energy transfer correlated well with the known denaturation properties of this protein<sup>13</sup>. While the folded structure displayed efficient energy transfer, guanidine HCl induced denaturation resulted in a dramatic decrease in energy transfer (Fig. 5-3). Thus, it can be concluded that AEDANS modification of apoE3(1-183) does not alter the

stability properties of the protein. Second, from changes in energy transfer observed upon protein unfolding, it is evident that changes in the conformation of apoE3(1-183) will be reflected in FRET measurements. Similar conclusions were drawn from experiments performed using TFE as a co-solvent. Decreased energy transfer observed as a function of TFE concentration are consistent with the hypothesis that, above 20 % (v/v), TFE induces conformational opening of the helix bundle through replacement of helix-helix contacts with helix-TFE interactions. In this case hydrophobic contacts between helices in the bundle conformation would be lost, with the protein no longer constrained to retain its globular structure. Studies in the presence of either TFE or guanidine HCl were complicated by the fact that tryptophan fluorescence quenching is observed. For example, the transition from 20 % TFE to 30 % TFE induced a large decrease in AEDANS emission whereas this was not accompanied by a corresponding increase in tryptophan fluorescence emission, due to a progressive quenching by TFE of Trp fluorescence. By contrast, the quantum yield of AEDANS fluorescence emission in AEDANS•apoE3(1-183) was unaffected between 20 and 75 % TFE (direct excitation at 336 nm) yet increased between 0 % TFE and 10 % TFE. Thus, distance measurements under these conditions must take into account changes in donor and/or acceptor fluorescence quantum yield, which have a direct effect on energy transfer.

When complexed with DMPC, the fluorescence quantum yield of tryptophan in unlabeled apoE3(1-183) was not significantly altered. However, lipid-associated AEDANS•apoE3(1-183) displayed reduced energy transfer compared to the lipid free state, resulting in an increase in the measured distance between the compound energy donor and the AEDANS moiety from 23 Å to 44 Å. Since the secondary structure content of the protein was not affected by DMPC binding, we conclude that interaction of apoE3(1-183) with lipid surfaces induces a conformational change that increases the distance between helix 1 and helix 3. While these data are consistent with the open conformation model presented in Fig. 5-1, a simple opening of the helix bundle would be expected to yield a larger distance between donor and acceptor moieties in this protein (Table 5-2). Further experiments will be required to better define the

precise nature of the conformational change and to minimize potential sources of error in the FRET-derived distance calculations. Experimental factors which could contribute error to the observed results include 1) alterations in the orientation factor,  $k^2$ , of the donor or acceptor species in the different conformations; 2) the presence of multiple energy donors (e.g. 4 Trp) in the molecule or 3) possible effects of the transition of Trp residues from an aqueous medium to a lipid/water interface on the efficiency of energy transfer. With regard to the first point, we have elected to use the averaged value of  $k^2 = 2/3$  because, in the present system, the compound energy donor is represented by the sum of the four tryptophan residues. Also, in other systems, anisotropy measurements suggest rapid movement in the AEDANS moiety, suggesting that random orientation may prevail during the energy transfer process (the lifetime of the tryptophan excited state). The problems introduced by the presence of multiple energy donors in this system (i.e. 4 Trp) can most readily be solved by sequential site-directed mutagenesis of tryptophan residues in apoE3(1-183) to yield a protein with a single energy donor species. In this case greater accuracy can be achieved in FRET-derived distance measurements. Toward this end, we have recently replaced Trp20 with a tyrosine (W20Y) by site-directed mutagenesis. In buffer, AEDANS labeled W20YapoE3(1-183) showed an increased energy transfer efficiency compared to corresponding wild type apoE3(1-183), consistent with the fact that, in the four helix bundle crystal structure, W20 resides furthest from the site of AEDANS modification (cysteine 112 in helix 3). This data, which illustrates the sensitivity of FRET measurements to alterations in the donor chromophore population in this system, suggests that creation of single tryptophan mutant apoE3(1-183) will permit highly accurate distance measurements to be obtained. Furthermore, the availability of a Trp-null apoE3(1-183) can be used to “dilute” AEDANS-labeled apoE3(1-183) samples, thereby providing an internal control for possible intermolecular energy transfer in the case of disc complexes and spherical lipoprotein recombinants. Finally, further mutations which place a tryptophan residue and/or the cysteine residue on different helical pairs in the bundle will permit detailed characterization of helix repositioning which accompanies lipid

interaction and, conceivably, reconstruction of a lipid-bound structure. The general applicability of FRET methods to the class of amphipathic exchangeable apolipoproteins provides a promising approach to study these proteins in their biologically active, lipid-associated state.

## 5.5 Bibliography

---

1. Innerarity, T.L., Friedlander, E.J., Rall Jr., S.C., Weisgraber, K.H. & Mahley, R.W. The receptor-binding domain of human apolipoprotein E: Binding of apolipoprotein E fragments. *J. Biol. Chem.* **258**, 12341-12347 (1983).
2. Innerarity, T.L., Pitas, R.E. & Mahley, R.W. Binding of arginine-rich (E) apoprotein after recombination with phospholipid vesicles to the low density lipoprotein receptors of fibroblasts. *J. Biol. Chem.* **254**, 4186-4190 (1979).
3. Wilson, C., Wardell, M.R., Weisgraber, K.H., Mahley, R.W. & Agard, D.A. Three-dimensional structure of the LDL receptor-binding domain of human apolipoprotein E. *Science* **252**, 1817-1822 (1991).
4. Breiter, D.R., Kanost, M.R., Benning, M.M., Wesenberg, G., Law, J.H., Wells, M.A., Rayment, I. & Holden, H.M. Molecular structure of an apolipoprotein determined at 2.5-Å resolution. *Biochemistry* **30**, 603-608 (1991).
5. Wang, J., Gagné, S., Sykes, B.D. & Ryan, R.O. Insight into lipid surface recognition and reversible conformational adaptation of an exchangeable apolipoprotein by multidimensional heteronuclear NMR techniques. *J. Biol. Chem.* **272**, 17912-17920 (1997).
6. Weisgraber, K.H. Apolipoprotein E: structure-function relationships. *Ad. Protein Chem.* **45**, 249-302 (1994).
7. Weisgraber, K.H., Lund-Katz, S. & Phillips, M.C. Apolipoprotein E: structure-function correlations. in *High density lipoproteins and atherosclerosis III* (eds. Miller, N.E. & Tall, A.R.) 175-181 (Elsevier, Amsterdam, 1992).
8. Selvin, P.R. Fluorescence resonance energy transfer. *Methods Enzymol.* **246**, 300-334 (1995).
9. Chapman, E.R., Alexander, K., Vorherr, T., Carafoli, E. & Storm, D.R. Fluorescence energy transfer analysis of calmodulin-peptide complexes. *Biochemistry* **31**, 12819-12825 (1992).
10. Lakowicz, J.R. *Principles of fluorescence spectroscopy*, (Plenum Press, New York, 1983).
11. Ryan, R.O., Oikawa, K. & Kay, C.M. Conformational, thermodynamic, and stability properties of *Manduca sexta* apolipophorin III. *J. Biol. Chem.* **268**, 1525-1530 (1993).

12. Aggerbeck, L.P., Wetterau, J.R., Weisgraber, K.H., Wu, C.C. & Lindgren, F.T. Human apolipoprotein E3 in aqueous solution: II. Properties of the amino- and carboxyl-terminal domains. *J. Biol. Chem.* **263**, 6249-6258 (1988).
13. Wetterau, J.R., Aggerbeck, L.P., Rall, S.C., Jr. & Weisgraber, K.H. Human apolipoprotein E3 in aqueous solution: I. Evidence for two structural domains. *J. Biol. Chem.* **263**, 6240-6248 (1988).
14. Narayanaswami, V., Kay, C.M., Oikawa, K. & Ryan, R.O. Structural and binding characteristics of the carboxyl terminal fragment of apolipoprotein III from *Manduca sexta*. *Biochemistry* **33**, 13312-13320 (1994).
15. Weisgraber, K.H. Apolipoprotein E distribution among human plasma lipoproteins: role of the cysteine-arginine interchange at residue 112. *J. Lipid Res.* **31**, 1503-1511 (1990).
16. Lakey, J.H., Baty, D. & Pattus, F. Fluorescence energy transfer distance measurements using site-directed single cysteine mutants: the membrane insertion of colicin A. *J. Mol. Biol.* **218**, 639-653 (1991).
17. Lakey, J.H., Baty, D. & Pattus, F. Fluorescence energy transfer distance measurements. The hydrophobic helical hairpin of colicin A in the membrane-bound state. *J. Mol. Biol.* **230**, 1055-1067 (1993).
18. Steer, B.A. & Merrill, A.R. The colicin E1 insertion-competent state: detection of structural changes using fluorescence resonance energy transfer. *Biochemistry* **33**, 1108-1115 (1994).
19. Isaac, V.E., Patel, V.L., Curran, T. & Abate-Shen, C. Use of fluorescence energy transfer to estimate intramolecular distances in the Msx-1 homeodomain. *Biochemistry* **34**, 15276-15281 (1995).
20. De Pauw, M., Vanloo, B., Weisgraber, K. & Rosseneu, M. Comparison of lipid-binding and lecithin:cholesterol acyltransferase activation of the amino- and carboxyl-terminal domains of human apolipoprotein E3. *Biochemistry* **34**, 10953-10960 (1995).
21. Dong, L.M., Parkin, S., Trakhanov, S.D., Rupp, B., Simmons, T., Arnold, K.S., Newhouse, Y.M., Innerarity, T.L. & Weisgraber, K.H. Novel mechanism for defective receptor binding of apolipoprotein E2 in type III hyperlipoproteinemia. *Nature Struct. Biol.* **3**, 718-722 (1996).



## Chapter 6

### **The Lipid-associated Conformation of the Receptor Binding Domain of Human Apolipoprotein E**

## **6.1 Introduction**

---

The ability of apoE to clear remnant particles from circulation is accomplished primarily through its ability to bind to cell surface receptors with high affinity<sup>1</sup>. An intriguing requirement of this capability is that apoE must be lipid-associated<sup>2,3</sup>. Such binding is accompanied by little change in the  $\alpha$ -helical content of the N-terminus<sup>4-6</sup>, suggesting that there is a tertiary structural alteration in which the helical boundaries are maintained. Since the lipid-bound conformation is critical for receptor interaction, the determination of its structure would be a significant contribution to our understanding of this phenomenon.

Previously, FRET analysis of recombinant apoE3(1-183) indicated that there was movement of helix 1 away from helix 3 upon lipid binding. This finding was consistent with the "Open Conformation" model which suggests that the helix bundle of the N-terminal domain of apoE opens up about a "hinge" region between helices 2 and 3 such that helices 1 and 2 move away from helices 3 and 4, exposing the hydrophobic interior for interaction with a lipid surface. In the present paper, analysis of FRET in mutants of apoE3(1-183) possessing a single tryptophan located on a unique helix and incorporation of Trp-null protein into phospholipid disc complexes to minimize intermolecular energy transfer, permitted the mapping of the relative position of helices in the lipid-bound state. We present a model representing the arrangement of helices in the lipid-bound N-terminal domain of apoE.

## **6.2 Materials and Methods**

---

### **Materials**

DMPC was obtained from Avanti Polar-lipids, Inc. (Alabaster, AL) and IAEDANS from Sigma Chemical Co., St. Louis, MO. Fine chemicals were supplied by Fisher Scientific (Nepean, ON).

## **Mutagenesis**

Mutations in apoE3(1-183) were performed using the Altered Sites II *in vitro* mutagenesis kit (Promega, Madison, WI). In wild-type (WT) apoE3(1-183), there are four Trp all located within or adjacent to helix 1. To generate a protein containing a single Trp, the first three Trp residues (amino acid positions 20, 26, and 34) were mutated to Phe to generate the protein apoE3(1-183){W39}, where {W39} denotes that there is a single Trp at position 39. Trp 39 was then replaced with a Phe to create a Trp-null protein (apoE3(1-183){Trp-null}). The other single Trp mutants were created by replacing a naturally occurring Tyr with a Trp. Where possible, primers were designed to incorporate silent mutations which altered a restriction site, aiding the screening of mutants. DNA was sequenced prior to transformation into the *E. coli* BL21(DE3) used for expression.

## **Protein Expression, Purification, and Labeling**

As per Chapter 5.

## **Phospholipid Disc Complex Formation**

As per Chapter 5.

## **Fluorescence Measurement**

As per Chapter 5.

## **Calculation of Donor-acceptor Separation**

The efficiency of energy transfer ( $E$ ) used to determine distances in lipid-bound protein was calculated using: i) the change in donor fluorescence emission and ii) the excitation spectrum of the energy acceptor<sup>7</sup>. The  $E$  values should be approximately equivalent if there are no interfering environmental or quenching factors<sup>8</sup>,

i)  $E$  was calculated by quantitating the change in donor fluorescence as follows:

$$E = 1 - \frac{Q_{DA}}{Q_D} \quad (1)$$

where  $Q_D$  and  $Q_{DA}$  are the quantum yield of the donor in the absence and presence of acceptor, respectively.

ii) Excitation spectra were used to determine  $E$  as per Lakey et al.<sup>8</sup> using the following formula:

$$E = \left[ \frac{F_{290}}{F_{340}} - \frac{\epsilon_{A290}}{\epsilon_{A340}} \right] \times \frac{\epsilon_{A340}}{\epsilon_{D290}} \quad (2)$$

where  $F_{290}$  and  $F_{340}$  are the fluorescence intensities at 290 and 340 nm respectively, and  $\epsilon_{A290}$  ( $1.2 \times 10^3 \text{ M}^{-1} \text{ cm}^{-1}$ ) and  $\epsilon_{A340}$  ( $6.0 \times 10^3 \text{ M}^{-1} \text{ cm}^{-1}$ ) are the AEDANS extinction coefficients, at 290 (excitation wavelength for Trp) and 340 nm (excitation wavelength of AEDANS), respectively.  $\epsilon_{D290}$  is the extinction coefficient of the tryptophan donor at 290 nm.

The remaining FRET parameters were calculated as described in Chapter 5.

### NMR Spectroscopy

WT, {Trp-null}, and {W162} were suspended in 50 mM acetate buffer with 5% D<sub>2</sub>O at pH 4.0 and spectra collected. One-dimensional NMR experiments were carried out on a Varian Unity-500 NMR spectrometer at a temperature of 30°C.

### Other Methods

Absorption spectra were obtained using a Hewlett Packard 8453 spectrophotometer. Electrospray mass spectrometry was performed as described in Chapter 2. Protein concentration was determined using the bicinchoninic acid assay (Pierce, Rockford, IL).

## 6.3 Results

### Protein Constructs

FRET analyses are optimal when there is one energy donor and one energy acceptor within each molecule since multiple energy donors contribute differentially to energy transfer depending upon their position relative to the acceptor, complicating interpretation of the resultant data. Since WT apoE3(1-183) possesses four Trp (intrinsic energy donors), this protein was modified using site-directed mutagenesis to yield proteins containing a single Trp. **Table 6-1** lists the proteins produced and indicates the mutations that were created.

**Table 6-1** Mutations introduced into apoE3(1-183) and the wavelength of tryptophan peak emission ( $\lambda$  max).

Protein <sup>a</sup>	Mutations	Trp(s) Location [Helix (residues)]	$\lambda$ Max (nm) <sup>b</sup>
WT		1 (44-53)	344
{W 39}	W20F, W26F, W34F	1 (44-53)	351
{Trp-null}	W20F, W26F, W34F, W39F		
{W74}	Trp-null, Y74W	2 (54-81)	341
{W118}	Trp-null, Y118W	3 (87-122)	336
{W162}	Trp-null, Y162W	4 (130-165)	339

<sup>a</sup> WT denotes wild-type apoE3(1-183); {Wx} denotes a mutant protein derived from apoE3(1-183) and indicates the amino acid position of the lone Trp.

<sup>b</sup> excitation wavelength was 295 nm

It was anticipated that, in the lipid-bound state, adjacent proteins have the potential to transfer energy between one another, complicating energy transfer analysis. This potential complication can be minimized by including in disc preparations an excess of a protein that lacks an energy donor. Thus, {Trp-null} was created by replacing the lone Trp in {W39} with a Phe. This construct was not needed for lipid-free analyses since the N-terminal fragment of apoE3 is monomeric up to 15 mg/ml<sup>4</sup> and, thus, at the protein concentrations used, any intermolecular energy transfer would be negligible.

### **Maintenance of Structural Integrity**

Mutations introduced into a protein may cause significant structural perturbations, thereby preventing the protein from functioning normally. To minimize the likelihood of disrupting the protein structure, the amino acid substitutions made were conservative, replacing bulky, hydrophobic residues (such as Trp) with those having similar side chain properties (i.e. Phe). One indication that mutant proteins retained native functionality was the ability of all the proteins generated to convert DMPC vesicles into high molecular weight complexes of comparable dimensions to that produced by wild-type apoE3(1-183) (as judged by non-denaturing PAGE; data not shown). Additionally, one dimensional NMR was performed on a representative sampling of proteins to gain insight into the  $\alpha$ -helicity and global fold (data not shown). In the resultant spectra, the dispersion of peaks indicated that these proteins were structured and the chemical shift of the amide region (8.4 - 7.7 ppm) suggested that the structure was predominantly  $\alpha$ -helical.

### **Efficient Energy Transfer in Lipid-free Protein**

As is evident in **Fig. 6-1**, unlabeled Trp-containing protein ( $\{W39\}$ ) exhibits a single emission peak centered at 351 nm when excited at 295 nm. Similar spectra were generated for all of the mutants produced and the  $\lambda$  max values are listed in **Table 6-1**. Wild-type apoE3(1-183) had a  $\lambda$  max of 344 nm, in agreement with previously determined values<sup>4,5,9</sup>. There was a considerable red shift (towards longer wavelengths) in the emission maxima of  $\{W39\}$  when compared to that of the other mutants (10 – 12 nm) suggesting that this Trp is more solvent exposed than the other three Trp residues. Analysis of the X-ray crystal structure of the N-terminal fragment of apoE confirmed that Trp 39 is oriented towards the solvent rather than the protein interior. In contrast, residues 118 and 162, which point towards the center of the helix bundle, have  $\lambda$  max values that are blue shifted, 336 and 339 nm respectively, indicative of their presence in a non-polar environment.

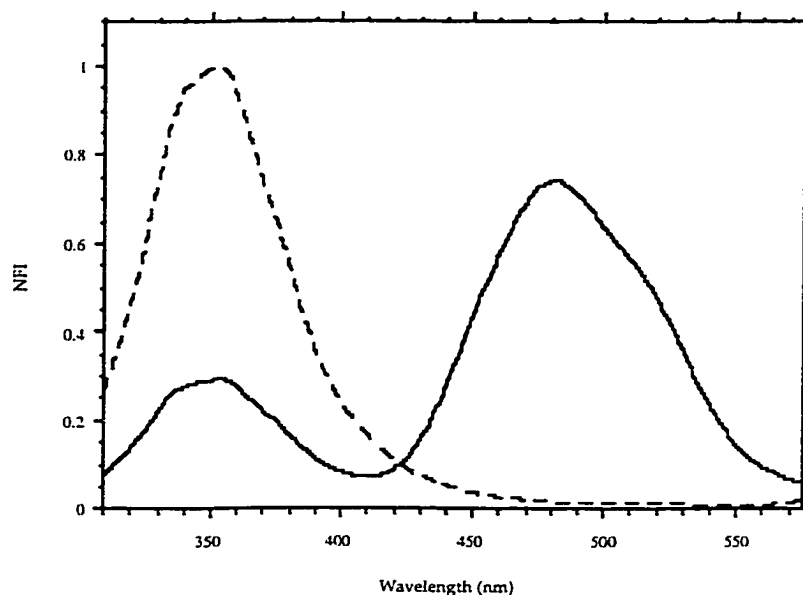


**Fig. 6-1** Efficient energy transfer in AEDANS labeled {W39}. (---), {W39}; (—), AEDANS•{W39}. One  $\mu\text{M}$  protein in 20 mM phosphate buffer pH 7.0. Spectra were recorded at room temperature, 295 nm excitation wavelength and were normalized to the maximal fluorescence intensity (NFI).

Following covalent attachment of the energy acceptor, AEDANS, at the lone Cys present in all the proteins analyzed (position 112 on helix 3), excitation (295 nm) resulted in a diminishment of the tryptophan peak and the appearance of a new peak centered at  $\sim 480$  nm (AEDANS emission), indicative of energy transfer from the excited Trp (Fig. 6-1). The relative peak intensities are dependent upon the distance between the fluorophores which is reflected in the efficiency of energy transfer ( $E$ ). **Table 6-2** lists  $E$  derived from the alteration in: i) the donor (Trp) emission peak intensity in AEDANS-labeled versus unlabeled samples and ii) the excitation spectra values for the energy acceptor. For {W72} and {W162},  $E$  values were in good agreement independent of the method used to calculate them while WT apoE3(1-183) and {W39} had significantly different values for the emission-derived versus the excitation-derived data.

**Table 6-2** Efficiency of energy transfer for lipid-free and lipid-bound proteins<sup>a</sup>

Protein	<i>E</i>					
	Lipid-free		+ DMPC			
	Em	Ex	Em	Ex	+ W-null	
	Em	Ex	Em	Ex	Em	Ex
WT	0.46±0.09	0.41±0.06	0.023 <sup>b</sup>	0.069	0.13±0.08	0.038±0.03
{W39}	0.52±0.2	0.50±0.02	0.17±0.09	0.072	0.22±0.01	0.090±0.02
{W74}	0.44±0.01	0.30±0.01	0.065±0.01	0.078±0.01	0.066±0.02	0.067±0.01
{W162}	0.54±0.06	0.42±0.02	0.70±0.03	0.58±0.04	0.28±0.1	0.27±0.05

<sup>a</sup> Values are the average of two or three independent experiments; determined as described in Materials & Methods.

<sup>b</sup>As determined in Chapter 5.



**Table 6-3** lists other parameters employed in FRET-derived distance determinations.

**Table 6-3** Parameters of resonance energy transfer

	WT	{W39}	{W74}	{W118}	{W162}
Quantum Yield, $Q_D$	0.19	0.054	0.15	0.089	0.18
Overlap Integral, $J^a$ (cm <sup>6</sup> /mol)	$5.9 \times 10^{-15}$	$7.9 \times 10^{-15}$	$1.0 \times 10^{-14}$	$1.4 \times 10^{-14}$	$8.3 \times 10^{-15}$
Distance at 50% efficiency, $R_0$ (Å)	22	19	23	21	23

Values are the average of three independent experiments.

Quantum yield is based on a value of 0.20 for 30 mM Trp in butanol.

<sup>a</sup>Determined as described in Materials and Methods.

There was significant variability in Trp quantum yield ( $Q$ ), ranging from 0.19 for WT to 0.054 for {W39}. It was apparent that  $Q$  was not additive since proteins containing a single Trp do not all have values that were 1/4 of that determined for the WT protein. Variability in these values is at least partially due to the quenching of energy by the different environments in which the Trp residues reside.

### Monitoring Gross Conformational Changes with FRET

To verify the ability of this system to monitor positional alterations, AEDANS•{W39} was analyzed by collecting emission spectra under progressively denaturing conditions using increasing concentrations of guanidine HCl (GdnHCl) (**Fig. 6-2**). The denaturant concentration at which tryptophan fluorescence increases markedly indicates commencement of the complete loss of protein structure and this value approximates the midpoint of denaturation as determined by circular dichroism (see Chapter 5). Similar to WT apoE3(1-183), the concentration of GdnHCl at which there was a pronounced increase in Trp fluorescence for this mutant was between 2 and 2.5 M, consistent with the

previously determined denaturation midpoint concentration of 2.2 M for the N-terminal fragment<sup>10</sup>.

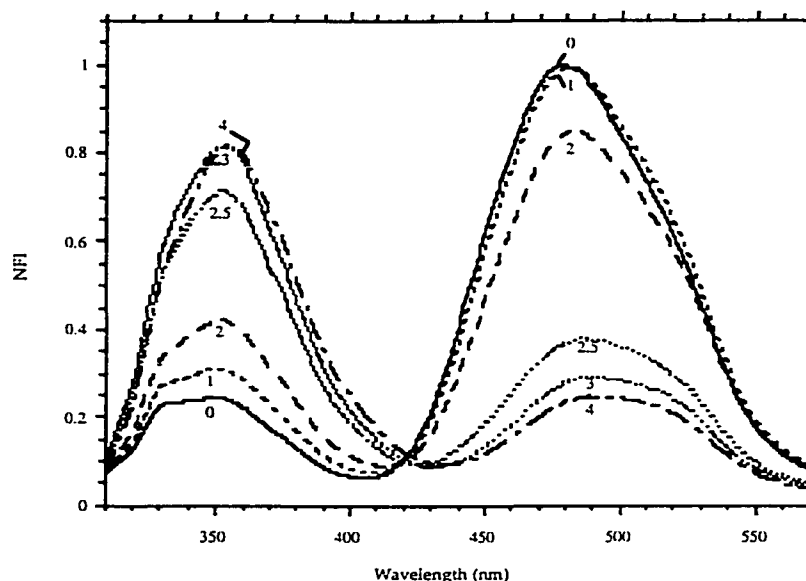


**Fig. 6-2** Protein unfolding monitored by FRET. AEDANS•{W39} (1  $\mu$ M) was incubated in 20 mM phosphate buffer, pH 7.0 in the indicated concentration of denaturant (GdnHCl) for 30 min at room temperature prior to spectra generation.

There was also a concomitant red shift in the tryptophan emission peak due to increased solvent exposure of the Trp as the protein unfolds. These results demonstrate that the mutants generated possessed stability properties comparable to WT apoE3(1-183) and that FRET is a faithful measure of conformational alterations.

### Altered Energy Transfer in Lipid-bound Protein

If there is movement of fluorophore-containing helices away from one another upon lipid interaction, a decrease in the efficiency of energy transfer should result. When AEDANS•{W39} bound to lipid, a significant reduction in the efficiency of energy transfer occurred, as indicated by the increase in Trp emission peak intensity (340 nm) and a decrease in the AEDANS (480 nm) peak (**Fig. 6-3**). As expected, there was a diminishment in  $E$  (Table 6-2), indicating that there was

movement of helix 1 away from helix 3, in agreement with previous results investigating WT apoE3(1-183)(Chapter 5).

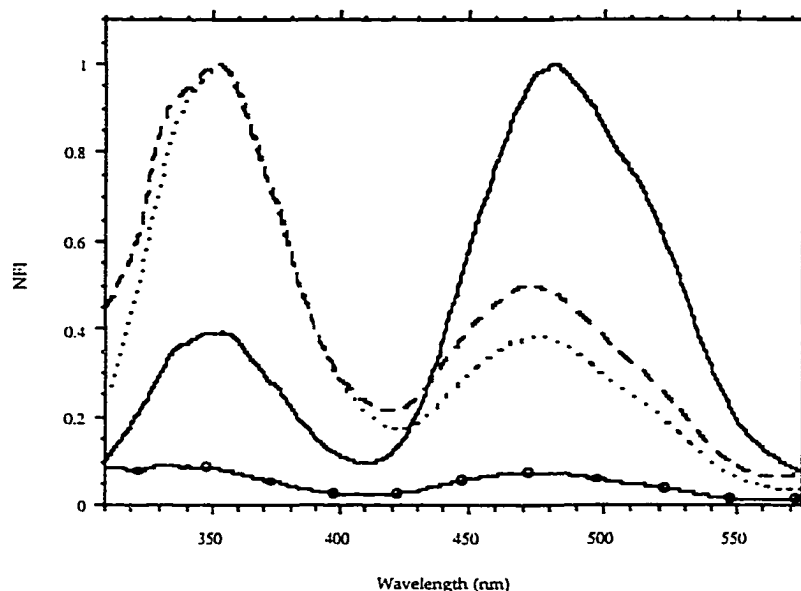


**Fig. 6-3** Diminished energy transfer in lipid-bound {W39}. (—), AEDANS•{W39}; (.....), AEDANS•{W39} + DMPC; (---), AEDANS•{W39} + {Trp-null} + DMPC; (-O-), AEDANS•{Trp-null} + {Trp-null} + DMPC. Discs were produced by sonicating a mixture of {Trp-null} and AEDANS-labeled protein (4:1, w/w) with DMPC in buffer.

This finding was also reflected in the distance measurements shown in **Table 6-4**.

**Table 6-4** Distance measurements derived from FRET analysis of AEDANS-labeled proteins in the absence and presence of lipid.

	R(Å)			
	Lipid-free		+ DMPC	
	Measured <sup>a</sup>	Calculated <sup>b</sup>	Measured <sup>c</sup>	Calculated <sup>b</sup>
WT	23.1±0.4	21	36.0±3.0	58
{W39}	19.4±2.0	17	28.3±2.0	69
{W74}	24.5±0.9	24	40.1±0.1	44
{W162}	23.1±0.8	24	32.4±0.1	72

DMPC discs were made as per Chapter 2;  
<sup>a</sup> from FRET measurements;

<sup>b</sup> distance calculations determined using the program InsightII (Biosym, San Diego); lipid-bound values were derived from the "extended open conformation" model depicted in Fig. 6-6.

<sup>c</sup>  $R_0$  used in distance measurements was obtained from discs made in the absence of {Trp-null}.

In contrast to the result shown in Fig. 6-3, when AEDANS•{W162} was complexed with lipid under the same conditions, there was no apparent difference in the emission spectra in comparison to the lipid-free state (Fig. 6-4).

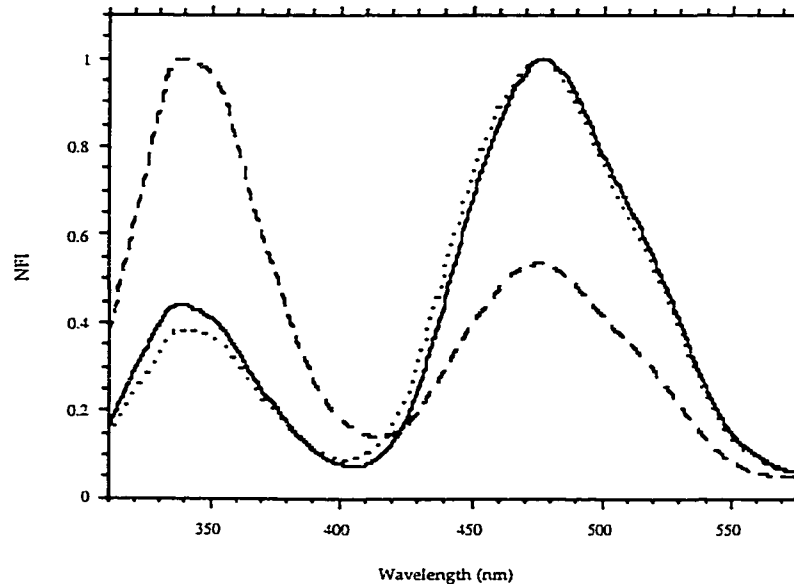


**Fig. 6-4.** Intermolecular energy transfer reduction on discs containing Trp-null and {W162}. AEDANS•{W162}, (—); AEDANS•{W162} + DMPC, (.....); AEDANS•{W162} + {Trp-null} + DMPC, (---). Discs were produced as in Fig. 6-3.

The lack of alteration in the efficiency of energy transfer in the AEDANS•{W162} spectra suggested that: i) there was no movement of helix 4 relative to helix 3 when the protein is lipid-bound or ii) there was movement, but this was masked by intermolecular energy transfer.

### Minimization of Intermolecular Energy Transfer Indicates Movement of Helix 3 away from Helix 4

In discoidal complexes of phospholipid and protein, apoE is believed to orient itself around the periphery of a bilayer of phospholipid, perpendicular to the acyl

chains which it shields from the aqueous environment (Chapter 4). In this configuration, it can be predicted that energy transfer could occur between chromophores present on adjacent protein molecules which would then lead to elevated  $E$  values resulting in an underestimation of FRET-derived distances. To minimize the possibility of intermolecular energy transfer, unlabeled {Trp-null} was incorporated into discoidal complexes by sonicating DMPC at a ratio of one AEDANS•apoE3(1-183) mutant to four {Trp-null}. Since chemical crosslinking has shown that there are 3 to 4 apoE3(1-183) molecules per disc (Chapter 4), the likelihood of there being two adjacent molecules participating in intermolecular energy transfer would be greatly diminished using this strategy. Following excitation (295 nm) of discoidal complexes containing an excess of AEDANS•{Trp-null} with unlabeled {Trp-null} (1:4 weight ratio), an emission spectra was produced with minimal 340 nm fluorescence (confirming the absence of Trp) and a minor peak at ~470 nm due to direct excitation of AEDANS (Fig. 6-3). As indicated by the emission spectra of Fig. 6-3 and the  $E$  values listed in Table 6-2, complexes formed using AEDANS labeled WT, {W39} or {W74} and unlabeled {Trp-null} produced spectra that were not significantly different from those generated from discs prepared using only AEDANS-labeled protein. The absence of a significant difference in spectra suggested that there was minimal intermolecular energy transfer occurring in these complexes.

Discs containing AEDANS•{W162} and unlabeled {Trp-null} exhibited a pronounced increase in Trp peak intensity (340 nm) and a diminishment in the AEDANS peak intensity (480 nm) indicating reduced energy transfer (Fig. 6-4).

This alteration in  $E$  (Table 6-2) was in stark contrast to the condition in which {Trp-null} was not present, suggesting that there was movement of helix 4 away from helix 3 during transition from the lipid-free to the lipid-bound state. This rearrangement was apparently masked in previous experiments by confounding intermolecular energy transfer.

As Table 6-4 indicates, the FRET-determined distances derived from lipid-free AEDANS-labeled protein are in good agreement with those obtained from the X-ray crystal structure, verifying that this system can provide accurate distance measurements. For the lipid-bound protein, there was considerable

variability in the model versus derived distances. The distance change between helices 2 ({W74}) and 3 was approximately equal to that predicted on the basis of a simple bundle opening hypothesis (40.1 Å versus 44 Å respectively). By contrast, the change in distance for the other proteins was significantly smaller than anticipated based on analysis of the distances *in silico*. The distance between helices 1 ({W39}) and 3 increased from 19.4 to 28.3 Å upon lipid binding, while that between helices 4 ({W162}) and 3 increased from 23.2 to 32.4 Å. A minor discrepancy in the FRET-derived distance values in comparison to the model structure may have resulted from the use of a linear model that does not account for the curvature of a discoidal particle. Thus, there may be an overestimation of expected distances. Additionally, there is probably still some intermolecular energy transfer between adjacent {W162} molecules even when a 1:4 dilution (labeled protein:{Trp-null}) was used. There was, however, an increased distance in all cases indicating movement of helices away from helix 3.

The marked difference in AEDANS•{W162} disc spectra in the absence and presence of {Trp-null} suggested that helices 3 and 4 might be in an extended conformation relative to each other which would then allow them to reestablish similar molecular contacts, albeit with helices from an adjacent molecule. As a result, the apparent efficiency of energy transfer would be unaltered when this mutant was the sole protein present on discs. To gain further support for such a reorientation, the relative extent of intermolecular energy transfer was evaluated by producing discs which contained an excess of AEDANS•{Trp-null} protein with an unlabeled single Trp protein (4:1 mass ratio). In this manner, it was anticipated that the AEDANS (on helix 3) would only be able to accept a significant amount of energy if the donor was located on a helix from an adjacent molecule that was in close proximity (< 70 Å). Following excitation at 295 nm, AEDANS emission peak intensities were compared by normalizing data based on the excitation spectra intensity at 340 nm, the absorption maxima for this moiety (**Fig. 6-5**). In the presence of {W39}, there was minimal transfer of energy from the Trp to AEDANS as evidenced by the comparable intensity of the ~ 480 nm peak to that produced by discs containing only unlabeled {Trp-null}. When {W162} was present, there was a pronounced

increase in the intensity of the AEDANS emission peak indicating significant energy transfer and considerably closer proximity of the energy acceptor to the Trp than would be expected if helices 3 and 4 from adjacent molecules were distal.

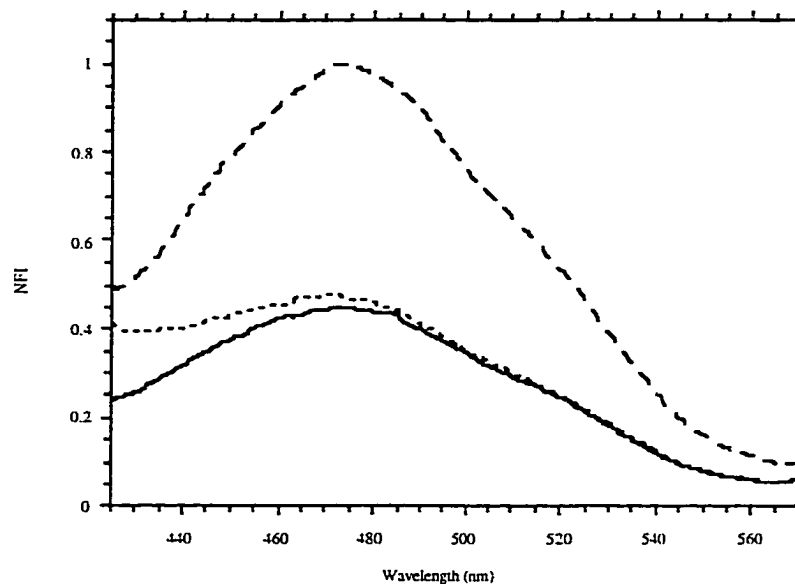


**Fig. 6-5.** Emission spectra resulting from intermolecular energy transfer between AEDANS•{Trp-null} and single Trp protein complexed with DMPC. (—), {Trp-null}; (---), {W39}; (-.-), {W162}. Discs were produced by co-sonicating DMPC with a mixture of AEDANS•{Trp-null} and unlabeled protein at a mass ratio of 4:1. The excitation value at the absorption maxima of AEDANS (340 nm) was used to adjust the intensity of the fluorescence spectra to allow comparisons to be made. Emission spectra were produced by excitation at 295 nm.

## 6.4 Discussion

---

ApoE is a critical component of the metabolism of triglyceride-rich lipoproteins, primarily due to its role in the clearance of remnant particles from circulation. This property is only manifest when apoE (specifically the amino terminal domain) is lipid-associated. It is evident that determination of the conformation of this protein in complex with lipid may yield valuable insight into its ability to interact with cell surface receptors.

There is a paucity of data describing the tertiary structure of the lipid-bound, receptor binding domain of apoE. FTIR data has indicated that the orientation of helices is perpendicular with respect to the acyl chains of phospholipid disc complexes (Chapter 4), while the surface area occupied by this protein at an air-water interface suggested an opening of the helix bundle<sup>12</sup>. However, direct evidence of tertiary organization is lacking. Proteins in complex with lipid present a unique challenge for structural determination which taxes the two major techniques available today, X-ray crystallography and NMR.

A number of models can be envisioned to describe the lipid-bound structure of the N-terminal domain of apoE. i) *Open Conformation model*: Based on surface monolayer studies, Weisgraber et al.<sup>12</sup> proposed that the helix bundle opens about a “hinge” region between helices 2 and 3, allowing the residues in the hydrophobic interior to replace their helix-helix interactions with helix-lipid contacts. If one considers a discoidal complex, the helices would be arranged in a perpendicular orientation with respect to the acyl chains of phospholipid around the disc periphery, consistent with the ATR-FTIR data presented in Chapter 4. This orientation is comparable to that of another helix-bundle exchangeable apolipoprotein that possesses a similar architecture, the insect apoLp-III<sup>13</sup> and resembles the model proposed by Breiter et al. based on the X-ray crystal structure of this protein<sup>14</sup>. ii) *Picket Fence model*: Based on FTIR and geometric considerations, de Pauw et al.<sup>5</sup> proposed the “Picket Fence” model in which the helices of the N-terminal domain rearrange themselves into 17 residue anti-parallel helices oriented parallel to the acyl chains of the phospholipid bilayer of discoidal particles. This orientation is similar to that proposed for full-length human apoA-I by Brasseur et al. based on energy minimization modeling<sup>15</sup>. There is some doubt as to the validity of such a model since the extensive helical rearrangements proposed would be energetically costly and it would result in the disruption of a region of positive charge in helix 4 that is believed to be critical for receptor binding<sup>16</sup>. iii) *Extended Belt model*: Another possible rearrangement exists in which the helices are oriented in a linear fashion around the periphery of a discoidal complex. Such an orientation is analogous to the X-ray crystal structure



of an N-terminal deletion mutant of human apoA-I (apo $\Delta$ (1-43)A-I)<sup>17</sup>. In this structure, a tetramer of  $\alpha$ -helical, horseshoe-shaped molecules were assembled in a tight elliptical ring in an anti-parallel orientation. The helices were arranged in an extended conformation and it can be envisioned that, if they were present around the periphery of a discoidal complex, the helices would be oriented perpendicular to the acyl chains. Borhani and colleagues suggested that this structure may represent the lipid-associated conformation of this protein. Further support for a perpendicular orientation of apoA-I with respect to the phospholipid acyl chains was recently provided by Koppaka et al. who presented data in which the protein was analyzed in a more hydrated, and, thus, more physiological state using polarized internal reflection infrared spectroscopy<sup>18</sup>.

In Chapter 5, it was demonstrated that FRET had the potential to provide information on the lipid-bound, receptor-competent conformation of the N-terminal domain of apoE. Spectral data suggested that there was movement of helix 3 away from helix 1, consistent with the "Open Conformation" model. There were, however, a few limitations: i) multiple energy donors (four Trp within the region of helix 1) complicated interpretation of energy transfer data since proximal Trp contribute energy to a greater extent than more distal residues, increasing the uncertainty of the distances determined; ii) intermolecular energy transfer in lipid-associated particles was not addressed; and iii) there was no information about the relative position of helix 2 or helix 4 with respect to 3. In the present paper, we have addressed these limitations and present a model of the lipid-bound conformation.

Based on the data presented here, it was concluded that apoE is present around the periphery of discs in a partially extended conformation. The virtual identity of the initial AEDANS•{W162} emission spectra in the absence and presence of lipid suggested that either: i) helices 3 and 4 remain associated when the N-terminus of apoE is lipid-bound or ii) these helices actually do move apart but they establish similar molecular contacts with their complementary helix in the adjacent molecule. The data generated utilizing {Trp-null} is only consistent with the second interpretation. Presumably, when AEDANS•{W162} was combined with an excess of unlabeled {Trp-null}, it was able to interact with an adjacent

molecule but it was unable to engage in intermolecular energy transfer due to the absence of a proximal acceptor moiety. In these complexes, the bulk of the energy transfer that is occurring is intramolecular and, thus, the increase in the Trp emission intensity detected indicates a reduction in energy transfer and, thus, movement of helix 3 away from helix 4 upon adoption of the lipid-bound conformation. The continued intimacy of these helices upon lipid binding was further supported by FRET analysis of discs which contained {W162} and excess AEDANS•{Trp-null}. **Fig. 6-6** depicts a model which is a hybrid between the “Extended Belt” and the “Open Conformation” models.

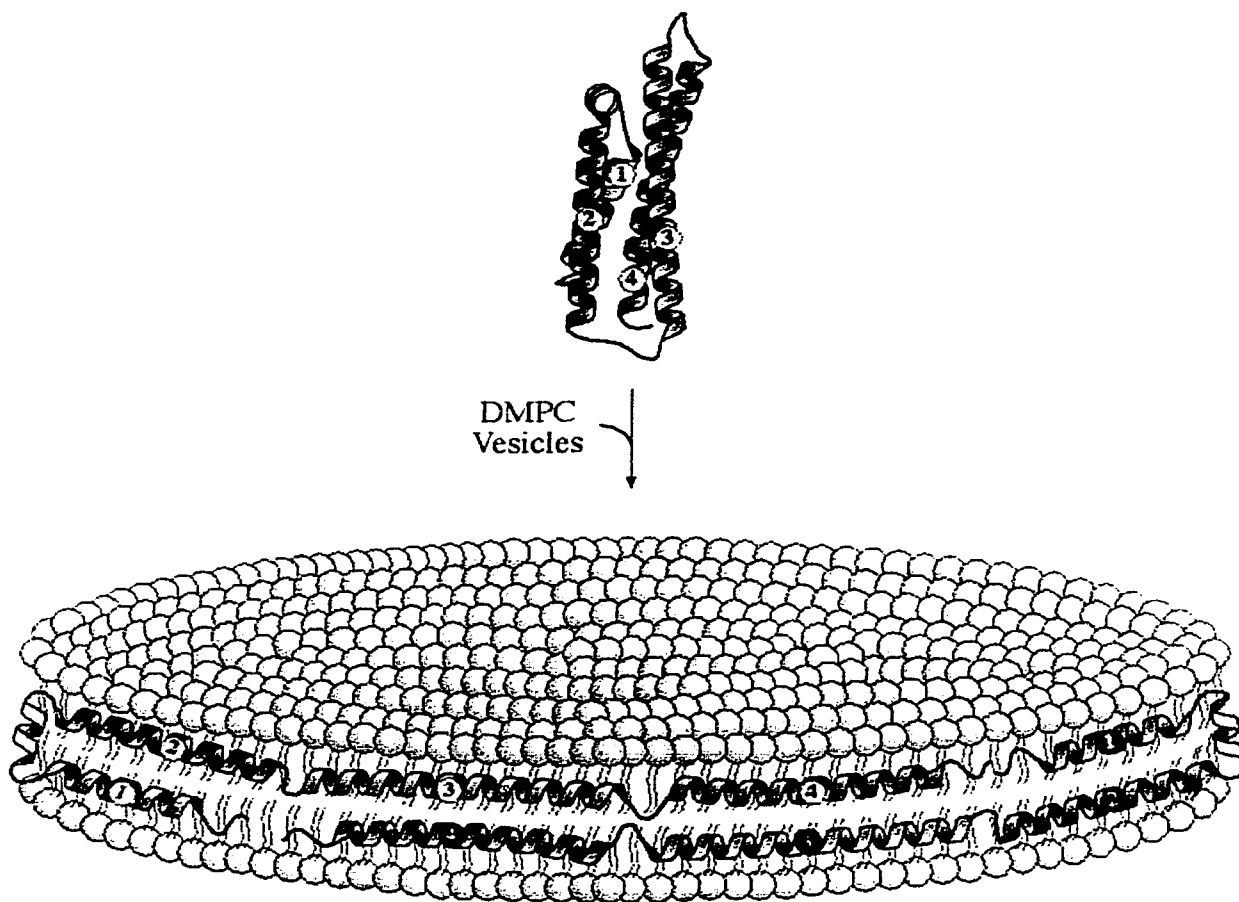


**Fig. 6-6** Model depicting the lipid-bound conformation of the N-terminal domain of apoE. Protein associates with the acyl chains of a DMPC bilayer forming a discoidal particle.

Helices 1 and 2 maintain contact replacing their intramolecular hydrophobic helix-helix interactions (H1-H2 to H3-H4) with helix-lipid interactions, while

helices 3 and 4 move away from one another generating an overall semi-extended conformation. Binding to a lipid or hydrophobic surface according to the model proposed would necessitate the disruption of numerous interactions that are important for the maintenance of the native helix bundle structure. Among these interactions are those occurring between the series of Leu residues which are believed to stabilize the interface between helix 1 and helix 4 in addition to that between helix 2 and helix 3. An opening of the bundle would permit these Leu residues to exchange their helix-helix interactions for helix-lipid ones. As a result of such an exchange, the precise orientation of the solvent-exposed, amino acid side chains may be altered such that the surface charge profile presented facilitates high affinity receptor interaction. Alternatively or additionally, residues which are in disordered regions of the X-ray structure (residues 1-22 and 167-191) may associate with lipid adopting a structure (possibly  $\alpha$ -helical) that further facilitates receptor binding. Additionally, the extension of helices 3 and 4 may permit the adoption of an  $\alpha$ -helical secondary structure in the loop region connecting these helices resulting in the formation of an extended, continuous stretch of  $\alpha$ -helix. The secondary structure prediction algorithms of King and Sternberg<sup>19</sup> in addition to those of Rost and Sander<sup>20</sup> indicated that this region has a high probability of forming  $\alpha$ -helix. Fragments or synthetic peptides of regions of exchangeable apolipoproteins often require lipid-association to adopt a significant amount of  $\alpha$ -helical structure<sup>21-23</sup>, suggesting that contact with lipid may drive loops to acquire this secondary structure. The amino acid sequence of apoE3(1-183) was also submitted to the Protein Sequence Analysis System of the BioMolecular Engineering Research Center at Boston University ([bmerc-www.bu.edu/psa/](http://bmerc-www.bu.edu/psa/))<sup>24-26</sup> and it was determined that the probability of the residues from 58 to 178 being in a helix was greater than 50%. The only turn was predicted to be centered at ~ residue 53 supporting the potential adoption of a helical arrangement in which helices 1 and 2 remained paired while the remainder may form an uninterrupted stretch of helix. Additionally, analysis of the amino acid residues in this region indicates that there is a repeating pattern of hydrophobic residues reminiscent of a heptad repeat that is indicative of a coiled coil structure<sup>27</sup>. This organization of residues in the interhelical junction is

analogous to that which occurs in the crystal structure of the apoA-I N-terminal deletion mutant<sup>17</sup> and may result in the adoption of an alignment of solvent exposed residues which facilitates receptor interaction.

Complete mapping of the repositioning of the helices of the N-terminal domain of apoE will require the production of mutants which contain a cysteine residue located on helix 1 or 2 to which an energy acceptor can be attached. Such constructs should permit the determination of the relative positions of these two helices with respect to one another and confirm their relation to helices 3 and 4.

The N-terminal domain of apoE may have greater freedom to adopt possibly alternative, energetically favorable conformations on the surface of a sphere than around the relatively spatially constrained periphery of a discoidal particle, a possibility that has some experimental support<sup>28,29</sup>. If molecules of the N-terminal domain of apoE come into close enough proximity to one another, they may form contacts as depicted in Fig. 6-6 modulating its receptor binding properties. Experiments with spherical complexes, such as recombinant lipoproteins, should provide insight into this question.

Utilizing site-directed mutagenesis and a combination of intrinsic and extrinsic fluorophores, we have provided insight into the relative positioning of helices with respect to one another in an exchangeable apolipoprotein in its bioactive, lipid-bound state. This structural reorganization has implications for our understanding of the mechanism by which apolipoproteins adapt their structure to fulfill their function.

## 6.5 Bibliography

---

1. Weisgraber, K.H. Apolipoprotein E: structure-function relationships. *Ad. Protein Chem.* **45**, 249-302 (1994).
2. Innerarity, T.L. & Mahley, R.W. Enhanced binding by cultured human fibroblasts of apo-E-containing lipoproteins as compared with low density lipoproteins. *Biochemistry* **17**, 1440-1447 (1978).
3. Innerarity, T.L., Pitas, R.E. & Mahley, R.W. Binding of arginine-rich (E) apoprotein after recombination with phospholipid vesicles to the low density lipoprotein receptors of fibroblasts. *J. Biol. Chem.* **254**, 4186-4190 (1979).
4. Aggerbeck, L.P., Wetterau, J.R., Weisgraber, K.H., Wu, C.C. & Lindgren, F.T. Human apolipoprotein E3 in aqueous solution: II. Properties of the amino- and carboxyl-terminal domains. *J. Biol. Chem.* **263**, 6249-6258 (1988).
5. De Pauw, M., Vanloo, B., Weisgraber, K. & Rosseneu, M. Comparison of lipid-binding and lecithin:cholesterol acyltransferase activation of the amino- and carboxyl-terminal domains of human apolipoprotein E3. *Biochemistry* **34**, 10953-10960 (1995).
6. Raussens, V., Fisher, C.A., Goormaghtigh, E., Ryan, R.O. & Ruyschaert, J.-M. The low density lipoprotein receptor active conformation of apolipoprotein E. Helix organization in N-terminal domain-phospholipid disc particles. *J. Biol. Chem.* **273**, 25825-25830 (1998).
7. Stryer, L. Fluorescence energy transfer as a spectroscopic ruler. *Annu. Rev. Biochem.* **47**, 819-846 (1978).
8. Lakey, J.H., Baty, D. & Pattus, F. Fluorescence energy transfer distance measurements using site-directed single cysteine mutants: the membrane insertion of colicin A. *J. Mol. Biol.* **218**, 639-653 (1991).
9. Fisher, C.A., Wang, J., Francis, G.A., Sykes, B.D., Kay, C.M. & Ryan, R.O. Bacterial overexpression, isotope enrichment, and NMR analysis of the N-terminal domain of human apolipoprotein E. *Biochem. Cell Biol.* , 45-53 (1997).
10. Wetterau, J.R., Aggerbeck, L.P., Rall, S.C., Jr. & Weisgraber, K.H. Human apolipoprotein E3 in aqueous solution: I. Evidence for two structural domains. *J. Biol. Chem.* **263**, 6240-6248 (1988).
11. Fisher, C.A. & Ryan, R.O. Lipid binding-induced conformational changes in the N-terminal domain of human apolipoprotein E. *J. Lipid Res.* **40**, 93-99 (1999).
12. Weisgraber, K.H., Lund-Katz, S. & Phillips, M.C. Apolipoprotein E: structure-function correlations. in *High density lipoproteins and atherosclerosis III* (eds. Miller, N.E. & Tall, A.R.) 175-181 (Elsevier, Amsterdam, 1992).
13. Raussens, V., Narayanaswami, V., Goormaghtigh, E., Ryan, R.O. & Ruyschaert, J.-M. Alignment of the apolipoprotein III  $\alpha$ -helices in complex with dimyristoylphosphatidylcholine. A unique spatial orientation. *J. Biol. Chem.* **270**, 12542-12547 (1995).

14. Breiter, D.R., Kanost, M.R., Benning, M.M., Wesenberg, G., Law, J.H., Wells, M.A., Rayment, I. & Holden, H.M. Molecular structure of an apolipoprotein determined at 2.5-Å resolution. *Biochemistry* **30**, 603-608 (1991).
15. Brasseur, R., Lins, L., Vanloo, B., Ruyschaert, J.-M. & Rosseneu, M. Molecular modeling of the amphipathic helices of the plasma apolipoproteins. *Proteins* **13**, 246-257 (1992).
16. Lalazar, A., Weisgraber, K.H., Rall, S.C., Jr, Giladi, H., Innerarity, T.L., Levanon, A.Z., Boyles, J.K., Amit, B., Gorecki, M. & Mahley, R.W. Site-specific mutagenesis of human apolipoprotein E. Receptor binding activity of variants with single amino acid substitutions. *J. Biol. Chem.* **263**, 3542-3545 (1988).
17. Borhani, D.W., Rogers, D.P., Engler, J.A. & Brouillette, C.G. Crystal structure of truncated human apolipoprotein A-I suggests a lipid-bound conformation. *Proc. Natl. Acad. Sci. U.S.A.* **94**(1997).
18. Koppaka, V., Silvestro, L., Engler, J.A., Brouillette, C.G. & Axelsen, P.H. The structure of human lipoprotein A-I: evidence for the "belt" model. *J. Biol. Chem.* **274**, 14541-14544 (1999).
19. King, R.D. & Sternberg, M.J. Identification and application of the concepts important for accurate and reliable protein secondary structure prediction. *Protein Sci.* **5**, 2298-2310 (1996).
20. Rost, B. & Sander, C. Combining evolutionary information and neural networks to predict protein secondary structure. *Proteins* **19**, 55-72 (1994).
21. Clayton, D., Brereton, I.M., Kroon, P.A. & Smith, R. NMR studies of the low-density lipoprotein receptor-binding peptide of apolipoprotein E bound to dodecylphosphocholine micelles. *Protein Sci.* **8**, 1797-1805 (1999).
22. Gazzara, J.A., Phillips, M.C., Lund-Katz, S., Palgunachari, M.N., Segrest, J.P., Anantharmaiah, G.M. & Snow, J.W. Interaction of class A amphipathic helical peptides with phospholipid unilamellar vesicles. *J. Lipid Res.* **38**, 2134-2146 (1997).
23. Narayanaswami, V., Weers, P.M.M., Bogerd, J., Kooiman, F.P., Kay, C.M., Scraba, D.G., Van der Horst, D.J. & Ryan, R.O. Spectroscopic and lipid binding studies on the amino and carboxyl terminal fragments of *Locusta migratoria* apolipoprotein III. *Biochemistry* **34**, 11822-11830 (1995).
24. Stultz, C.M., Nambudripad, R., Lathrop, R.H. & White, J.V. Predicting Protein Structure with Probabilistic Models. in *Protein Structural Biology in Bio-Medical Research*, Vol. 22B (ed. Bittar, E.E.) (JAI Press, Greenwich, 1997).
25. Stultz, C.M., White, J.V. & Smith, T.F. Structural Analysis Based on State-space Modeling. *Protein Sci.* **2**, 305-314 (1993).
26. White, J.V., Stultz, C.M. & Smith, T.F. Protein Classification by Stochastic Modeling and Optimal Filtering of Amino-Acid Sequences. *Math. Biosci.* **119**, 35-75 (1994).
27. Lupas, A. Coiled coils: new structures and new functions. *Trends Biochem. Sci.* **21**, 375-382 (1996).

28. Lund-Katz, S., Weisgraber, K.H., Mahley, R.W. & Phillips, M.C. Conformation of apolipoprotein E in lipoproteins. *J. Biol. Chem.* **268**, 23008-23015 (1993).
29. Narayanaswami, V., Wang, J., Kay, C.M., Scraba, D.G. & Ryan, R.O. Disulfide bond engineering to monitor conformational opening of apolipoprotein III during lipid binding. *J. Biol. Chem.* **271**, 26855-26862 (1996).

# **Chapter 7**

## **General Discussion and Comments**

---



ApoE is an exchangeable apolipoprotein that has stimulated intense study due to its critical participation in lipid homeostasis. Many roles have been suggested for this protein but the one of primary interest for my thesis has been the conformational changes that allow it to promote the uptake of lipid- and cholesterol-rich lipoprotein particles from circulation. The importance of this function has been clearly demonstrated by the propensity to develop atherosclerosis as a result of dyslipidemias in individuals possessing mutations in apoE and by the dysfunction that occurs in mice in which the gene for this protein is disrupted.

ApoE, as with other exchangeable apolipoproteins, has the capability of existing in both lipid-free and lipid-bound states. In the latter environment, apoE is able to aid in the solubilization of lipoprotein particles during their delivery to sites of storage or metabolism. It is also in this form that apoE is able to mediate high affinity binding to cell surface lipoprotein receptors. Thus, the determination of the lipid-bound conformation of apoE should provide us with insight into the structural flexibility required by these molecules to fulfill their function and how this alteration results in the presentation of a profile that permits high affinity receptor interaction.

## **7.1 Development of an Expression and Purification System for ApoE3(1-183)**

As a starting point for in-depth structural analysis of the amino terminal domain of apoE, we designed and developed a bacterial expression system for

this protein. Expression of this protein in commonly employed systems resulted in relatively low yields. The modular nature of apoE allows the expression of individual domains permitting us to focus on the region harboring the receptor binding potential, the N-terminal domain. We chose to express the first 183 amino acids since this fragment encompassed all of the residues contained within the ordered region of the X-ray crystal structure and those that were deemed important for high affinity receptor binding. Bacterial expression was employed due to the ease of culture preparation and the potential that it presented to incorporate isotopes into the media during protein expression to produce protein that is amenable to multidimensional NMR analysis. We were also encouraged by the success that this lab has had with another exchangeable apolipoprotein, apoLp-III, from the insect *Manduca sexta*. Bacterial expression of apoLp-III had resulted in the fortuitous accumulation of this protein in the culture media producing a yield of ~ 150 mg/L. Expression of apoE3(1-183) in a similar system yielded protein which also accumulated in the media and resulted in a yield of approximately 50 mg protein/L.

Analytical ultracentrifugation indicated that the protein was monomeric, mass spectrometry showed the expected molecular weight and circular dichroism produced data indicative of a protein that was predominantly  $\alpha$ -helical in structure. As with other exchangeable apolipoproteins, not only could recombinant apoE3(1-183) convert phospholipid vesicles to discoidal complexes, but it prevented the aggregation of LDL particles that were being overloaded with lipid. The native-like functioning of this protein was further

confirmed by the ability of apoE3(1-183)-DMPC complexes to compete with LDL for binding to the LDLr on the surface of human skin fibroblasts.

One of the most powerful techniques available today for structural determination is NMR. One of its key features is the ability to provide structures of proteins in their hydrated state. Despite the availability of the X-ray structure of this protein, there may be significant differences between this and that derived by NMR. Additionally, there has been some success in obtaining structural information from lipid-associated proteins. NMR analyses of  $^{15}\text{N}$ -labeled apoE3(1-183) yielded 2-dimensional spectra in which the crosspeaks were reasonably well dispersed although the pH necessary for data collection was 3.6, considerably below that encountered *in vivo*. Even at this low pH, however, apoE3(1-183) possesses the bulk of its secondary structure suggesting that information obtained would still be relevant. Despite the spectral dispersion that was obtained, complete unambiguous assignment of all of the crosspeaks as a step towards elucidation of the tertiary structure will require the use of multidimensional NMR.

## **7.2 Displacement of ApoLp-III from LDLp to Create a Receptor-active Molecule**

The ability to bind lipid and the extent to which this occurs is a primary determinant of the ability of apoE to modulate receptor binding. Exchangeable apolipoproteins compete for space on the surface of lipoproteins as a requisite for fulfilling their functions. The protein that will have the greatest success in

this endeavor is the one which has the highest lipid affinity and is most adept at accommodating changes in the local environment. ApoE can form complexes with lipid in which the small particle size dictates that only a portion of this protein can remain associated, attesting to the conformational versatility of this protein<sup>1</sup>. Studying the relative lipid binding affinity of apoE on spherical particles may provide some insight into its conformational adaptability in comparison to other exchangeable apolipoproteins.

LDLp isolated from *Manduca sexta* was chosen for these studies based on the thorough characterization of this molecule and the presence of a readily exchangeable apolipoprotein, apoLp-III. Incubation of LDLp with apoE3(1-183) displaced the resident apoLp-III, producing apoE-rich particles that were subsequently shown to effectively compete with LDL for LDLr binding. When apoE was co-incubated with apoA-I, the resultant particles contained primarily apoA-I, indicating that the relative lipid binding affinity of these proteins is apoA-I > apoE3(1-183) > apoLp-III. Relating this data to conditions *in vivo*, prior to apoE exerting a significant role in lipoprotein clearance (via receptor binding), the concentration of apoA-I may need to be diminished or reduced below a level that allows the less lipophilic N-terminal domain of apoE to undergo the conformational changes necessary for receptor interaction.

In addition to delineating the relative lipid affinity of these apolipoproteins, we have produced a spherical particle that can be used as a tool to mimic the physiological environment in which these proteins often find

themselves (i.e. bound to spherical lipoprotein particles), enabling the functional consequences of directed mutations to be analyzed.

### **7.3 Determination of the Lipid-bound Orientation of ApoE3(1-183)**

ApoE is only bioactive in the lipid-bound state. The varied components of lipoprotein particles present a considerable challenge to the study of an individual constituent. A model system that has proven its utility for studying lipid-associated apolipoproteins has been that involving the sonication of phospholipid and protein to form discoidal particles. There is a scarcity of structural data on proteins in such an environment due to the difficulties of tertiary structural determination by standard methods. In lieu of detailed tertiary information, several models have been proposed to describe the lipid-bound conformation of the N-terminal fragment of apoE (described in detail earlier). One of the points of contention for the lipid-bound conformation has been the orientation of helices in relation to the phospholipid acyl chains in disc complexes. ATR-FTIR data, derived from analysis of discoidal particles, indicated that the orientation of helices in relation to the plane of the germanium plate (and, thus, the disc surface) is perpendicular. There was even some indication that the small helix located between helices 1 and 2 (i.e. H') was oriented parallel to the acyl chains, consistent with the "open conformation" and even the "extended belt" models. With this knowledge, the myriad of possible helical rearrangements around the disc periphery is diminished. One proposal that is not consistent with such an orientation is that of de Pauw et al. who

proposed a configuration in which the helices rearrange into 17 residue stretches such that they orient parallel to the acyl chains, spanning the width of the disc<sup>2</sup>. It is unfortunate that the FTIR data upon which these authors based their conclusions was not actually presented in their paper, preventing critical analysis of their hypothesis.

An interesting exercise would be repeating our measurements using a form of polarized internal reflection infrared spectroscopy that permits the analysis of lipoprotein complexes in a hydrated, more native-like state<sup>3</sup>. Using this system, the orientation of the helices of apoA-I in discoidal complexes was determined to be perpendicular to the acyl chains, in contrast to earlier FTIR data<sup>4</sup> and in support of the recently published X-ray structure of an N-terminal deletion mutant of apoA-I<sup>5</sup>.

#### **7.4 Determination of the Lipid-bound Conformation of ApoE3(1-183)**

Determining the tertiary structure of proteins in complex with lipids presents considerable challenges. In the presence of lipid, it is difficult to grow the crystals that are required for X-ray diffraction precluding the determination of higher order structure with this technique. NMR holds some promise since the formation of crystals is not a requisite although it is not without its limitations. Lipoprotein particles can reach 1000 kDa in size and even the smallest particles are close to 100 kDa<sup>1</sup>. Since the current limit of NMR spectroscopy is closer to 40 kDa, determination of the structure of lipoprotein complexes using this technique is still not feasible. While the level of detail may

not be quite as exquisite as that of those techniques previously mentioned, FRET can provide considerable information on the relative position of various regions of a protein, making it possible to map conformational alterations occurring in a protein present in different environments. The N-terminal domain of apoE was a prime candidate for FRET analysis for a number of reasons: i) structural information in the lipid-free state was readily available; ii) transition from a lipid-free to a lipid-bound state does not alter its secondary structure; iii) this domain has four Trp residues all within the vicinity of the first helix; iv) there is a Cys near the middle of helix 3 to which an energy acceptor can be readily attached; and v) a bacterial expression system has been established, facilitating the production of mutants.

Following confirmation of the structural soundness of AEDANS-labeled protein and the ability of this construct to monitor conformational changes, binding of apoE to lipid resulted in a decrease in the efficiency of energy transfer indicating movement of helix 1 away from helix 3, a positional alteration that is in agreement with the "Open Conformation" model. However, there were a few limitations with this system: i) the presence of multiple energy donors; ii) a restriction to analysis of movement between helices 1 and 3, and iii) the possibility of intermolecular energy transfer. In the final chapter, these limitations were overcome by creating mutants of apoE3(1-183), each possessing a single Trp on a different helix. Further, a Trp-null protein was designed for incorporation into discs to minimize energy transfer between adjacent molecules. Analysis of alterations in energy transfer for protein in the

presence and absence of lipid permitted the proposal of a model in which the helices are partially extended around the periphery of a disc with helices 1 and 2 remaining associated while helices 3 and 4 are extended.

## 7.5 Comments

Determining the lipid-bound conformation of the N-terminal domain of apoE may yield new insights into the structural adaptability of exchangeable apolipoproteins in general and adoption of a receptor competent conformation in particular. Exchangeable apolipoproteins can exist in both a lipid-free and a lipid-bound state. To accommodate such a dual existence, its structure must somehow adapt so that a readily reversible interaction can occur. A common characteristic of these proteins is that they are composed of amphipathic  $\alpha$ -helices. As such, their sequestered hydrophobic residues must exchange their helix-helix interactions for helix-lipid ones. One of the attributes that may permit such an alteration is the relatively loose packing of the helices. Recently, Prévost and Kocher performed molecular dynamics simulations on the receptor binding domain of apoE and their results suggested that this domain has relatively weak tertiary compactness in comparison to proteins of similar size, as evidenced by a higher incidence of atomic-size cavities<sup>6</sup>. In support of a model in which helices 1 and 2 move away from helices 3 and 4, it was found that cavities larger than 1 Å radius occurred more frequently at the interface between helices 1 and 2 (H1-H2) and helices 3 and 4 (H3-H4) than between the helical pairs H1-H4/H2-H3. Additionally, the presence of apolar side chains that are



more flexible than in other native proteins suggested that the structure of this protein is molten globule-like, which may account for its conformational flexibility. Other exchangeable apolipoproteins such as apoA-I<sup>7</sup> and apoLp-III<sup>8</sup> appear to have similar structural properties and a propensity for conformational plasticity.

Based on the model shown in Fig. 6-6, it can be predicted that the region between helices 2 and 3 may have an opportunity to form  $\alpha$ -helical secondary structure. When the amino acid sequence of apoE3(1-183) was analyzed by the program "SOPMA" (self-optimized prediction method)<sup>9</sup>, a continuous stretch of  $\alpha$ -helix was predicted to be present between residues 44 and 125, the sequence that encompasses helices 2 and 3 based upon the X-ray structure. This is despite the presence of a proline in the central region of this stretch of residues. It seems possible then that the opening of the helix bundle might allow the formation of a continuous stretch of helix which may stabilize the final structure. This stretch is also predicted to form a coiled coil as indicated by the program "Coils"<sup>10</sup> although there is a disruption due to the proline at position 84. A proline in the middle of a helix would impart a twist of 100° between the interfacial planes<sup>11</sup>. This may simply result in the adoption of a curvature in the helix which aids in the association of the protein with a curved surface such as that encountered in spherical or discoidal lipoprotein particles.

There is also some evidence that the loop between helices 3 and 4 can form a continuous stretch of  $\alpha$ -helix. The secondary structure prediction algorithms of King and Sternberg<sup>12</sup> along with Rost and Sander<sup>13</sup> indicated that

this region has a high probability of forming  $\alpha$ -helix. Additionally, the sequence of apoE3(1-183) was submitted to the Protein Sequence Analysis System ([bmerc-www.bu.edu/psa/](http://bmerc-www.bu.edu/psa/)) of the BioMolecular Engineering Research Center at Boston University<sup>14-16</sup>. It was predicted that the probability of the residues from 58 to 178 being in a helix was greater than 50%. The only turn was predicted to be centered at ~ residue 53 supporting a helical arrangement in which helices 1 and 2 remain paired with the remainder forming an uninterrupted stretch of helix.

This thesis presents evidence for the possibility of a partially extended conformation for the lipid-bound N-terminal domain of apoE as depicted in Fig. 6-6. What such a conformation suggests is that lipid association permits the rearrangement of helices so that certain stretches of amino acids that span the interhelical gaps may be stimulated to adopt structure. Changes in these regions may induce alterations in the orientation of the surface profile such that the charge density presented to other molecules is favorable for interactions. It is also likely that receptor binding is modulated by the alteration in the orientation of the helices' hydrophilic face as a result of the replacement of helix-helix interactions with helix-lipid contacts. It is interesting that helices 3 and 4 appear to reestablish some of the molecular contacts present in the lipid-free protein. The contacts that occurred between this pairing and helices 1 and 2 are replaced by helix-lipid interactions, possibly introducing an alteration in the solvent exposed, unpaired charged residues that are available for receptor binding although the precise orientation of these residues remains undefined.

FRET has provided insight into the relative positioning of helices in the lipid-associated N-terminal domain of apoE. The resulting helical arrangement provides clues to the resultant effects on receptor interaction but the precise complement of residues that dictate receptor binding awaits further study.

There are a number of questions that remain which may be answered by extending the work that I have outlined in this thesis. While discoidal particles possess receptor binding activity, what is the conformation of the N-terminus when freed from the constraints of a disc periphery? Are proteins clustered together on the surface of spherical particles and is this protein density necessary for receptor interaction? It has been hypothesized that the most important contribution of lipoprotein binding to receptor interaction is the provision of a scaffold upon which multiple copies of receptor competent protein can be brought into close enough proximity to promote high affinity receptor interaction. Considerable insight might be gained by producing spherical reconstituted lipoprotein particles in which fluorophore-containing apoE3(1-183) is incorporated thereby allowing the relative positions of these molecules, and their component helices, to be monitored.

The focus of my thesis has been the N-terminal domain since it contains the receptor binding region, but there is considerable evidence that interaction between the two domains exists. Expression and fluorophore labeling of full-length apoE might permit determination of the dynamic interaction that exists between these two regions. A similar construct may prove insightful in situations where apoE resides on the surface of lipoproteins but in a receptor-

inactive state. Since the primary lipid binding capacity resides in the C-terminal domain, a scenario can be envisioned in which apoE remains anchored to the surface of a lipoprotein particle by its C-terminus while its N-terminal portion adopts a lipid-free helix bundle structure until such time as the surface conditions permit its lipid association, presumably with opening of the bundle as envisioned in Fig. 6-6. In this manner, native apoE may be able to prolong its residence time on the lipoprotein surface.

While several questions have been addressed by my thesis, the system that I have employed is poised to answer many of those that await resolution.

## **Bibliography**

---

1. Jonas, A., Steinmetz, A. & Churgay, L. The number of amphipathic  $\alpha$ -helical segments of apolipoproteins A-I, E, and A-IV determines the size and functional properties of their reconstituted lipoprotein particles. *J. Biol. Chem.* **268**, 1596-1602 (1993).
2. De Pauw, M., Vanloo, B., Weisgraber, K. & Rosseneu, M. Comparison of lipid-binding and lecithin:cholesterol acyltransferase activation of the amino- and carboxyl-terminal domains of human apolipoprotein E3. *Biochemistry* **34**, 10953-10960 (1995).
3. Koppaka, V., Silvestro, L., Engler, J.A., Brouillette, C.G. & Axelsen, P.H. The structure of human lipoprotein A-I: evidence for the "belt" model. *J. Biol. Chem.* **274**, 14541-14544 (1999).
4. Brasseur, R., DeMeutter, J., Vanloo, B., Goormaghtigh, E., Ruyschaert, J.-M. & Rosseneu, M. Mode of assembly of amphipathic helical segments in model high-density lipoproteins. *Biochim. Biophys. Acta.* **1043**, 245-253 (1990).
5. Borhani, D.W., Rogers, D.P., Engler, J.A. & Brouillette, C.G. Crystal structure of truncated human apolipoprotein A-I suggests a lipid-bound conformation. *Proc. Natl. Acad. Sci. U.S.A.* **94**(1997).
6. Prévost, M. & Kocher, J.-P. Structural characterization by computer experiments of the lipid-free LDL-receptor-binding domain of apolipoprotein E. *Protein Eng.* **12**, 475-483 (1999).
7. Gursky, O. & Atkinson, D. Thermal unfolding of human high-density apolipoprotein A-I: implications for a lipid-free molten globular state. *Proc. Natl. Acad. Sci. USA* **93**, 2991-2995 (1996).

8. Soulages, J.L. & Bendavid, O.J. The lipid binding activity of the exchangeable apolipoprotein apolipoprotein III correlates with the formation of a partially folded conformation. *Biochemistry* **37**, 10203-10210 (1998).
9. Geoujon, C. & Deléage, G. SOPMA: significant improvement in protein secondary structure prediction by consensus prediction from multiple alignments. *Cabios* **11**, 681-684 (1995).
10. Lupas, A., Van Dyke, M. & Stock, J. Predicting coiled coils from protein sequences. *Science* , 1162-1164 (1991).
11. Gazzara, J.A., Phillips, M.C., Lund-Katz, S., Palgunachari, M.N., Segrest, J.P., Anantharmaiah, G.M. & Snow, J.W. Interaction of class A amphipathic helical peptides with phospholipid unilamellar vesicles. *J. Lipid Res.* **38**, 2134-2146 (1997).
12. King, R.D. & Sternberg, M.J. Identification and application of the concepts important for accurate and reliable protein secondary structure prediction. *Protein Sci.* **5**, 2298-2310 (1996).
13. Rost, B. & Sander, C. Combining evolutionary information and neural networks to predict protein secondary structure. *Proteins* **19**, 55-72 (1994).
14. Stultz, C.M., Nambudripad, R., Lathrop, R.H. & White, J.V. Predicting Protein Structure with Probabilistic Models. in *Protein Structural Biology in Bio-Medical Research*, Vol. 22B (ed. Bittar, E.E.) (JAI Press, Greenwich, 1997).
15. Stultz, C.M., White, J.V. & Smith, T.F. Structural Analysis Based on State-space Modeling. *Protein Sci.* **2**, 305-314 (1993).

16. White, J.V., Stultz, C.M. & Smith, T.F. Protein Classification by Stochastic Modeling and Optimal Filtering of Amino-Acid Sequences. *Math. Biosci.* **119**, 35-75 (1994).